Performance of WRF Large-Eddy Simulations in summertime CBL characteristics over the Taklimakan Desert: A Real Test Case

Journal:	*Journal of Meteorological Research (JMR)*
Manuscript ID	ACTA-E-2018-0001.R2
Manuscript Type:	Original Article
Date Submitted by the Author:	15-Jul-2018
Complete List of Authors:	Xu, Hongxiong Wang, Minzhong Wang, Yinjun; Chinese Academy of Meteorological Sciences, State Key Laboratory of Severe Weather
Keywords:	WRF, Large Eddy Simulation, Convective Boundary Layer, Taklimakan
Speciality:	Large Eddy Simulation, Convective Boundary Layer

Performance of WRF Large Eddy Simulations in modeling the convective boundary layer over the Taklimakan Desert, China

Hongxiong Xu[1], Minzhong Wang[124], Yinjun Wang[1], Wenyue Cai[13]

1 State Key Laboratory of Severe Weather, Chinese Academy of Meteorological Sciences
Beijing, China 100081

2 Institute of Desert Meteorology, CMA (Chinese Meteorological Administration),
Urumqi, China
3National Climate Center, Chinese Meteorological Administration,
Beijing, China 100081

4 Taklimakan Desert Atmospheric Environment Observation Experimental Station, Tazhong 841000,
China

Submitted to ***Journal of Meteorological Research***

January 2, 2018

Corresponding author:
Dr. Minzhong Wang
Institute of Desert Meteorology,
CMA (Chinese Meteorological Administration),
No. 46, Zhongguancun South Street, Haidian District, Beijing
P. R. China, 100081
Email: wangmz@idm.cn
dorn1984@163.com

Abstract

The maximum height of the convective boundary layer (CBL) over the Taklimakan Desert can exceed 5000 m during the summer and has a crucial role in simulating the regional circulation and weather. We combined Weather Research and Forecasting Large Eddy Simulations with data from Global Positioning System (GPS) radiosondes and eddy covariance stations to evaluate the performance of the model in predicting the characteristics of the deep convective planetary boundary layer over the central Taklimakan Desert. The model reproduced the evolution of planetary boundary layer processes reasonably well, but the simulations predicted warmer and more moist conditions than the observations as a result of the over-prediction of surface fluxes and large-scale advection. Further simulations were performed with multiple configurations and sensitivity experiments. The sensitivity tests for the lateral boundary conditions (LBCs) showed that the model results are sensitive to changes in the time resolution and domain size of the specified LBCs. A larger domain size varies the distance of the area of interest from the LBCs and reduces the influence of large forecast errors near the LBCs. Comparing the model results using the original land surface parameterized sensible heat flux with the Noah land surface scheme and those of the sensitivity experiments showed that the desert CBL is sensitive to the sensible heat flux produced by the land surface scheme during daytime in summer. A reduction in the sensible heat flux can correct overestimates of the potential temperature profile. However, increasing the sensible heat flux significantly reduces the total time needed to increase the CBL to a relatively low altitude (<3 km) in the middle and initial stages of the development of the CBL rather than producing a higher CBL in the later stages.

Keywords: Weather Research and Forecasting Model, Large Eddy Simulations, convective boundary layer, Taklimakan Desert

1 Introduction

The Taklimakan Desert in south-central Xinjiang Province, China is the world's second-largest flow desert and has a profound influence on the regional weather and climate. As a result of the extreme range in near-surface temperatures, the planetary boundary layer (PBL) in this region commonly reaches 4–6 km in height during the boreal summer (Wang et al.), the deepest on Earth. This deep PBL, which is significantly higher than that over the surrounding mountains and oases, plays an important role in the regional circulation and weather. The accurate forecast of PBL processes over the Taklimakan Desert is an important problem in northwest China.

The atmosphere over large deserts (such as the Sahara and Taklimakan deserts) is a key component in the Earth's climate system. Surface heating from intense solar radiation leads to the development of a near-surface, low-pressure thermal system, commonly referred to as a heat low (Engelstaedter et al. 2015). However, despite the vital role that deserts have in the Earth's climate system, observations are extremely sparse and the available data are usually obtained from surrounding areas (Marsham et al. 2011). This lack of observational data has restricted the development of our understanding of deserts and has led to large discrepancies in analyses and significant biases in operational numerical weather prediction (NWP) models. The ability of local models to simulate real-world examples is often hindered by a lack of data with which to assess the performance of the model (Garcia-Carreras et al. 2015).

To fill in the gaps in the available data for the Taklimakan Desert, a field observation experiment was carried out during July 2016 in Tazhong, located in the center of the Taklimakan Desert near the Institute of Desert Meteorology, Chinese Meteorological

Administration, Urumqi (Liu et al. 2012; Wang et al. 2016a; Wang et al. 2016b). These data will allow the evaluation of the performance of the deep PBL process in NWP models over the Taklimakan Desert.

The motion of the atmosphere interweaves small-scale, complex interactions with multiscale nonlinear interactions. As a result of their limited resolution in both time and space, mesoscale atmospheric models are unable to represent all these processes (Talbot et al. 2012), which include turbulent motion on a scale that is too small to be resolved by simplified processes in atmospheric models. Turbulent mixing throughout the PBL can have a large impact on forecasts by NWP models (Shin; Hong 2011; Shin; Hong 2015).

Complex turbulent flows in NWP models can be analyzed by large eddy simulation (LES) techniques, which can explicitly resolve the energy-containing turbulent motions responsible for turbulent transport (Moeng et al. 2007). LES techniques have been used intensively to examine the detailed structure of turbulence, to generate statistics and to study physical processes (Garcia-Carreras et al. 2015; Heinold et al. 2013; Heinold et al. 2015; Heinze et al. 2015; Sun; Xu 2009). However, most applications of LES techniques to the PBL have been limited to idealized physical conditions. Recently, some studies have attempted to test and assess the performance of LES in simulating real-world case studies (Liu et al. 2011; Talbot et al. 2012). Liu et al. (2011) suggested that the Weather Research and Forecasting Large Eddy Simulation (WRF-LES) is a valuable tool with which to simulate real-world microscale weather flows and to develop real-time forecasting systems, although further modeling to determine the accuracy of synoptic forcing and the effect of resolution has been highly recommended. Talbot et al. (2012) suggested that the ability of WRF-LES to simulate real-world examples is hindered by a lack of favorable synoptic forcing. The initial and lateral boundary conditions (LBCs) were found to be more important in the LES results than subgrid-scale turbulence closures. Thus the LBCs can significantly alter the status of high-resolution LESs via inflow boundaries (Rai et al. 2017).

Most of the LES research over desert regions has been limited to idealized physical conditions (Garcia-Carreras et al. 2015) or conducted outside the Taklimakan Desert (Liu et al. 2011; Talbot et al. 2012). The aim of this study was to apply LES to a real example of a deep convective boundary layer (CBL) over the Taklimakan Desert. An important aspect of this work is to assess the skillfulness of the WRF-LES in simulating real examples of deep desert PBL processes at a relatively coarse resolution (333 m) over the Taklimakan Desert during the boreal summer. We first use a combination of the WRF-LES and Global Positioning System (GPS) radiosonde and surface fluxes over the central Taklimakan Desert calculated using an eddy covariance method to evaluate the performance of the WRF-LES in a real-world example. We then assess the potential errors related to the LBCs. One of our aims is to evaluate the relative contribution of uncertainties in the surface model to the typical behavior of PBL processes by conducting sensitivity experiment. We therefore studied the sensitivity of the model performance to the surface sensible heat flux. Section 2 gives a brief description of the synoptic conditions of the case study and describes the data, model configuration and design of the numerical experiments. The results of the numerical simulations are presented in Section 3 and our conclusions are summarized in Section 4.

2 Methods

2.1 Model configuration

We used version 3.8.1 of the WRF model (Skamarock et al. 2008) at a sub-kilometer resolution to simulate an extreme CBL over the Taklimakan Desert. The model is integrated for 12 h, starting from 0800 BJT (Beijing Time) on 1 July 2016. We use one-way nested WRF model from the mesoscale down to LES scales. All the domains consist of 51 levels extended to 50 hPa. The altitudes for the lowest 20 levels are 1130.473, 1157.705, 1207.765, 1294.703, 1423.873, 1591.895, 1795.526, 2021.868, 2272.33, 2558.433, 2882.675, 3248.113, 3658.499, 4118.481, 4633.882, 5212.111, 5855.802, 6517.111, 7151.295 and 7757.151 m and the horizontal spacing of the model is 12, 3, 1 and 0.33 km for d01, d02, d03, and d04. We used (411 × 321), (791 × 651), (211 × 201) and (403 × 406) model grids. Figure 1. shows the domain used for all the experiments except BDY_T3. A smaller grid size (205 × 208) is used in experiment BDY_T3 to verify the effect of domain size on the LES.

The initial and LBCs are provided at the coarsest mesoscale simulations from the National Centers for Environmental Prediction Global Data Assimilation System Final Operational Global Analyses dataset. The analyses are 0.25° × 0.25° grids operationally prepared every six hours and available on the surface and at 32 mandatory (and other pressure) levels from 1000 to 10 mbar (National Centers for Environmental Prediction 2015).

The physical options in the model include the WSM5 microphysics scheme (Hong; Lim 2006), the Yonsei University PBL scheme (Hong; Pan 1996), the Kain–Fritsch cumulus parameterization scheme (Kain 1993; Kain 2004), the rapid update cycle (RUC) land surface model (Smirnova Tatiana et al. 2000; Smirnova et al. 1997), the rapid radiative transfer model (Mlawer et al. 1997) at long wavelengths and the Dudhia shortwave radiation scheme (Dudhia 1989). The cumulus parameterization scheme is only applied to the d01 (12 km) grid domain to parameterize the convective rainfall and the LES is only applied to d04 (0.333 km).

Table 1 lists the experiments. Experiment 1 was the control experiment, denoted as CTRL. Experiments 2 (six-hourly updated LBC; denoted BDY_T2) and 3 (with domain sizes 205 × 208, denoted BDY_T2) were conducted as in the CTRL experiment, but with different domain sizes and frequency of LBC updates. In experiments 4 (HFX_%75) and 5 (HFX_%125), the sensible heat flux was reduced to 75 and 125%, respectively, of that in the CTRL experiment in the RUC land surface scheme to highlight the impact of the sensible heat flux on the deep CBL in the Taklimakan Desert. In experiment 6 (denoted Noah), the Noah land surface model (Chen; Dudhia 2001a, 2001b) replaced the RUC land surface model in the CTRL experiment to discriminate the influence of different land surface models on the deep CBL.

2.2 Data

The model simulations are compared with the Tazhong field experiment carried out throughout the month of July 2016 by the Institute of Desert Meteorology, Chinese Meteorological Administration, Urumqi. The main station was located at (86.63° E, 39.03° N). The location is relatively flat with few hills and is covered by sand combined with grass (Figure 1. c). The deep PBL in our simulation was under a cloudless sky in a dry environment.

The surface fluxes were measured by an eddy correlation system using an R3-50 supersonic anemometer developed by Gill (UK) deployed at a height of 10 m. The frequency of data acquisition was 20 Hz and the surface sensible heat flux was calculated by the eddy covariance method.

The vertical profiles were measured using soundings. Upper air soundings of the temperature, pressure, humidity, and wind speed and direction were conducted three to six times per day with the CASIC23 GPS sounding system developed by the No. 23 Institute of China Aerospace Science & Industry. The sounding times were 01:15, 07:15, 10:15, 13:15, 16:15 and 19:15.

2.3 Synoptic patterns

Figure 2 shows the synoptic patterns at 0800 BJT on 1 July 2016 at 850, 700, 500 and 100 hPa. There were cyclonic vortexes from 850 to 500 hPa centered at 55° N (Figure 2. a, b and c). The Taklimakan Desert was located east of the cyclonic vortex and embedded in an east–west elongated ridge at 0800 BJT on 1 July 2016. To the southwest, influenced by the South Asian High centered over the eastern Iranian Plateau, the upper air over the Taklimakan Desert was controlled by the westerly jet stream at 100 hPa (Figure 2. d). A low-pressure system at low levels, termed a heat low (Figure 3.), dominated most of southern Xinjiang and resulted in continuous high temperatures over the desert. This situation favored subsidence and served as a triggering mechanism for the deep PBL in the region in the subsequent two to three days (not shown).

3 Results

3.1 Validation of the deep CBL structure

The time series of the surface variables at Tazhong station from the CTRL simulation for 1 July 2016 are presented in Figure 4. a and b. The results show that there are large discrepancies in the thermodynamic surface variables (surface temperature and the sensible and latent heat fluxes) between the model and the observations. The surface sensible heat flux is far lower in the observations (maximum 243 W m^{-2}) than in the model (maximum 613 W m^{-2}), indicating that the sensible heat flux from the WRF simulation is 2.5 times than that of the observations when they are both at their maximum. By contrast, the model shows a significant cold bias for the surface temperature, which is much higher in the observations (maximum 70°C) than in the model (maximum 50°C). To further verify the surface variables, the root-mean-square error (RMSE) and mean bias (BIAS) are calculated including integration hours from 3 to 12 h for Tazhong station (Table 2). The model significantly overestimates the sensible heat flux (RMSE 263.636 W m^{-2}, BIAS:250.14 W m^{-2}) and dramatically underestimates the surface temperature (RMSE 14.65°C, BIAS −13.37°C).

There are two possible reasons for the model sensible heat flux being far greater than that of the observations. First, mismatches in land use between the model and the observations. The WRF models uses land use categories to assign static parameters and initial values to each grid cell (e.g. the albedo and surface roughness; Schicker et al. 2016). However, Figure 1. c shows that station EC is surrounded by a mixture of grass and sand. This complex underlying surface may not be adequately reproduced by the model and may have an impact on the overestimation of the sensible heat flux. Second, the sensible heat flux and the latent heat flux based on the eddy correlation method may be underestimated (LeMone et al. 2013). It has been shown that if the other two terms in the budget (the net radiation and flux into the soil) are accurate, then the data used for the whole experiment to find the sensible and latent heat fluxes for Tazhong station are, on average 75%, of the values required to balance the surface energy budget.

In contrast with the large differences in the surface variables between the model and the observations, the near-surface variables (the 2 m temperature, the relative humidity and the 10 m wind speed; Figure 4. e, f and g) in the model are higher than in the observations. The time series evolution of the 2 m temperatures follow those of the observations (RMSE 1.66, BIAS 1.61), but the model produces a surface warmer by about 3 K at the beginning of integration and 1 K when the model and observations both reach their maximum temperature.

The results indicate that the near-surface relative humidity in the model is close to the initial observations (Figure 4. f). However, the humidity in the model increases during the first few hours of model integration, while the observed humidity decreases. After three hours of spin-up, the model reproduces the evolution of humidity reasonably well, in agreement with the observations (RMSE 1.22), but the values are higher than the observed values (BIAS 1.11).

One reason for this discrepancy is the overestimation of the soil moisture content during the simulation. The soil moisture content can have a strong influence on the near-surface humidity. An overestimation of the soil moisture content in the initial condition of the model may result in a considerable difference in the humidity of the near-surface layer (Talbot et al. 2012). In our simulations, the model produces large overestimates of the soil moisture content. At initialization of the model in the CTRL simulation, the soil moisture content at 5 cm depth at station EC was 0.230 $m^3 m^{-3}$, whereas the initial value in the model was 0.6 $m^3 m^{-3}$ (Figure 4. d). This large overestimate of the soil moisture content results in a continuing increase in the latent heat in the model (Figure 4. b, f). As a result, the near-surface in the model is far moister than in the observations during the first few hours of model integration. The model simulation has the ability to correct some of the bias due to the initial conditions of the surface and the results from the CTRL experiment are closer to the observed values after three hours of spin-up.

Figure 5. (solid lines) compares the potential temperatures simulated by the model with the GPS sounding measurements (dash lines) at Tazhong from 0800 to 2000 BJT on 1 July 2016. The radiosonde was about 7 km away from Tazhong when it reached a height of 6 km. The profiles of the model simulations are therefore averaged at a radius of 3.5 km from the measurement station. When the model is initialized at 0800 BJT, the nocturnal inversion reaches 300 m (not shown). This inversion is eroded in the model by 1100 BJT, in agreement with the observations, and both the model results and the observations reach about 300 m at 1100 BJT (Figure 5. a). However, the simulated CBL grows faster in the morning than that in the observations due to a larger sensible heat flux, reaching 3500 m (3000 m in the observations) at 1400 BJT (Figure 5. b). The simulated and observed CBL heights exceed 4000 and 5000 m, respectively, at 1700 BJT (Figure 5. c). This indicates that the simulated CBL increases more slowly in the afternoon than the observed CBL. Compared with the measurements, the model is initially cooler, but with a faster heating rate in the morning. As a result, the model is warmer than the observations in the afternoon, but in agreement with the observations by the end of the day. This may be due to the differences in the potential temperature lapse rate above the top of the mixing layer between the observations and the simulated results. The stronger simulated inversion layer restricts the development of the CBL.

The model initially simulates a cooler and drier CBL at 1100 BJT on July 2016 than the observations (Figure 5. a). Compared with the observed potential temperature profile, the CBL appears earlier in model forecasts due to an obvious warming in the surface layer. The residual layer may play a key part in the deep PBL over the Taklimakan Desert. At 1100 BJT, when the CBLH (Convective Boundary Layer Height) in the observations was about 300 m, the potential temperature was about 317 K in the PBL and 320 K in the residual layer. When the potential temperature in the CBL increased to the value in the residual layer (320 K), the CBL merged with the residual layer and the height of the PBL in the observations reached 3000 m at 1400 BJT. These results are in good agreement with those of Han et al. (2012), who, by analyzing observations from a CBL in the Badanjilin region, found that the CBL developed rapidly after 1200 LST, possible as a result of the disappearance of the inversion layer.

When the sensible heat flux reached its maximum at 1400 BJT (Figure 5. b), the potential temperature profile was closer to the observations than at the initial time and their value was higher than the observed values. By 2000 BJT (Figure 5. d), the height of the CBL in the model reached its maximum value, consistent with the observations, despite being about 0.4 K cooler at lower levels (<2.5 km). One cause of the higher temperatures produced in the model may be the large difference in the surface heat fluxes and we concluded that the surface sensible heat flux from the land surface parameterization was the crucial factor affecting the CBL processes during the daytime in summer. Differences in the surface sensible heat flux create differences in the vertical development of the PBL. Thus the large difference in the surface sensible heat flux between the model and the observations may lead to differences in the growth of the CBL during the daytime and in its peak depth during the simulation. Fortunately, the surface sensible heat flux computed by the land surface model can artificially be modified to control the calculation of the surface fluxes. Sensitive simulations will be realized and discussed in next section.

Figure 5. also shows vertical profiles of the vapor mixing ratio (dashed lines) at Tazhong station. The simulated profiles with a lower residual layer are much drier than the observations from 1500 to 3500 m at 1100 BJT. Vertical mixing results in a uniform structure of the vapor mixing ratio within the CBL, so the differences between the profiles of the simulated results and the observations are remarkably reduced when the CBL is above 4000 m at 1400 BJT. The differences are generally <1 g kg^{-1} at 1100 BJT, reaching a maximum of 0.3 g kg^{-1} at 1400 BJT. However, the PBL shows an inverse layer at lower levels (≤2000 m) with a measured moisture content of 2.8–3.6 g kg^{-1}, which is not captured by the model. As the CBL grows, the inversion moisture structure below 3000 m develops and is maintained below 3000 m from 1400 to 2000 h BJT. By the end of the day, the simulated humidity of the CBL is higher than in the observations because the model cannot reproduce the inverse moisture layer within the CBL.

The inverse pattern in humidity may be caused by the interactions between the heterogeneous pattern of humidity and large-scale advection over the underlying surface. For instance, the interaction of an oasis with the desert environment may lead to an inverse humidity layer in the PBL above the desert. One possible reason for the discrepancy between the model results and the observations may be an error in the classification of land use type. The USGS land use data in the ARW-WRF model is based on Advanced Very High Resolution Radiometer 1 km resolution satellite data during the time period 1992–1993 and this land use data may no longer be accurate in the Taklimakan Desert. Misclassifications have also been found in the USGS land use data, which is the default land use dataset in the WRF model (Schicker et al. 2016). This is confirmed by the discrepancies in land use between the simulation and the observations at Tazhong station. The large-scale advection of dry air can affect the moisture profile. The moisture content is also variable in the horizontal direction, so advection at low levels may contribute to the drier conditions in the lower PBL and more moist conditions in the upper PBL between 1100 and 2000 BJT.

The mismatch between the model results and the observations in terms of moisture content suggest that the effects of land use type and large-scale advection need to be quantified and that more detailed data may be required for the Taklimakan Desert (both land and atmosphere) to realize more realistic results. Extra care should also be taken with the sparse and limited data at the periphery of the Taklimakan Desert (ter Maat et al. 2012).

3.2 Sensitivity to the lateral boundary conditions

After verifying the details of the LES experiments, we assessed the sensitivity of the simulations to the time resolution and domain size of the specified LBCs. For a one-way nest, the specified LBCs are obtained from coarser simulations. The analysis and forecast times from a previously run larger area simulation are used to specify the LBC. The primary cause of the differences in the structure of the PBL was diagnosed as the difference in the domain sizes and frequency provided by the coarser resolution. The aim was to assess the sensitivity of the finer LESs to uncertainties of the specified LBC forcing by model simulations with a larger area.

Figure 5. compares the profiles of the simulated potential temperature and vapor

mixing ratio profiles from the LBC sensitivity experiments and observations. The results show that there is a distinct relationship between the development of the LBCs and the CBL. The profiles produced by the model are almost all the same at the initial time (not shown). However, the results show that there are large discrepancies in the CBL structure among the different experiments. The results indicate that a larger domain size and higher time frequency for the LBCs leads to a warmer and drier PBL, but a cooler and moister free troposphere. This sensitivity is monotonic with respect to the LBCs (Figure 5.). Over the next three hours, the differences between the sensitivity experiments increase over time (Figure 5. a, b). The potential temperature profiles within the CBL diverge at 1100 BJT. However, the results show a greater convergence in the afternoon as the CBL continues to grow (Figure 5. c) but the largest discrepancies are found at end of the day (Figure 5. d) when the model CBL potential temperature is warmer than the observations by up to 0.7 and 0.9 K in BDY_T2 and BDY_T1, respectively.

Figure 6. shows cross-sections of the horizontal winds along 39.03° N, superposed with theta and the vapor mixing ratio. Less frequent updates of the LBCs are desirable in the cold zone near the LBCs, which results in cold advection of the temperature and moisture to the area of interest (Figure 6. b, c). A larger domain size, which changes the distance of the area of interest from the LBC, is efficient in reducing the influence of large forecast errors near the LBCs on the area of interest (CMP, Figure 6. a, c).

To further examine the impact of the LBCs on the turbulence in the deep Taklimakan Desert CBL, the instantaneous vertical velocity fields are shown in Figure 7. By 1400 BJT, the convection of the CTRL simulation had clearly intensified under strong surface heating

(Xu et al. 2018). Thus the maximum vertical velocity reached 9 m s^{-1} and the depth of the mixed layer grew to about 4.3 km (Figure 7 a). The distances between the boundary layer rolls correspondingly increased to about 12 km and the height of the peak up-draft was raised to just under 4 km. The cellular shape of the up- and down-drafts characteristic of the boundary layer rolls is clear in the horizontal view showing the strength of convection. The BDY_T2 and BDY_T3 experiments (Figure 7b, c) both reproduce motions with much weaker maximum and minimum values at the boundary of the domain. In BDY_T3, Tazhong station at the center of the model is directly influenced by the inflow of cold advection produced by the low-frequency LBCs, resulting in much weaker maximum and minimum values of *w* (about 6 m s^{-1}). However, despite the underestimation of the potential temperature, the *w* fields in the BDY_T2 experiment are similar to those in the CTRL experiment in plan view and the horizontal extent of the up-/down-drafts agrees with the CTRL experiment.

To further examine the vertical structure of the desert CBL, Figure 8 presents vertical cross-sections of *w* along Tazhong station (39° N). Wide and regularly spaced up-drafts along A1–A2 split into stronger and more irregular motions in the CTRL and BDY_T2 experiments. The up-drafts are much weaker in experiment BDY_T3 (Figure 8. c). The peak up-drafts in BDY_T3 are about 4 m s^{-1}, much weaker than in the CTRL (9 m s^{-1}) and BDY_T2 (8 m s^{-1}) experiments. The inflow boundary is wider in BDY_T2 and BDY_T3 and the intensity of the convection is weaker at the boundary. The horizontal distribution of the vertical velocity at Tazhong station in BDY_T3 is much weaker than in BDY_T2. The results suggest that the model results are sensitive to changes in the time resolution and domain size of the specified LBCs. The mismatch among sensitive experiments means that the effect of the LBCs needs to be quantified to realize a more realistic performance in sub-kilometer-scale simulations.

3.3 Simulations with different surface sensible heat fluxes and land surface models

An important cause of the differences in the structure of the PBL was determined to be the differences in sensible heat flux predicted by the land surface schemes. The sensible heat flux is a key factor affecting the height of the CBL during daytime in summer. The difference between the models and observations may therefore lead to differences in the growth of the PBL during the day. To further confirm whether this occurs, three additional sensitive simulations were realized based on the CTRL experiment. The Noah land surface model replaced the RUC land surface model in the CTRL experiment and the sensible heat fluxes for HFX-125% and HFX-75% are %125 and %75 that of the CTRL (HFX -100%) experiment while the other parameters remain the same.

The results in Figure 10. and Table 2 show that HFX-75% successively improved the simulation of the sensible heat flux with an RMSE of 151.12 compared with 263.64 and 357.11 in the CTRL and HFX-125% experiments, respectively. The Noah land surface experiment yielded the best performance in terms of the sensible heat flux, the surface temperature and the air temperature. However, the Noah land surface model showed large discrepancies with the observations in terms of the soil moisture content, resulting in a dramatic overestimate of the latent heat flux and relative humidity compared with the CTRL experiment.

A further examination of the potential temperature and vapor mixing ratio (Figure 9.) indicates that a smaller sensible heat flux leads to a cooler, more moist lower PBL and a warmer, drier free atmosphere. This sensitivity is monotonic with respect to the sensible heat flux. The structure of the CBL from the HFX-75% and Noah experiments matches the GPS radiosonde measurements better than the CTRL (HFX-100%) simulations. The potential temperature profiles from the CTRL (HFX-100%) and HFX-125% experiments are consistently warmer than the observations by about 0.4 and 0.5 K, respectively, whereas the results from the HFX-75% and Noah experiments are within about 0.2 K at 1400 BJT (Figure 9. b). These results suggest that the model is sensitive to changes in the sensible heat flux from the land surface model. The simulations converge at the end of the day, although there are still differences at 2000 BJT (Figure 9. d). The HFX-75% and Noah experiments with a weaker surface sensible heat flux still produce almost the same deep CBL as the CTRL and HFX-125% experiments. This indicates that the sensible heat flux may not the dominant factor in the formation of the deep CBL over the Taklimakan Desert.

The results of the simulations of the desert PBL in the morning agree with previous studies of the sensitivities the land surface model in other areas (Hu et al. 2010; Zhang et al. 2017). However, all the experiments produce nearly the same height of the CBL and moisture content from 1700 to 2000 BJT on 1 July 2016 (Figure 9. b, d), in agreement with the observations in the PBL. The effects of the sensible heat flux on the evolution of the PBL structures in the Taklimakan Desert during this period need to be examined further to determine why the simulations are insensitive to land surface processes at the end of the day. As reported by Stull (1988), the development of the CBL is mainly influenced by the effects of thermodynamic and turbulent entrainment if we do not consider factors such as large-scale advection or subsidence. In addition to the surface sensible heat, the intensity of the entrainment process determines the increase in the CBL. Thus the entrainment rate w_e is a valuable indicator of the development of the structure of the PBL. The rate of growth of the CBL is mainly determined by the entrainment rate w_e at the inversion layer without considering large-scale vertical motion. w_e usually has a positive correlation with the amount of heat flux at the inversion layer $\overline{(w'\theta_v')_h}$ and LES experiments show that $\overline{(w'\theta_v')_h}$ is about 0.2 times the surface flux of the buoyancy $\overline{(w'\theta_0')}$. During the period from 1100 to 1400 BJT, a larger sensible heat flux is clearly correlated with stronger turbulent entrainment and warmer air from the free atmosphere entraining into the Mixing Layer (ML) . As a result, the CBL develops rapidly and warms too quickly in the early simulation phase due to the clear increase in temperature and strong vertical mixing in the model. The reduction in the sensible heat flux reproduces the evolution of the desert PBL better in the early simulation phase because the HFX-75% and Noah simulations produce the smallest simulation errors in both temperature and moisture. However, the height of the CBL and the potential temperature for HFX-75% and Noah reach >5000 m and 323.2 K, respectively, at 1700 BJT (Figure 9. a). For the rest of the day, the rate of increase in the height of the CBL slows due to the deep CBL (>5000 m), which requires more heat for the increase in the depth of the PBL. w_e decreases with increasing intensity of the inversion, which inhibits the mixing and entrainment processes. These two factors limit the growth of the CBL when the height is >5000 m in this deep desert event. Therefore increasing the sensible heat flux from 75 to 125% significantly reduced the total time required for the increase in the CBL to a relatively low altitude (<5000 m) at the middle and preliminary stages of the development of the CBL, rather than produces a higher CBL at a later stage. When the height of the CBL over the

Taklimakan Desert exceeds 5000 m, it may not change in proportion to the sensible heat flux (Figure 9. d). As a result, the PBL is basically the same in the WRF simulations and is not sensitive to the sensible heat flux at the end of the day.

4 Summary

In this paper, we assessed the performance of the WRF model LES in an example of a deep convective PBL over the Taklimakan Desert. The tests were performed with multiple configurations and sensitivity experiments. The sensitivity tests for the LBCs showed that the model results are sensitive to changes in the size of the time resolution and domain of the specified LBC. A larger domain size changes the distance of the area of interest from the LBC and is efficient in reducing the influence of the large forecast error near the LBC.

The model reproduces the evolution of PBL processes reasonably well with the configuration used in this study. The model shows discrepancies between the main CBL characteristics in the morning, including the thermal and moisture structures. The model simulates the relatively colder and drier morning CBL, underestimating the temperature in the near-surface layer at Tazhong station by up to 1.5 K and the moisture content by 1 g kg^{-1}. The overestimation of the CBL profile may be caused by initial discrepancies between the model and the observations. This indicates that the results are sensitive to the initial conditions of the model, although the simulation seems to be able to correct some of the bias due to the initial conditions. The model correctly reproduces the thermal structure in the afternoon, but the simulations are relatively warmer and moister than the observations. The potential temperature profile at the CBL appears warmer than the observations by about 0.4 K. The model seriously overestimates the moisture content in the afternoon and overestimates the vapor mixing ratio in the CBL by about 1–2 g kg^{-1}. The largest discrepancies are found in 0–3 km layer, where the model vapor mixing ratio is twice as moist as that of the observations (up to about 3 g kg^{-1}).

Three additional simulations were realized to confirm whether the large differences in the sensible heat flux lead to differences in growth of the CBL during the daytime relative to the CTRL experiment. The results suggest that the model results are sensitive to changes in the sensible heat flux and different land surface models. The large difference between the model and observations may lead to differences in the growth of the CBL during the daytime. It was concluded the surface sensible heat flux is an important factor affecting the processes of the CBL over the Taklimakan Desert during the daytime in summer. However, its peak depth during the simulation was less sensitive to the sensible heat flux because w_e had decreased by the end of the day. One should note that the CBL of Taklimakan need several days of favorable environment to reach its super depth (> 4000m), and sustained high temperature and SH is the crucial factor for CBL to develop from shallow to deep CBL. The SH is not dominant factor, but still an important factor affecting the deep CBL.

Future work will study several other examples of a deep CBL over the Taklimakan Desert to determine their common features. We hope to use high-resolution models and observations to describe the fine characteristics of a typical deep CBL over the Taklimakan Desert, particularly the turbulent and vertical mixing and its impact on the regional weather forecast. This research aims to improve our understanding of the deep CBL over the Taklimakan Desert and its influence on the regional weather and climate.

Conflict of interests

The authors declare that there is no conflict of interests regarding the publication of this paper.

Acknowledgments

This study is supported by the National Natural Science Foundation of China (Grant no. 41575008 and 41775030). The author thanks the reviewers and editors for their professional advice in improving this paper.

Captions:

Figure 1. Simulation domains used in the ARW model with (a) the terrain height (shaded, units:m), (b) the land use categories for domains D03 and D04 and (c) photograph of the area around Tazhong station.

Figure 2. Horizontal distribution of the geopotential height (solid lines, units: da gpm), wind speed (shaded, units: knots) and wind barbs from the NCEP FNL analysis at 0800 BJT on 1 July 2016 at (a) 850, (b) 700, (c) 500 and (d) 100 hPa.Figure 2. Horizontal distribution of the geopotential height (solid lines, units: da gpm), wind speed (shaded, units: knots) and wind barbs from the NCEP FNL analysis at 0800 BJT on 1 July 2016 at (a) 850, (b) 700, (c) 500 and (d) 100 hPa.

Figure 3. NCEP FNL 700 hPa potential temperature (colors) and mean sea level pressure (white lines) at 0800 BJT on 1 July 2016. The black dot shows the location of Tazhong station in Xingjiang province.

Figure 4. Time series of the initial simulated surface variables from the innermost domain of the simulations and the surface observations at Tazhong station (83.63° E, 39.03° N) at 0800 BJT on 1 July 2016: (a) sensible heat flux; (b) latent heat flux; (c) surface temperature; (d) soil moisture content; (e) temperature at 2 m; (f) relative humidity at 2 m; (g) wind speed at 10 m; and (h) wind direction at 10 m.

Figure 5. Vertical profiles of the potential temperature (solid line, units: K) and vapor mixing ratio (dashed line, units: g kg^{-1}) from the innermost domain of the simulations and the observations from GPS sounding at Tazhong station (83.63° E, 39.03° N) at (a) 1100, (b)

1400, (c) 1700 and (d) 2000 BJT on 1 July 2016. The profiles of the model output are averaged over a radius of 3.5 km.

Figure 6. Cross-sections along 39.03° N of the horizontal winds (barbs, units: m s^{-1}) at intervals of 5 m s^{-1} superposed with theta (shaded, units: K) and the vapor mixing ratio (contours, units: g kg^{-1}) from the (a) BDY_T1, (c) BDY_T2 and (e) BDY_T3 experiments at 1400 BJT on 1 July 2016 and the (b) BDY_T1, (d) BDY_T2 and (f) BDY_T3 experiments at 2000 BJT on 1 July 2016.

Figure 7. Instantaneous vertical velocity fields (shading: m s^{-1}) at 3000 m for the (a) BDY_T1 (CTRL), (b) BDY_T2, (c) BDY_T3 and (d) Noah experiments at 1400 BJT on 1 July 2016.

Figure 8. Vertical cross-sections of the instantaneous vertical velocity fields (shading: m s^{-1}) along A1–A2 in for the (a) BDY_T1 (CTRL), (b) BDY_T2, (c) BDY_T3 and (d) Noah experiments at 1400 BJT on 1 July 2016.

Figure 9. Vertical profiles of the potential temperature (solid line, units: K) and vapor mixing ratio (dashed line, units: g kg^{-1}) for the sensible heat flux sensitivity and Noah land surface experiments at (a) 1100, (b) 1400, (c) 1700 and (d) 2000 BJT on 1 July 2016. The profiles of the model output are averaged over a radius of 3.5 km.

Figure 10. Time series of the initial simulated surface variables for the sensible heat flux sensitivity and Noah land surface experiments: (a) sensible heat flux; (b) latent heat flux; (c) surface temperature; (d) soil moisture content; (e) temperature at 2 m; (f) relative humidity at 2 m; (g) wind speed at 10 m; and (h) wind direction at 10 m.

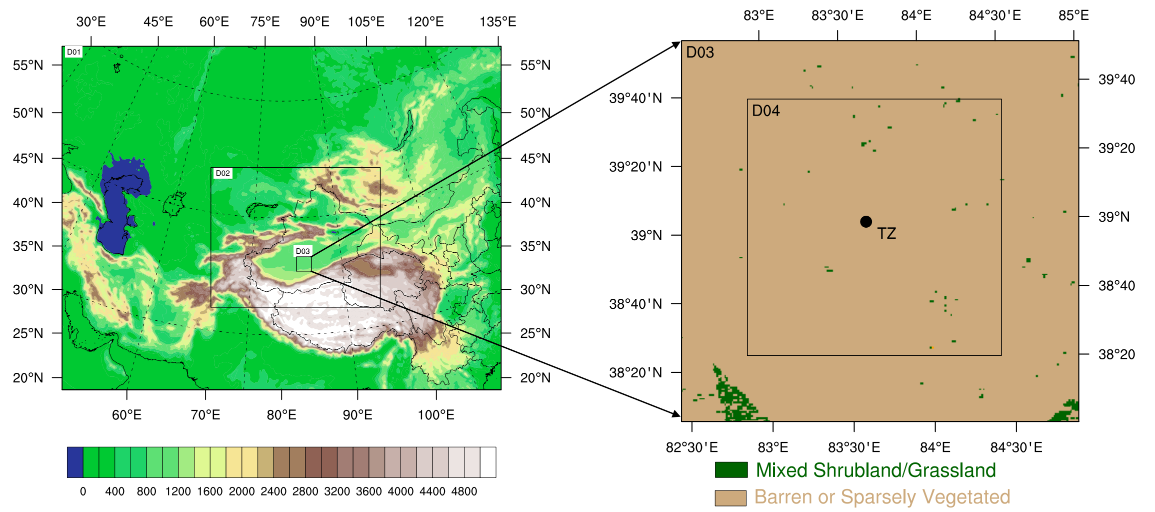

（a） （b）

（c）

Figure 1. Simulation domains used in the ARW model with (a) the terrain height (shaded, units:m), (b) the land use categories for domains D03 and D04 and (c) photograph of the area around Tazhong station.

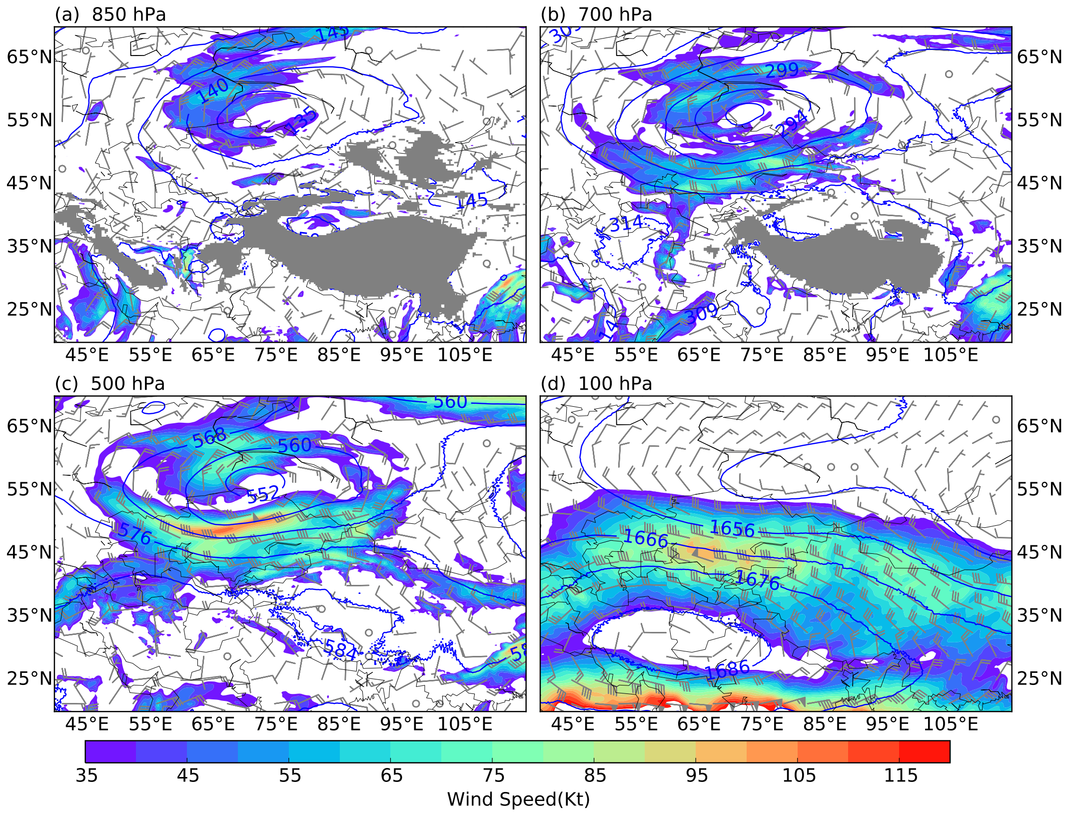

Figure 2. Horizontal distribution of the geopotential height (solid lines, units: da gpm), wind speed (shaded, units: knots) and wind barbs from the NCEP FNL analysis at 0800 BJT on 1 July 2016 at (a) 850, (b) 700, (c) 500 and (d) 100 hPa.

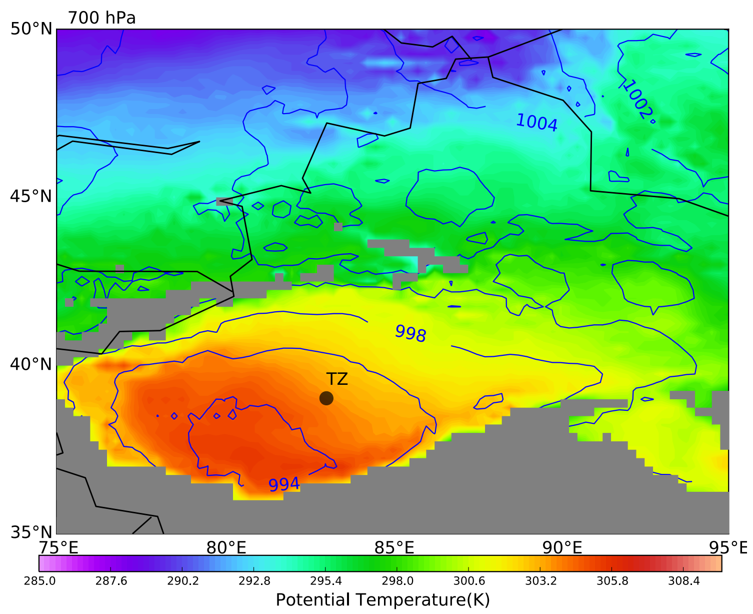

Figure 3. NCEP FNL 700 hPa potential temperature (colors) and mean sea level pressure (white lines) at 0800 BJT on 1 July 2016. The black dot shows the location of Tazhong station in Xingjiang province.

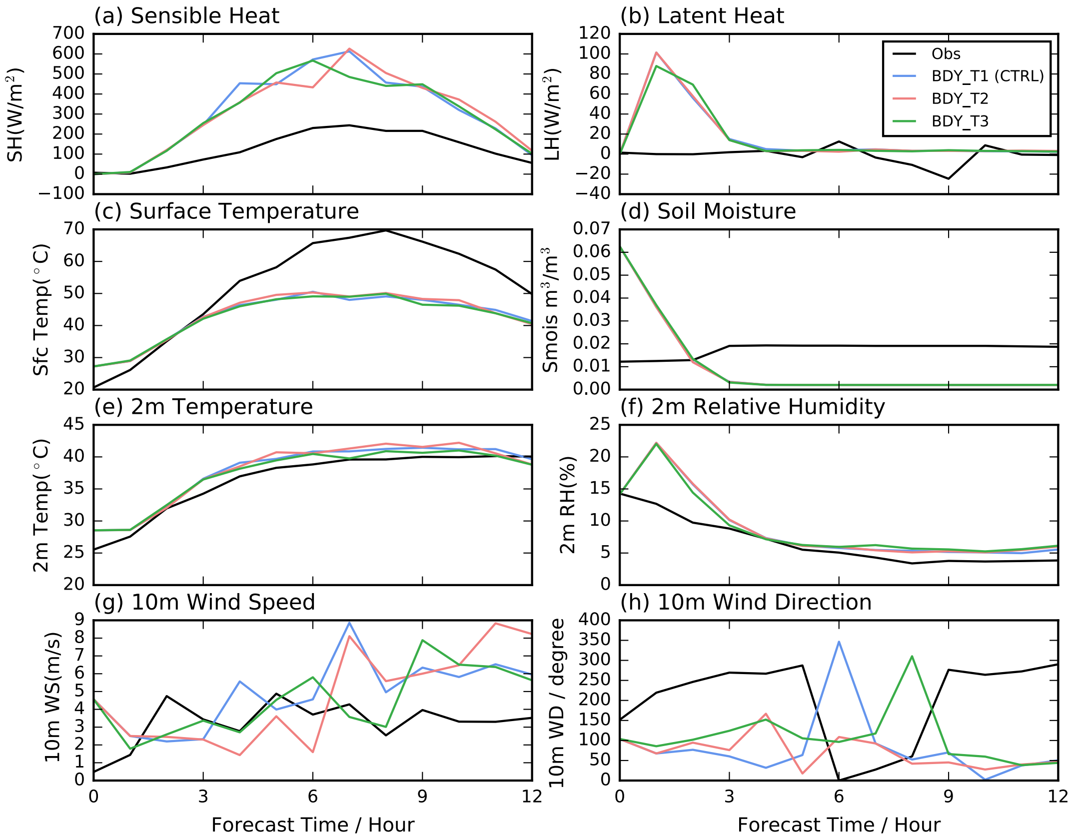

Figure 4. Time series of the initial simulated surface variables from the innermost domain of the simulations and the surface observations at Tazhong station (83.63° E, 39.03° N) at 0800 BJT on 1 July 2016: (a) sensible heat flux; (b) latent heat flux; (c) surface temperature; (d) soil moisture content; (e) temperature at 2 m; (f) relative humidity at 2 m; (g) wind speed at 10 m; and (h) wind direction at 10 m.

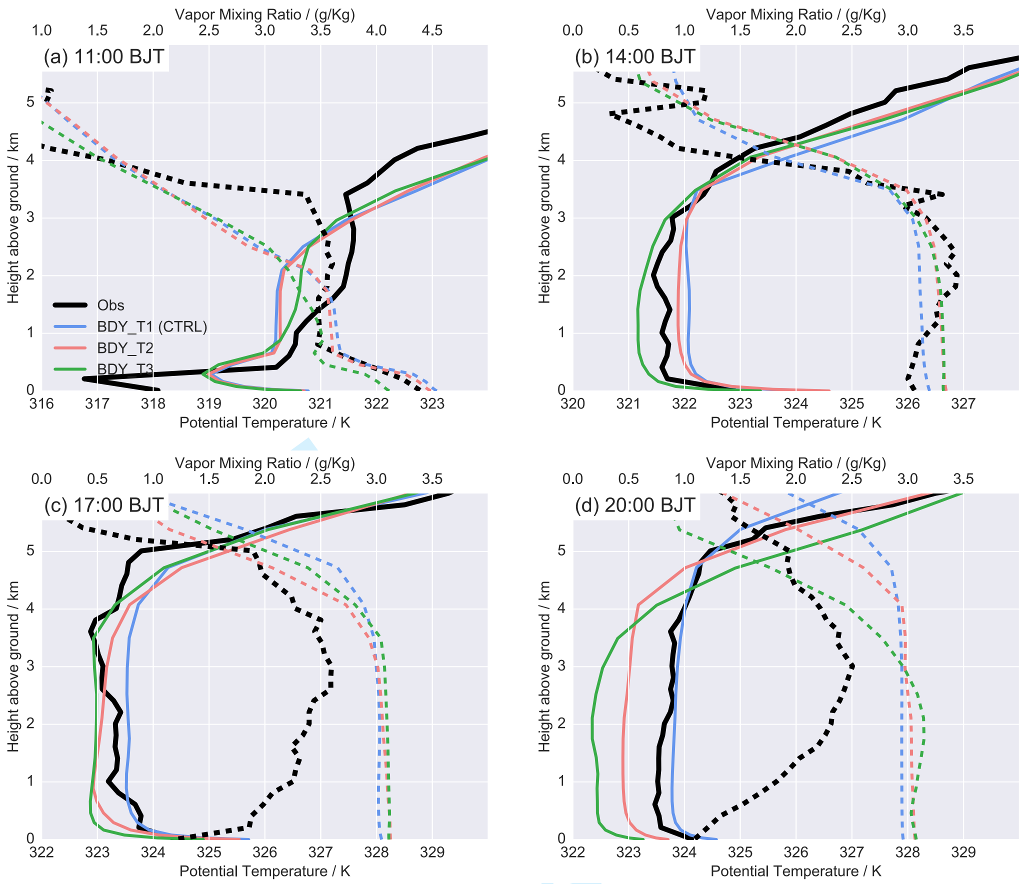

Figure 5. Vertical profiles of the potential temperature (solid line, units: K) and vapor mixing ratio (dashed line, units: g kg^{-1}) from the innermost domain of the simulations and the observations from GPS sounding at Tazhong station (83.63° E, 39.03° N) at (a) 1100, (b) 1400, (c) 1700 and (d) 2000 BJT on 1 July 2016. The profiles of the model output are averaged over a radius of 3.5 km.

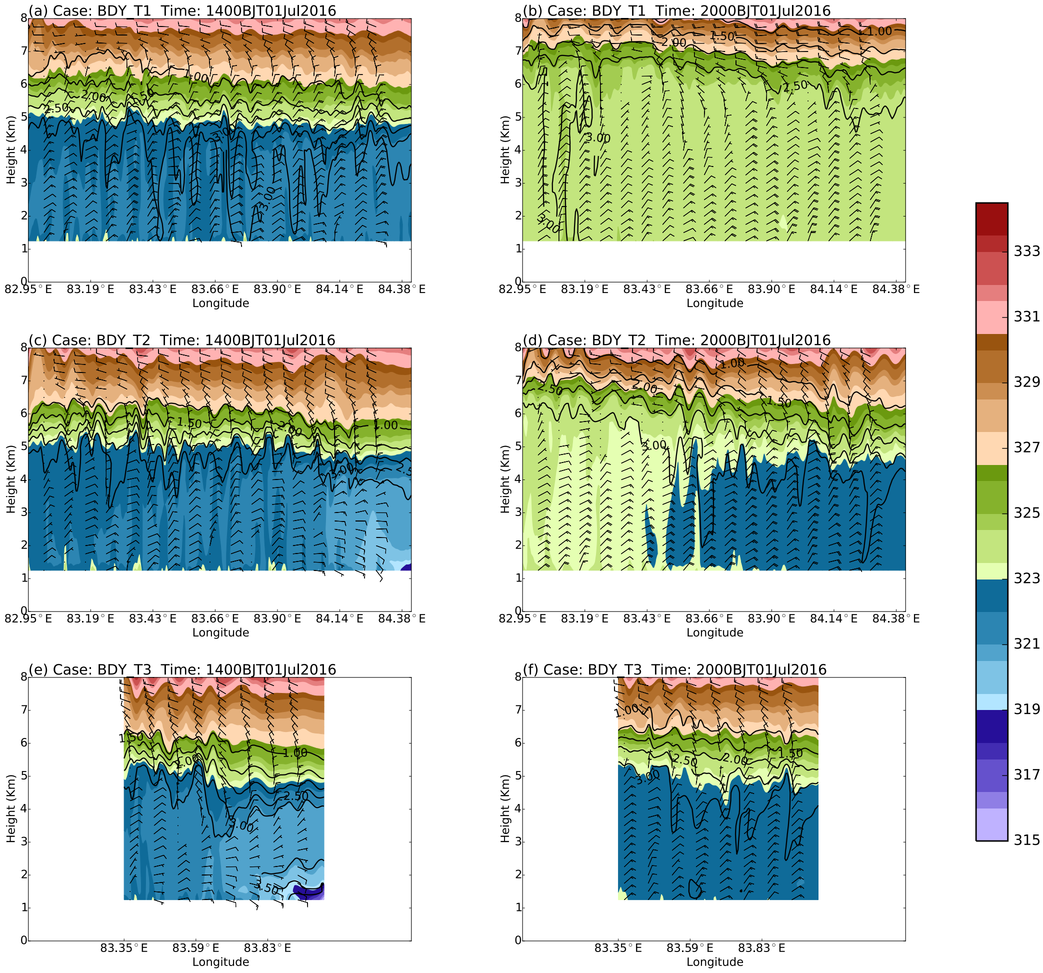

Figure 6. Cross-sections along 39.03° N of the horizontal winds (barbs, units: m s^{-1}) at intervals of 5 m s^{-1} superposed with theta (shaded, units: K) and the vapor mixing ratio (contours, units: g kg^{-1}) from the (a) BDY_T1, (c) BDY_T2 and (e) BDY_T3 experiments at 1400 BJT on 1 July 2016 and the (b) BDY_T1, (d) BDY_T2 and (f) BDY_T3 experiments at 2000 BJT on 1 July 2016.

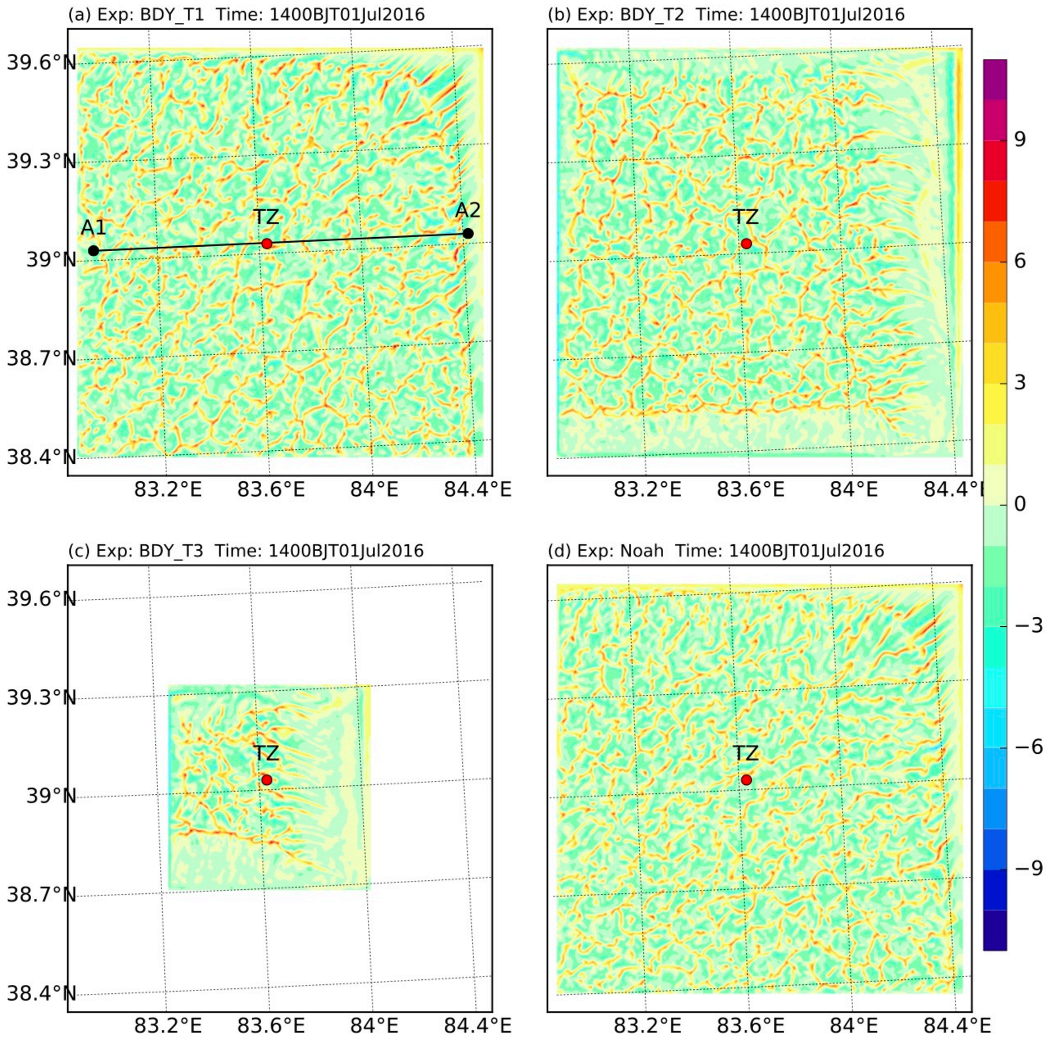

Figure 7. Instantaneous vertical velocity fields (shading: m s^{-1}) at 3000 m for the (a) BDY_T1 (CTRL), (b) BDY_T2, (c) BDY_T3 and (d) Noah experiments at 1400 BJT on 1 July 2016.

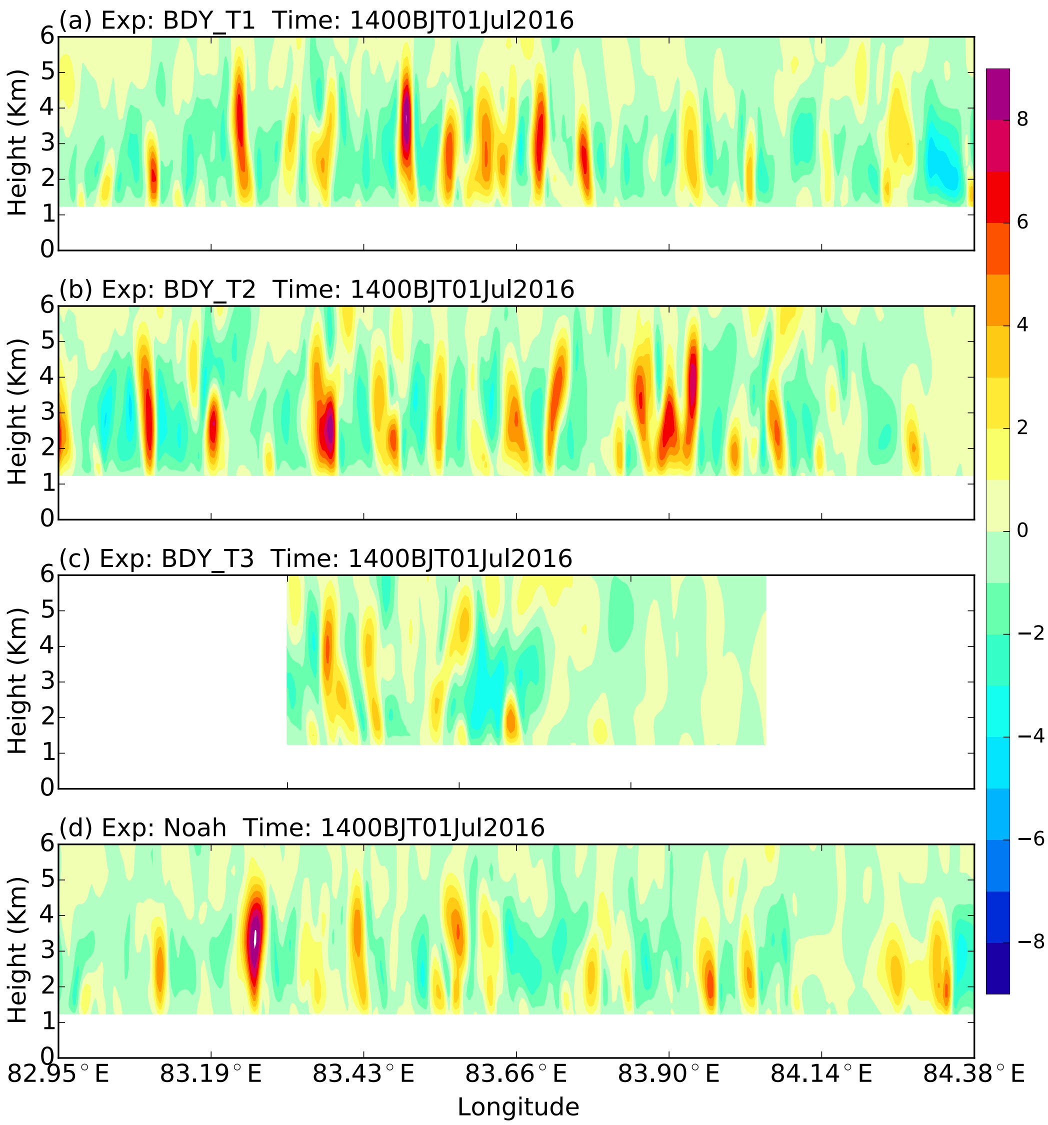

Figure 8. Vertical cross-sections of the instantaneous vertical velocity fields (shading: m s^{-1}) along A1–A2 in for the (a) BDY_T1 (CTRL), (b) BDY_T2, (c) BDY_T3 and (d) Noah experiments at 1400 BJT on 1 July 2016.

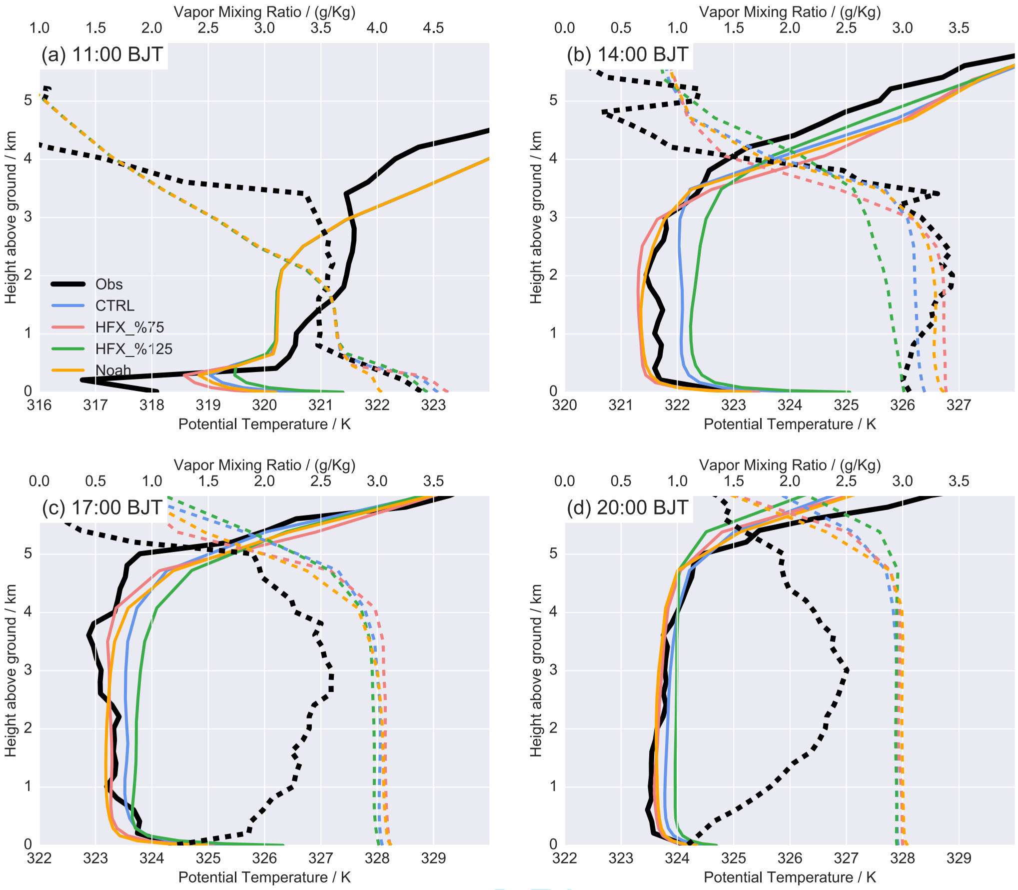

Figure 9. Vertical profiles of the potential temperature (solid line, units: K) and vapor mixing ratio (dashed line, units: g kg^{-1}) for the sensible heat flux sensitivity and Noah land surface experiments at (a) 1100, (b) 1400, (c) 1700 and (d) 2000 BJT on 1 July 2016. The profiles of the model output are averaged over a radius of 3.5 km.

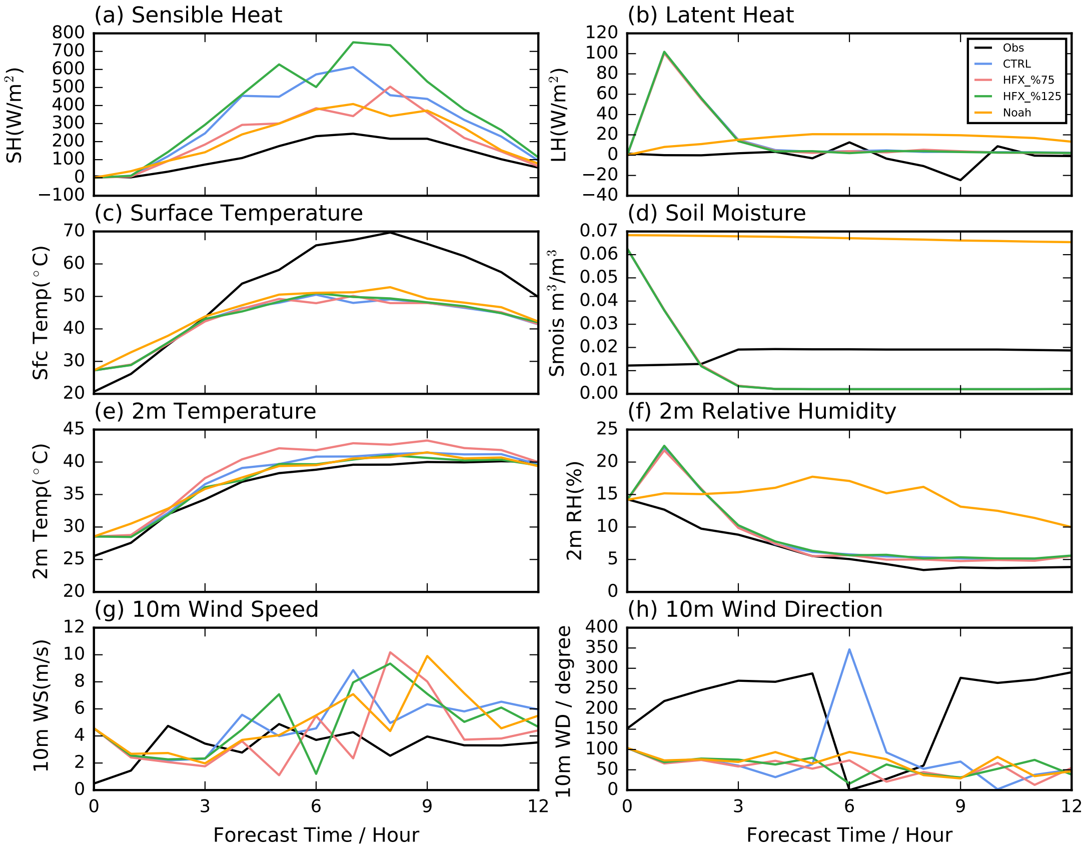

Figure 10. Time series of the initial simulated surface variables for the sensible heat flux sensitivity and Noah land surface experiments: (a) sensible heat flux; (b) latent heat flux; (c) surface temperature; (d) soil moisture content; (e) temperature at 2 m; (f) relative humidity at 2 m; (g) wind speed at 10 m; and (h) wind direction at 10 m.

Experiment	Name	Remarks
1	BDY_T1(CTRL)	LBC of D04 is provided by d03 every one hour with 403 × 406 model grids
2	BDY_T2	As BDY_T1, but LBC of D04 is provided by d03 every six hours
3	BDY_T3	As BDY_T2, but with 205 ×208 model grids
4	HFX_%75	As CTRL_T2, but with a sensible heat flux of 75%
5	HFX_%125	As CTRL_T2, but with a sensible heat flux of 125%
6	Noah	As CTRL_T2, but with the Noah land surface model

Table 1. List of designed experiments.

Experiments	Sensible heat flux		Latent heat flux		Surface temperature		Soil moisture content		Temperature at 2 m		Relative humidity at 2 m		Wind speed at 2 m	
	RMSE	BIAS	RMSE	BIAS	RMSE	BIAS	RMSE	BIAS	RMSE	BIAS	RMSE	BIAS	RMSE	BIAS
CTRL	263.636	250.140	12.398	6.674	14.654	−13.373	0.017	−0.017	1.666	1.613	1.220	1.109	2.579	1.864
BDY_T2	249.395	240.660	12.383	6.253	14.116	−12.853	0.017	−0.017	1.912	1.817	1.275	1.162	2.943	1.307
BDY_T3	241.681	232.705	12.251	6.328	14.929	−13.737	0.017	−0.017	1.227	1.046	1.483	1.280	2.118	1.287
HFX_%75	151.119	134.594	12.544	6.354	14.740	−13.426	0.017	−0.017	3.078	3.016	0.956	0.826	3.335	0.874
HFX_%125	357.711	335.556	12.439	6.152	14.244	−13.043	0.017	−0.017	1.026	0.860	1.303	1.231	3.265	2.052
Noah	125.695	120.313	23.350	20.664	12.757	−11.502	0.048	0.048	1.046	0.983	10.116	9.904	2.788	1.795

Table 2. Summary of the verification of surface and air variables including the integration hours from 3 to 12 h for Tazhong station.

Reference:

Chen, F., and J. Dudhia, 2001a: Coupling an Advanced Land Surface–Hydrology Model with the Penn State–NCAR MM5 Modeling System. Part II: Preliminary Model Validation. *Monthly Weather Review*, **129,** 587-604.

——, 2001b: Coupling an advanced land surface-hydrology model with the Penn State-NCAR MM5 modeling system. Part I: Model implementation and sensitivity. *Monthly Weather Review*, **129,** 569-585.

Dudhia, J., 1989: Numerical study of convection observed during the winter monsoon experiment using a mesoscale two-dimensional model. *J. Atmos. Sci.*, **46,** 3077-3107.

Engelstaedter, S., R. Washington, C. Flamant, D. J. Parker, C. J. T. Allen, and M. C. Todd, 2015: The Saharan heat low and moisture transport pathways in the central Sahara—Multiaircraft observations and Africa-LAM evaluation. *Journal of Geophysical Research: Atmospheres*, **120,** 2015JD023123.

Garcia-Carreras, L., and Coauthors, 2015: The Turbulent Structure and Diurnal Growth of the Saharan Atmospheric Boundary Layer. *Journal of the Atmospheric Sciences*, **72,** 693-713.

Han, B., S. Lü, and Y. Ao, 2012: Development of the convective boundary layer capping with a thick neutral layer in Badanjilin: Observations and simulations. *Adv. Atmos. Sci.*, **29,** 177-192.

Heinold, B., P. Knippertz, and J. H. Marsham, 2013: Large Eddy Simulations of Nocturnal Low-Level Jets over Desert Regions and Implications for Dust Emission. *EGU General Assembly Conference*.

Heinold, B., P. Knippertz, and R. J. Beare, 2015: Idealized large-eddy simulations of nocturnal low-level jets over subtropical desert regions and implications for dust-generating winds. *Quarterly Journal of the Royal Meteorological Society*, **141,** 1740–1752.

Heinze, R., D. Mironov, and S. Raasch, 2015: Second-moment budgets in cloud topped boundary layers: A large-eddy simulation study. *Journal of Advances in Modeling Earth Systems*, **7,** 510-536.

Hong, S.-Y., and H.-L. Pan, 1996: Nonlocal boundary layer vertical diffusion in a medium-range forecast model. *Monthly weather review*, **124,** 2322-2339.

Hong, S.-Y., and J.-O. J. Lim, 2006: The WRF single-moment 6-class microphysics scheme (WSM6). *J. Korean Meteor. Soc*, **42,** 129-151.

Hu, X.-M., J. W. Nielsen-Gammon, and F. Zhang, 2010: Evaluation of Three Planetary Boundary Layer Schemes in the WRF Model. *Journal of Applied Meteorology and Climatology*, **49,** 1831-1844.

Kain, J. S., 1993: Convective parameterization for mesoscale models: The Kain-Fritsch scheme. *The representation of cumulus convection in numerical models, Meteor. Monogr*, **46,** 165-170.

Kain, J. S., 2004: The Kain–Fritsch Convective Parameterization: An Update. *JOURNAL OF APPLIED METEOROLOGY*, **43,** 170-181.

LeMone, M. A., M. Tewari, F. Chen, and J. Dudhia, 2013: Objectively Determined Fair-Weather CBL Depths in the ARW-WRF Model and Their Comparison to CASES-97 Observations. *Monthly Weather Review*, **141,** 30-54.

Liu, Y., Q. He, H. Zhang, and A. Mamtimin, 2012: Improving the CoLM in Taklimakan Desert hinterland with accurate key parameters and an appropriate parameterization scheme. *Adv. Atmos. Sci.*, **29,** 381-390.

Liu, Y., and Coauthors, 2011: Simultaneous nested modeling from the synoptic scale to the LES scale for wind energy applications. *Journal of Wind Engineering and Industrial Aerodynamics*, **99,** 308-319.

Marsham, J. H., P. Knippertz, N. Dixon, D. J. Parker, and G. M. S. Lister, 2011: The importance of the representation of deep convection for modeled dust- generating winds over West Africa during summer. *Geophysical Research Letters*, **38**.

Mlawer, E. J., S. J. Taubman, P. D. Brown, M. J. Iacono, and S. A. Clough, 1997: Radiative transfer for inhomogeneous atmospheres: RRTM, a validated correlated-k model for the longwave. *J. Geophys. Res.*, **102,** 16663-16682.

Moeng, C.-H., J. Dudhia, J. Klemp, and P. Sullivan, 2007: Examining Two-Way Grid Nesting for Large Eddy Simulation of the PBL Using the WRF Model. *Monthly Weather Review*, **135,** 2295-2311.

National Centers for Environmental Prediction, N. W. S. N. U. S. D. o. C., 2015: NCEP GDAS/FNL 0.25 Degree Global Tropospheric Analyses and Forecast Grids. Research Data Archive at the National Center for Atmospheric Research, Computational and Information Systems Laboratory.

Rai, R. K., L. K. Berg, B. Kosović, J. D. Mirocha, M. S. Pekour, and W. J. Shaw, 2017: Comparison of Measured and Numerically Simulated Turbulence Statistics in a Convective Boundary Layer Over Complex Terrain. *Boundary-Layer Meteorology*, **163,** 69-89.

Schicker, I., D. Arnold Arias, and P. Seibert, 2016: Influences of updated land-use datasets on WRF simulations for two Austrian regions. *Meteorology and Atmospheric Physics*, **128,** 279-301.

Shin, H. H., and S. Y. Hong, 2011: Intercomparison of Planetary Boundary-Layer Parametrizations in the WRF Model for a Single Day from CASES-99. *Boundary-Layer Meteorology*, **139,** 261-281.

Shin, H. H., and S.-Y. Hong, 2015: Representation of the Subgrid-Scale Turbulent Transport in Convective Boundary Layers at Gray-Zone Resolutions. *Monthly Weather Review*, **143,** 250-271.

Skamarock, W. C., and Coauthors, 2008: A Description of the Advanced Research WRF Version 3. . *NCAR/TN–475+STR, NCAR TECHNICAL NOTE*.

Smirnova Tatiana, G., M. Brown John, G. Benjamin Stanley, and D. Kim, 2000: Parameterization of cold- season processes in the MAPS land- surface scheme. *Journal of Geophysical Research: Atmospheres*, **105,** 4077-4086.

Smirnova, T. G., J. M. Brown, and S. G. Benjamin, 1997: Performance of Different Soil Model Configurations in Simulating Ground Surface Temperature and Surface Fluxes. *Monthly Weather Review*, **125,** 1870-1884.

Stull, R. B., 1988: An Introduction to Boundary Layer Meteorology. *Atmospheric Sciences Library*, **8,** 89.

Sun, J., and Q. Xu, 2009: Parameterization of Sheared Convective Entrainment in the First-Order Jump Model: Evaluation Through Large-Eddy Simulation. *Boundary-Layer Meteorology*, **132,** 279-288.

Talbot, C., E. Bou-Zeid, and J. Smith, 2012: Nested Mesoscale Large-Eddy Simulations with WRF: Performance in Real Test Cases. *Journal of Hydrometeorology*, **13,** 1421-1441.

ter Maat, H. W., E. J. Moors, R. W. A. Hutjes, A. A. M. Holtslag, and A. J. Dolman, 2012: Exploring the Impact of Land Cover and Topography on Rainfall Maxima in the Netherlands. *Journal of Hydrometeorology*, **14,** 524-542.

WANG, and Coauthors, 2016a: Summer atmospheric boundary layer structure in the hinterland of Taklimakan Desert, China. *Journal of Arid Land*, **8,** 846-860.

Wang, M., X. Xu, and H. Xu: The possible influence of the summertime deep atmospheric boundary layer process over the Taklimakan Desert on the regional weather. *(submitted to Quarterly Journal of the Royal Meteorological Society)*.

Wang, M. Z., H. Lu, H. Ming, and J. Zhang, 2016b: Vertical structure of summer clear-sky atmospheric boundary layer over the hinterland and southern margin of Taklamakan Desert: The deep convective boundary layer of Taklamakan Desert. *Meteorological Applications*, **23,** 438-447.

Zhang, F., Z. Pu, and C. Wang, 2017: Effects of Boundary Layer Vertical Mixing on the Evolution of Hurricanes over Land. *Monthly Weather Review*, **145,** 2343-2361.

Reviewer(s)' Comments to Author:

Reviewer: 1

Comments to the Author

The content of the manuscript looks OK, but still needs focus on its main findings and contribution to the science. Moreover, it needs a lot of works/corrections for grammar and typos.

Thank you for the comments.

Main findings:

(1) SH may not be the dominant factor for the super deep CBL over the Taklimakan desert. As explained in lines 392~426, in addition to the surface sensible heat, the intensity of the entrainment process determines the increase in the CBL. The entrainment rate w_e is a valuable indicator of the development of the structure of the PBL. The rate of growth of the CBL is mainly determined by the entrainment rate w_e at the inversion layer without considering large-scale vertical motion. w_e usually has a positive correlation with the amount of heat flux at the inversion layer $\overline{(w'\theta_v')_h}$ and large LES experiments show that $\overline{(w'\theta_v')_h}$ is about 0.2 times the surface flux of the buoyancy $\overline{(w'\theta_0')}$. During the period from 1100 to 1400 BJT, a larger sensible heat flux is clearly correlated with stronger turbulent entrainment and warmer air from the free atmosphere entraining into the Mixing Layer. As a result, the CBL develops rapidly and warms too quickly in the early simulation phase due to the clear increase in temperature and strong vertical mixing in the model. The reduction in the sensible heat flux reproduces the evolution of the desert PBL better in the early simulation phase because the HFX-75% and Noah simulations produce the smallest simulation errors in both temperature and moisture. However, the height of the CBL and the potential temperature for HFX-75% and

Noah reach >5000 m and 323.2 K, respectively, at 1700 BJT. For the rest of the day, the rate of increase in the height of the CBL slows due to the deep CBL (>5000 m), which requires more heat for the increase in the depth of the PBL. w_e decreases with increasing intensity of the inversion, which inhibits the mixing and entrainment processes. These two factors limit the growth of the CBL when the height is >5000 m in this deep desert event. Therefore, increasing the sensible heat flux from 75 to 125% significantly reduced the total time required for the increase in the CBL to a relatively low altitude (<5000 m) at the middle and preliminary stages of the development of the CBL, rather than produces a higher CBL at a later stage.

(2) The SH is an important factor affecting the super deep CBL. Although SH is not dominant factor in this super deep CBL case, the CBL of Taklimakan need several days of favorable environment to reach its super depth (> 4000m), and Sustained high temperature and SH is the crucial factor for CBL to develop from shallow to deep CBL.

It needs a lot of works/corrections for grammar and typos.

We have used professional English language edit service (Lucid Paper) to correct grammar and typos in the manuscript.

Certificate

Editing for authors and publishers

Reference number: 2018-061601 **Date**: 21 June 2018

Contact author: Hongxiong XU

Manuscript: Performance of Weather Research and Forecasting Model Large Eddy Simulations in modeling the convective boundary layer over the Taklimakan Desert, China

This document certifies that the above-detailed manuscript was edited by a native English-speaking expert at LucidPapers on the date stated.

Following the editing process, the editor's overall assessment is that:

The manuscript will be ready for consideration by the target journal once the edits have been checked and approved/rejected as necessary.	
The manuscript may or will require modifications to the text in response to the editor's comments/queries, but further professional editing is unlikely to be needed.	
The manuscript requires modifications to the text in response to the editor's comments/queries, and further professional editing may be needed.	☑
The manuscript requires modifications to the text in response to the editor's comments/queries, and further professional editing is more than likely going to be needed.	
The manuscript requires modifications to the text in response to the editor's comments/queries, and further professional editing is strongly recommended.	

Signed:

C J Smith

Colin Smith
Chief Editor
LucidPapers

Reviewer: 2

Comments to the Author

Review comments on the revised version of "Characteristics over the Taklimakan Desert: A Real Test Case" (ACTA-E-2018-0001.R1)"

Many changes were made through the authors' efforts in the revised manuscript. However, the grammar errors continue to occur almost everywhere in this updated version. A heavy English edit work is required to improve the writing. It is strongly recommended to seek a professional language edit service.

Thank you for the comments.

We have used professional English language edit service (Lucid Paper) to edit and improve the English writing.

Certificate

Editing for authors and publishers

Reference number: 2018-061601	**Date**: 21 June 2018
Contact author: Hongxiong XU	**Manuscript:** Performance of Weather Research and Forecasting Model Large Eddy Simulations in modeling the convective boundary layer over the Taklimakan Desert, China

This document certifies that the above-detailed manuscript was edited by a native English-speaking expert at LucidPapers on the date stated.

Following the editing process, the editor's overall assessment is that:

The manuscript will be ready for consideration by the target journal once the edits have been checked and approved/rejected as necessary.	
The manuscript may or will require modifications to the text in response to the editor's comments/queries, but further professional editing is unlikely to be needed.	
The manuscript requires modifications to the text in response to the editor's comments/queries, and further professional editing may be needed.	☑
The manuscript requires modifications to the text in response to the editor's comments/queries, and further professional editing is more than likely going to be needed.	
The manuscript requires modifications to the text in response to the editor's comments/queries, and further professional editing is strongly recommended.	

Signed:

CJSmith

Colin Smith
Chief Editor
LucidPapers

As pointed out in the first turn review, it is not useful to present the impact of the ingest frequency of the lateral boundary conditions on the large-eddy simulation (LES) results if the WRF/LES has a capability of running the online-coupling mode.

Thank you for the comments.

Yes, it is not useful to test the frequency of the lateral boundary conditions especially in two-way nest mode (online-coupling). However, one of our aims is to assess the contribution of uncertainties in LBC to the typical behavior of super deep PBL processes. LBC frequency sensitive experiments are still kept, because these experiments can provide an explanation of the important role of LBC play in LES. As showed by the experiments, LBC may be more important than the physics schemes used in the model.

In addition, the simulated sensible and latent heat fluxes presented in Figures 4 and 10 are not accepted for publication without further improvement. As pointed by the authors, the observed sensible heat flux could be too low on July 1, 2016. What about the observational data for other days? Did the authors see the similar low observed sensible heat fluxes on other days since you have one-month data in July 2017?

Yes, we see the similar low observed sensible heat fluxes on other days in July 2017. Wang et.al., statics the PBL height of Tazhong during July 2016. The number of days when the PBL exceeds 4,000 m depth is 8, and that of higher than 3,000 m is 20. However, most of observed deep PBL cases show similar low observed sensible heat fluxes as on July 1, 2016 (Figure b3).

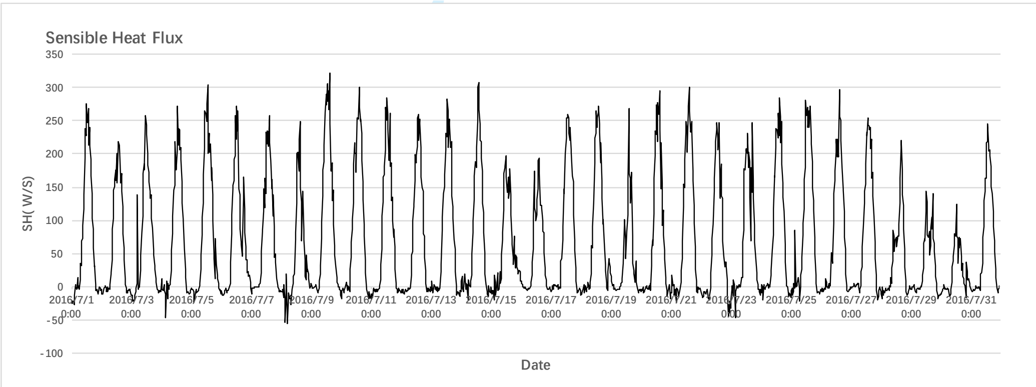

Over-predicted latent heat flux in the first several simulation hours should be alleviated by setting the initial soil moisture in the simulations as the observed value. Did the authors try that?

Thank you for the comments.

Yes, we have tried to set the initial soil moisture in the simulations as the observed value (experiment EXP_SMOIST). In EXP_SMOIST experiment, initial soil moisture was simply minus 0.05 (difference between model and observation over Tazhong station, Figure b1). Over-predicted latent heat flux the first several simulation hours are largely reduced in EXP_SMOIST. The large overestimate of soil moisture makes LH (Figureb2 b, f) from the model continue to increase. As a result, near-surface of model is in agreement with observation (Figure b2 d). However, the results from CTRL experiment are closer to EXP_SMOIST experiment after 3 hours' spin-up. The large overestimate of soil moisture at initial stage(0~3hours) may have little impact on the large over-prediction of sensible heat flux during 3~12 hours' simulation.

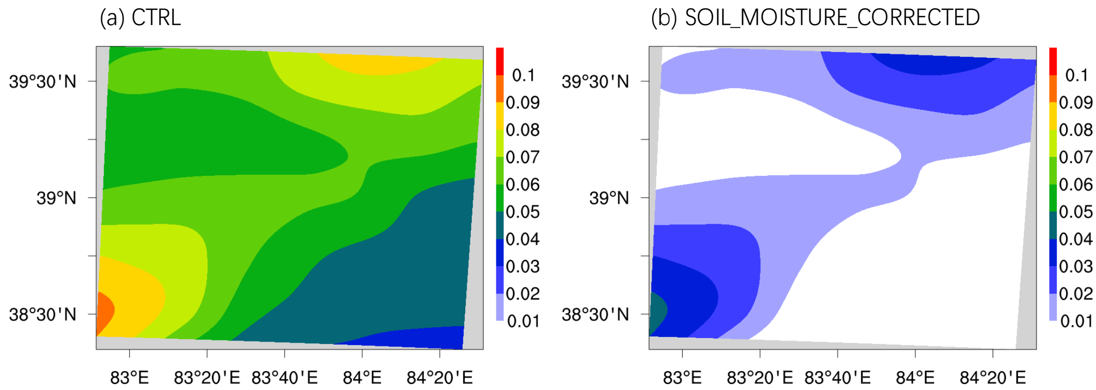

Figure b1 Soil moisture from model initial condition for (a) CTRL, (b) SOIL MOISTURE CORRECTED

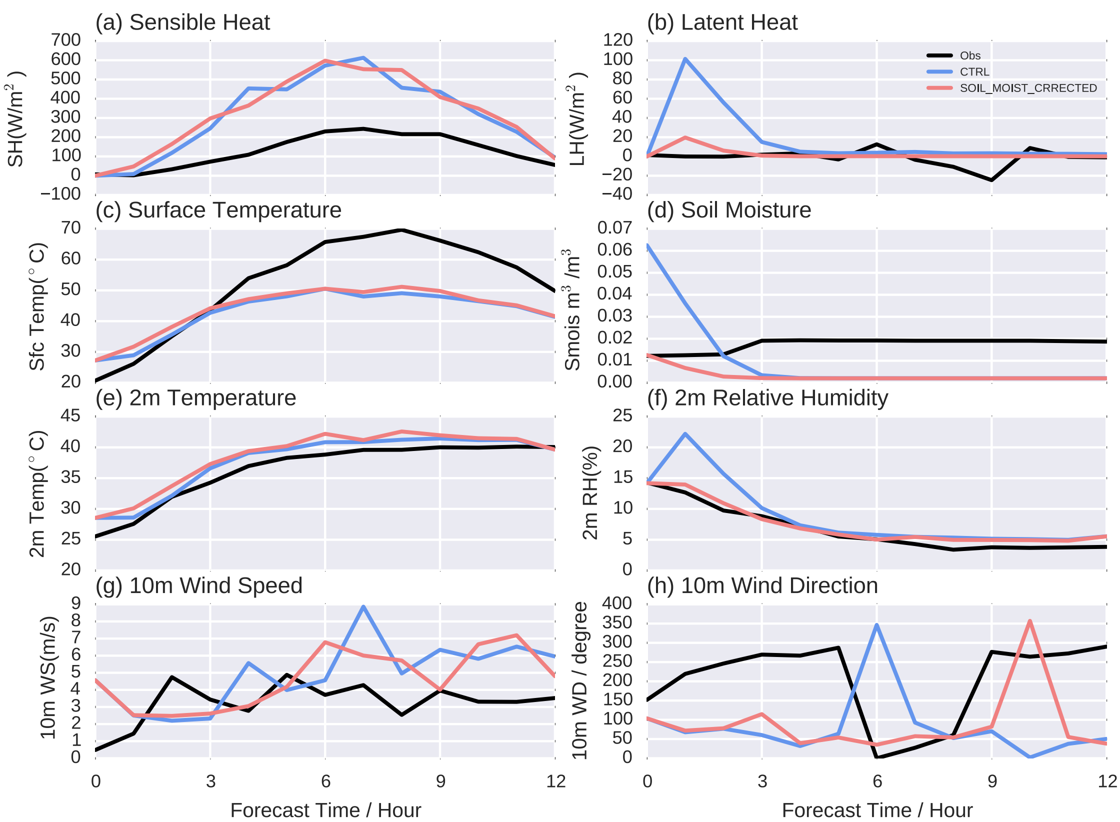

Figure b2 the same as Figure4, but for initial soil moisture sensitive experiment.

It is noted that the great efforts were made to improve the manuscript. However, another major revision is needed before it is accepted for publication.

Thank you for the comments.

More specific comments are found below.

1. The LES results presented in Figures 4 and 10 need further improvements. It is suggested to use the observed soil moisture as the initial condition for the new LES runs.

Yes, we have tried to set the initial soil moisture in the simulations as the observed value (experiment EXP_SMOIST). In EXP_SMOIST experiment, initial soil moisture was simply minus 0.05 (difference between model and observation over Tazhong station, Figure b1).

Over-predicted latent heat flux the first several simulation hours are largely reduced in EXP_SMOIST. The large overestimate of soil moisture makes LH (Figureb2 b, f) from the model continue to increase. As a result, near-surface of model is in agreement with observation (Figure b2 d). However, the results from CTRL experiment are closer to EXP_SMOIST experiment after 3 hours' spin-up. The large overestimate of soil moisture at initial stage(0~3hours) may have little impact on the large over-prediction of sensible heat flux during 3~12 hours' simulation.

2. Lines 398-399, the authors pointed out that the sensible heat (SH) may not be the dominant factor for the development of the deep CBL over the Taklimakan desert. However, in the conclusion part (line 461), the authors highlight that the SH is an important factor affecting the CBL depth over dominant. Please have double check and make them to be consistent? It should be very careful to make the former statement. If this were the case, that would be a big finding from this study?

Thank you for the comments.

(1) SH may not be the dominant factor for the super deep CBL over the Taklimakan desert. As explained in lines 392~426, in addition to the surface sensible heat, the intensity of the entrainment process determines the increase in the CBL. The entrainment rate w_e is a valuable indicator of the development of the structure of the PBL. The rate of growth of the CBL is mainly determined by the entrainment rate w_e at the inversion layer without considering large-scale vertical motion. w_e usually has a positive correlation with the amount of heat flux at the inversion layer $\overline{(w'\theta_v')_h}$ and large LES experiments show that $\overline{(w'\theta_v')_h}$ is about 0.2 times the surface flux of the buoyancy $\overline{(w'\theta_0')}$. During the period from 1100 to 1400 BJT, a larger sensible heat flux is clearly correlated with stronger turbulent entrainment and warmer air from the free atmosphere entraining into the Mixing Layer. As a result, the CBL develops rapidly and warms too quickly in the early simulation phase due to the clear increase in temperature and strong vertical mixing in the model. The reduction in the sensible heat flux reproduces the evolution of the desert PBL better in the early simulation phase because the HFX-75% and Noah simulations produce the smallest simulation errors in both temperature and moisture. However, the height of the CBL and the potential temperature for HFX-75% and Noah reach >5000 m and 323.2 K, respectively, at 1700 BJT. For the rest of the day, the rate of increase in the height of the CBL slows due to the deep CBL (>5000 m), which requires more heat for the increase in the depth of the PBL. w_e decreases with increasing intensity of the inversion, which inhibits the mixing and entrainment processes. These two factors limit the growth of the CBL when the height is >5000 m in this deep desert event. Therefore, increasing the sensible heat flux from 75 to 125% significantly reduced the total time required for the increase in the CBL to a relatively low altitude (<5000 m) at the middle and preliminary stages of the development of the CBL, rather than produces a higher CBL at a later stage.

(2) The SH is an important factor affecting the super deep CBL. Although SH is not dominant factor in this super deep CBL case, the CBL of Taklimakan need several days of favorable environment to reach its super depth (> 4000m), and Sustained high temperature and SH is the crucial factor for CBL to develop from shallow to deep CBL.

3. L136: The setting of vertical levels of the WRF/LES simulations is not correct. It is impossible that the vertical level starts from 1130.473m.

Sorry for the mistake, 1130.473m is altitude. We have changed "height for lowest 20 levels" to "altitude for lowest 20 levels"

4. Please make sure all the abbreviated terms are defined at the place where they appear at the first time. Please define GPS at Line 45, and check the same issue throughout the manuscript.

Ok.

5. Line 48: Change "relative warmer" to "relatively warmer".

Ok.

6. Lines 50-51, change "Lateral Boundary Layer(LBC)" to "lateral boundary layer (LBC)". Please add one space before "(". There are many similar errors in other places of the manuscript.

Ok.

7. Please be careful to use the upper case for the first letter of a word. Here "Lateral Boundary Layer" is one example （L50-51）. More similar problems include "china" (L73), "Vertical" (L288), "Large-scale" (L300), "Specified LBC" (L319), etc. I am not going to list all of them here. It is the authors' responsibility to correct all the problems.

Ok. We have changed "Lateral Boundary Layer" to "china", "Vertical", "Large-scale" (L300), and "Specified LBC" to "Lateral Boundary Condition (LBC)", "China", "vertical", "large-scale" (L300), and "specified LBC" respectively. We also carefully corrected similar problems in the manuscript.

8. Please pay more attention to the usage of past tense and singularity of verbs. Some examples include "model show…" (L206), "but model produce" (L223-224), "… temperature are …" (L245),

"Figure 5 compare" (L327), etc. There are too many errors like this. The authors should be able to correct and avoid them.

Ok.

9. Lines 52-54. Please rewrite the sentence starting with "It is found ….". It is difficult to understand the authors' meaning.

We have changed "It is found that larger domain size varies the distance of the area of interest from the LBC, is efficient to reduce the influences of large forecast error near the LBC." to "It is found that larger domain size varies the distance of the area of interest from the LBC, is efficient to reduce the influences of large forecast error near the LBC." to "It is found that larger domain size varies the distance from the area of interest to the LBC, which is efficient to reduce the influences of large forecast error near the LBC."

10. Please change "locates" to "located".

Ok.

11. Line 70: Please add year after Wang et al.

Thank your comment, we didn't add year because the paper is still under review.

12. Line 81, please rewrite the sentence "This fundamentally restrict the development of understanding desert and surrounding area".

Ok, we have changed "This fundamentally restrict the development of understanding desert and surrounding area" to "This fundamentally restrict further understanding desert and surrounding area"

13. Line 86, "To fill in the gaps of Taklimakan desert" is ugly.

Ok, we have changed "To fill in the gaps of Taklimakan desert" to "To fill in the gaps in the available data for the Taklimakan Desert".

14. Line 97, "PBL can heavily impacted"?

Ok, we have changed "PBL can heavily impacted" to "PBL can severely impacted".

15. Line 98, "One way to tackle complex turbulent flows in weather forecast models is Large eddy simulation (LES)….." needs an improvement. Please correct. Again, there is no need to redefine LES if it is defined previously.

Ok.

16. Line 112, what is the LBCs?

We have changed "lateral boundary conditions (LBCS)" to "lateral boundary conditions (LBCs)".

17. Line 118, For the statement of "this paper is to examine assess the skillfulness….", please delete examine or assess.

Ok, we have deleted "examine"

18. Lines 136-138, what is the unit of the height?

The units are meter.

19. Line 140, please change the sentence "The sizes of model grids are 411 ×321 791x651 211x201 and 403x406 respectively." to "The numbers of model grids from the outmost to the innermost domains are 411× 321, 791×651, 211×201, and 403×406, respectively". Several similar issues can be found in other places such as Lines 139, 207-208, etc. Please pay more attention on how to use ",".

Ok.

20. Lines 258-260, how can you attribute the reason to the potential temperature lapse rate?

Yes, this may be due to the differences in the potential temperature lapse rate above the top of the mixing layer between the observations and the simulated results. The stronger simulated inversion layer restricts the development of the CBL.

21. Line 266, please define CBLH. Please check out throughout the manuscript.

We have changed "CBLH" to "CBLH (Convective Boundary Layer Height)"

22. Line 301, "may resulted in" => "may result in".

Ok

23. Line 318, for "LES simulation", please delete "simulation" since LES has included.

Ok

24. Lines 330-331, for the sentence "However, the comparison results reveal that discrepancies among different experiments are large for CBL"? What does the "discrepancy" represent?

Thank you for the comments. "discrepancy" represent moisture and temperature profile in CBL. We have changed "However, the comparison results reveal that discrepancies among different experiments are large for CBL" to "the results show that there are large discrepancies in the CBL structure among the different experiments".

25. Using "The" or "the" correctly is a big challenge. It seems that the authors have a big trouble of using "the" or "The". For example, on Lines 331, "CBL" should be "the CBL". There are too many issues like this.

Ok.

26. Line 350, the sentence "CBL, the instantaneous vertical velocity fields for the horizontal are displayed in" is incomplete. Please correct.

Ok, we have changed "CBL, the instantaneous vertical velocity fields for the horizontal are displayed in" to "CBL, the instantaneous vertical velocity fields are shown in Figure 7"

27. L353-357, figure number is missing.

Ok, we have changed "(a)" and "(b, c)" to "(Figure 7a)"and "(Figure 7 b, c)"respectively.

28. Line 374: import or important?

Ok, we have changed "import" to "important".

29. Line 375, "surface-land schemes" should be "land-surface schemes".

Ok.

30. Line 376: "the difference between model and observation" should be "the difference between simulations and observations". Similar issues can be found other places too.

Ok.

31. Lines 382-384, please rewrite the sentence "The results … 125%".

Ok.

32. Line 414, what do the large LES experiments mean?

We have deleted "large".

33. Lines 446-447, please rewrite the sentence "Overestimation of CBL profile may be caused by discrepancy between model and measurement initially".

Ok.

34. Lines 527-528: (d) "surface temperature (°C)" is not matched with Figure 4.d.

Sorry for the mistake, we have corrected the caption of Figure 4.

35. Line 534, please add "," between (a), (b), (c), and (c).

Ok.

36. Line 535, change "01 Jul2016" to "01 July 2016". Check the same issues in other places too.

Ok.

37. Figure 7, please add labels to x-axis and y-axis for all the four panels.

Ok.

38. I have to say that it is difficult to list all of the writing errors here since there are too many.

Thank you for the comments. We have tried our best to avoid writing errors and used professional English language edit service (Lucid Paper) to edit and improve the English writing

Editor(s)' Comments to Author:

Comments to the Author:

While the reviewers appreciated the efforts the authors spent during the revision, they still raised issues regarding English writing and too large model bias of surface fluxes.

Please be more careful for writing and improve introduction to put this work into the perspective.

Also please carefully address the 2nd reviewer's remaining concern.

Thank you for the comments.

(1) We have carefully replied reviewers' remaining concern and rewritten part of the introduction to make it clear.

(2) We have used professional English language edit service (Lucid Paper) to edit and improve the English writing.

Performance of WRF Large Eddy Simulations in modeling the convective boundary layer over the Taklimakan Desert, China

Hongxiong Xu[1], Minzhong Wang[124], Yinjun Wang[1], Wenyue Cai[13]

1 State Key Laboratory of Severe Weather, Chinese Academy of Meteorological Sciences
Beijing, China 100081

2 Institute of Desert Meteorology, CMA (Chinese Meteorological Administration),
Urumqi, China

3National Climate Center, Chinese Meteorological Administration,
Beijing, China 100081

4 Taklimakan Desert Atmospheric Environment Observation Experimental Station, Tazhong 841000, China

Submitted to ***Journal of Meteorological Research***

January 2, 2018

Corresponding author:
Dr. Minzhong Wang
Institute of Desert Meteorology,
CMA (Chinese Meteorological Administration)
No. 46, Zhongguancun South Street, Haidian District, Beijing
P. R. China, 100081
Email: wangmz@idm.cn
dorn1984@163.com

删除的内容: **Weather Research and Forecasting Model**

删除的内容: **RF**

删除的内容: **-Eddy**

删除的内容: **in summertime**

删除的内容: **CBL characteristics**

删除的内容: **: A Real Test Case**

批注 [LP1]: The title of your paper has been edited for clarity – please check and confirm meaning is now correct.

删除的内容: Minzhong Wang[12]

删除的内容: ... [1]

删除的内容: ... [2]

删除的内容: ... [3]

删除的内容:

删除的内容:

删除的内容: Yinjun Wang

删除的内容:

删除的内容: State Key Laboratory of Severe Weather

删除的内容: Chinese Academy of Meteorological Sciences

删除的内容:

Abstract

The maximum height of the convective boundary layer (CBL) over the Taklimakan Desert can exceed 5000 m during the summer and has a crucial role in simulating the regional circulation and weather. We combined Weather Research and Forecasting Large Eddy Simulations with data from Global Positioning System (GPS) radiosondes and eddy covariance stations to evaluate the performance of the model in predicting the characteristics of the deep convective planetary boundary layer over the central Taklimakan Desert. The model reproduced the evolution of planetary boundary layer processes reasonably well, but the simulations predicted warmer and more moist conditions than the observations as a result of the over-prediction of surface fluxes and large-scale advection. Further simulations were performed with multiple configurations and sensitivity experiments. The sensitivity tests for the lateral boundary conditions (LBCs) showed that the model results are sensitive to changes in the time resolution and domain size of the specified LBCs. A larger domain size varies the distance of the area of interest from the LBCs and reduces the influence of large forecast errors near the LBCs. Comparing the model results using the original land surface parameterized sensible heat flux with the Noah land surface scheme and those of the sensitivity experiments showed that the desert CBL is sensitive to the sensible heat flux produced by the land surface scheme during daytime in summer. A reduction in the sensible heat flux can correct overestimates of the potential temperature profile. However, increasing the sensible heat flux significantly reduces the total time needed to increase the CBL to a relatively low altitude (<3 km) in the middle and initial stages of the development of the CBL rather than producing a higher CBL in the later stages.

Keywords: Weather Research and Forecasting Model, Large Eddy Simulations, convective boundary layer, Taklimakan Desert

删除的内容: Email: pbl_wyj@sina.cn

删除的内容:

带格式的: 行距： 1.5 倍行距

删除的内容: During the summer season over Taklimakan Desert, the …he maximum height of the CBL (…onvective ... [4]

删除的内容: p…sitioning Ss ... [5]

删除的内容:)…radiosondes and eddy-…covariance stations ... [6]

带格式的: 字体颜色: 文字 1

删除的内容: g

带格式的: 字体颜色: 文字 1

删除的内容: the

删除的内容: more frequently updated LBC is desirable to

删除的内容: The inhibit model errors near the LBCs are inhibited by more frequent updates of the LBCs., On the other hand, modelForecast errorbut are increased as the distance between the area of interest and the lateral boundaries decreasesd.

删除的内容: Furthermore,

删除的内容:

删除的内容: c…omparing the model results using the ... [7]

删除的内容: a reduction(increment) in SH decreases(increases) maximum PBL by roughly 15% over desert. …he desert It ... [8]

删除的内容: very …ensitivity… to the to…SH…ensible heat flux produced by surface …he land surface scheme during summer …ay ... [9]

删除的内容: e

删除的内容: SH

删除的内容: in the CBL during summer day time

删除的内容: SH…ensible heat flux significantly reduces the total time needed for…o CBL …ncrease the CBL to a relatively low altitude (< … km) at…n the middle and preliminary…nitial stages of the development of the CBL rather than produce…ng a higher CBL at ... [10]

删除的内容: WRF

删除的内容:

1 Introduction

The Taklimakan Desert in south-central Xinjiang Province, China, is the world's second-largest flow desert and has a profound influence on the regional weather and climate. As a result of the extreme range in near-surface temperatures, the planetary boundary layer (PBL) in this region commonly reaches 4–6 km in height during the boreal summer (Wang et al.), the deepest on Earth. This deep PBL, which is significantly higher than that over the surrounding mountains and oases, plays an important role in the regional circulation and weather. The accurate forecast of PBL processes over the Taklimakan Desert is an important problem in northwest China.

The atmosphere over large deserts (such as the Sahara and Taklimakan deserts) is a key component in the Earth's climate system. Surface heating from intense solar radiation leads to the development of a near-surface, low-pressure thermal system, commonly referred to as a heat low (Engelstaedter et al. 2015). However, despite the vital role that deserts have in the Earth's climate system, observations are extremely sparse and the available data are usually obtained from surrounding areas (Marsham et al. 2011). This lack of observational data has restricted the development of our understanding of deserts and has led to large discrepancies in analyses and significant biases in operational numerical weather prediction (NWP) models. The ability of local models to simulate real-world examples is often hindered by a lack of data with which to assess the performance of the model (Garcia-Carreras et al. 2015).

To fill in the gaps in the available data for the Taklimakan Desert, a field observation experiment was carried out during July 2016 in Tazhong, located in the center of the Taklimakan Desert near the Institute of Desert Meteorology, Chinese Meteorological

删除的内容: ,…locates at the…n south …center…al of the [11]

删除的内容: (Wang et al.)

删除的内容: making it probably …he deepest on earth…arth [12]

删除的内容: part

删除的内容: o…n then…regional circulation and weather. In [13]

删除的内容: ,…and Taklimakan et al.…eserts) [14]

删除的内容: conditions are very difficult

删除的内容: fundamentally …as restricted the development [15]

删除的内容: …o fill in the gaps of…n the available data for [16]

删除的内容: g

删除的内容: ,…Desert near by …the Institute of Desert [17]

Administration, Urumqi (Liu et al. 2012; Wang et al. 2016a; Wang et al. 2016b). These data will allow the evaluation of the performance of the deep PBL process in NWP models over the Taklimakan Desert.

The motion of the atmosphere interweaves small-scale, complex interactions with multiscale nonlinear interactions. As a result of their limited resolution in both time and space, mesoscale atmospheric models are unable to represent all these processes (Talbot et al. 2012), which include turbulent motion on a scale that is too small to be resolved by simplified processes in atmospheric models. Turbulent mixing throughout the PBL can have a large impact on forecasts by NWP models (Shin; Hong 2011; Shin; Hong 2015).

Complex turbulent flows in NWP models can be analyzed by large eddy simulation (LES) techniques, which can explicitly resolve the energy-containing turbulent motions responsible for turbulent transport (Moeng et al. 2007). LES techniques have been used intensively to examine the detailed structure of turbulence, to generate statistics and to study physical processes (Garcia-Carreras et al. 2015; Heinold et al. 2013; Heinold et al. 2015; Heinze et al. 2015; Sun; Xu 2009). However, most applications of LES techniques to the PBL have been limited to idealized physical conditions. Recently, some studies have attempted to test and assess the performance of LES in simulating real-world case studies (Liu et al. 2011; Talbot et al. 2012). Liu et al. (2011) suggested that the Weather Research and Forecasting Large Eddy Simulation (WRF-LES) is a valuable tool with which to simulate real-world microscale weather flows and to develop real-time forecasting systems, although further modeling to determine the accuracy of synoptic forcing and the effect of resolution has been highly recommended. Talbot et al. (2012) suggested that the ability of WRF-LES to simulate

删除的内容: (CMA)… Urumqi (Liu et al. 2012; Wang et al ... [18]

删除的内容: On the other hand, a…tmospheric… ... [19]

删除的内容: cannot

删除的内容: explicitly …epresent all these processes (Talbot ... [20]

删除的内容: planetary boundary layer (…BL) ... [21]

删除的内容: heavily …ave a large impacted…on ... [22]

删除的内容: One way to tackle c…omplex turbulent flows in ... [23]

删除的内容: S

删除的内容: LES …nd assess its …he performance of LES ... [24]

删除的内容:

删除的内容: LES …odeling tests,…such as elucidate… ... [25]

real-world examples is hindered by a lack of favorable synoptic forcing. The initial and lateral boundary conditions (LBCs) were found to be more important in the LES results than subgrid-scale turbulence closures. Thus, the LBCs can significantly alter the status of high-resolution LESs via inflow boundaries (Rai et al. 2017).

Most of the LES research over desert regions has been limited to idealized physical conditions (Garcia-Carreras et al. 2015) or conducted outside the Taklimakan Desert (Liu et al. 2011; Talbot et al. 2012). The aim of this study was to apply LES to a real example of a deep convective boundary layer (CBL) over the Taklimakan Desert. An important aspect of this work is to assess the skillfulness of the WRF-LES in simulating real examples of deep desert PBL processes at a relatively coarse resolution (333 m) over the Taklimakan Desert during the boreal summer. We first use a combination of the WRF-LES and Global Positioning System (GPS) radiosonde and surface fluxes over the central Taklimakan Desert calculated using an eddy covariance method to evaluate the performance of the WRF-LES in a real-world example. We then assess the potential errors related to the LBCs. One of our aims is to evaluate the relative contribution of uncertainties in the surface model to the typical behavior of PBL processes by conducting sensitivity experiment. We therefore studied the sensitivity of the model performance to the surface sensible heat flux. Section 2 gives a brief description of the synoptic conditions of the case study and describes the data, model configuration and design of the numerical experiments. The results of the numerical simulations are presented in Section 3 and our conclusions are summarized in Section 4.

2 Methods

2.1 Model configuration

删除的内容: -…orld cases are…xamples is hindered by a [26]

删除的内容: initial condition

删除的内容: of …an significantly alter the status of [27]

删除的内容: WRF land-surface model…nflow boundaries [28]

删除的内容: However, m…ost of the research above [29]

删除的内容: As far as we know,

删除的内容: is the first attempt to…as to applicate…only [30]

删除的内容: Thus, a

删除的内容: the ongoing …his paper [31]

删除的内容: examine

删除的内容: in relative coarse resolution (333m) over Taklimakan dessert

删除的内容: ,

删除的内容: cases …xamples of deep desert PBL processes [32]

删除的内容: First we assess the potential errors related to LBC. Then

删除的内容: First w…e first use a combination of the [33]

删除的内容: O

删除的内容: the …ensitivity experiment.s.…Thus, a [34]

删除的内容: . In Section 3

删除的内容: ,…and we …escribed… the data, and…odel [35]

删除的内容: 4

删除的内容: .…Finally, we…nd our [36]

删除的内容: <#>Data [37]

We used version 3.8.1 of the WRF model (Skamarock et al. 2008) at a sub-kilometer resolution to simulate an extreme CBL over the Taklimakan Desert. The model is integrated for 12 h, starting from 0800 BJT (Beijing Time) on 1 July 2016. We use one-way nested WRF model from the mesoscale down to LES scales. All the domains consist of 51 levels extended to 50 hPa. The altitudes for the lowest 20 levels are 1130.473, 1157.705, 1207.765, 1294.703, 1423.873, 1591.895, 1795.526, 2021.868, 2272.33, 2558.433, 2882.675, 3248.113, 3658.499, 4118.481, 4633.882, 5212.111, 5855.802, 6517.111, 7151.295 and 7757.151 m and the horizontal spacing of the model is 12, 3, 1 and 0.33 km for d01, d02, d03, and d04. We used (411 × 321), (791 × 651), (211 × 201) and (403 × 406) model grids. Figure 1. shows the domain used for all the experiments except BDY_T3. A smaller grid size (205 × 208) is used in experiment BDY_T3 to verify the effect of domain size on the LES.

The initial and LBCs are provided at the coarsest mesoscale simulations from the National Centers for Environmental Prediction Global Data Assimilation System Final Operational Global Analyses dataset. The analyses are 0.25° × 0.25° grids operationally prepared every six hours and available on the surface and at 32 mandatory (and other pressure) levels from 1000 to 10 mbar (National Centers for Environmental Prediction 2015).

The physical options in the model include the WSM5 microphysics scheme (Hong; Lim 2006), the Yonsei University PBL scheme (Hong; Pan 1996), the Kain–Fritsch cumulus parameterization scheme (Kain 1993; Kain 2004), the rapid update cycle (RUC) land surface model (Smirnova Tatiana et al. 2000; Smirnova et al. 1997), the rapid radiative transfer model (Mlawer et al. 1997) at long wavelengths and the Dudhia shortwave radiation scheme (Dudhia 1989). The cumulus parameterization scheme is only applied to the d01 (12 km) grid

删除的内容: convection-permitting

删除的内容: s…to simulate the ... [38]

删除的内容: rainfall

删除的内容: event in…ver the Taklimakan Desertdesert ... [39]

删除的内容: . Figure 1 shows the domain for two experiments. We use the outermost domain and three one-way nested domains.

删除的内容: conducted

删除的内容: a

删除的内容: -

已移动(插入) [1]

删除的内容: were

删除的内容: Height

删除的内容: A…he altitudes for the lowest 20 levels a... [40]

带格式的: 字体:12 pt

删除的内容: Figure 1. Figure 1Figure 1

带格式的: 字体:12 pt

删除的内容: for …DY_T3. S… smaller grid sizes (205 ... [41]

批注 [LP2]: Are units required for the grid sizes?

删除的内容: simulation

删除的内容:

删除的内容: (Figure 1).

已上移 [1]: All domains were 51 levels extended to 50 hPa.

删除的内容: .

删除的内容: ized condition …nd LBCslateral boundary ... [42]

删除的内容: on

删除的内容: -degree by…0.25°-degree…grids ... [43]

删除的内容: 26

删除的内容: millibars …o 10 millibars …bar (National ... [44]

删除的内容: model …hysical options in the model include ... [45]

删除的内容: (Smirnova Tatiana et al. 2000; Smirnova et al. 1997)the Noah land surface model(Chen; Dudhia 2001a, 2001b),

删除的内容: longwave,

domain to parameterize the convective rainfall and the LES is only applied to d04 (0.333 km).

Table 1 lists the experiments. Experiment 1 was the control experiment, denoted as CTRL. Experiments 2 (six-hourly updated LBC; denoted BDY_T2) and 3 (with domain sizes 205 × 208, denoted BDY_T2) were conducted as in the CTRL experiment, but with different domain sizes and frequency of LBC updates. In experiments 4 (HFX_%75) and 5 (HFX_%125), the sensible heat flux was reduced to 75 and 125%, respectively, of that in the CTRL experiment in the RUC land surface scheme to highlight the impact of the sensible heat flux on the deep CBL in the Taklimakan Desert. In experiment 6 (denoted Noah), the Noah land surface model (Chen; Dudhia 2001a, 2001b) replaced the RUC land surface model in the CTRL experiment to discriminate the influence of different land surface models on the deep CBL.

2.2 Data

The model simulations are compared with the Tazhong field experiment carried out throughout the month of July 2016 by the Institute of Desert Meteorology, Chinese Meteorological Administration, Urumqi. The main station was located at (86.63° E, 39.03° N). The location is relatively flat with few hills and is covered by sand combined with grass (Figure 1. c). The deep PBL in our simulation was under a cloudless sky in a dry environment.

The surface fluxes were measured by an eddy correlation system using an R3-50 supersonic anemometer developed by Gill (UK) deployed at a height of 10 m. The frequency of data acquisition was 20 Hz and the surface sensible heat flux was calculated by the eddy covariance method.

删除的内容: ….While,…nd the large-eddy-simulation (…ES) ... [46]

删除的内容: shows the …ists the of…experiments ... [47]

删除的内容: to…ith the Tazhong field experiment…which ... [48]

带格式的: 字体:12 pt

删除的内容: Figure 1. Figure 1Figure 1

带格式的: 字体:12 pt

删除的内容: ,… and t…he deep PBL of …n our simulation ... [49]

删除的内容: 1)…he surface fluxes:…were measured ... [50]

The vertical profiles were measured using soundings. Upper air soundings of the temperature, pressure, humidity, and wind speed and direction were conducted three to six times per day with the CASIC23 GPS sounding system developed by the No. 23 Institute of China Aerospace Science & Industry. The sounding times were 01:15, 07:15, 10:15, 13:15, 16:15 and 19:15.

2.3 Synoptic patterns

Figure 2 shows the synoptic patterns at 0800 BJT on 1 July 2016 at 850, 700, 500 and 100 hPa. There were cyclonic vortexes from 850 to 500 hPa centered at 55° N (Figure 2. a, b and c). The Taklimakan Desert was located east of the cyclonic vortex and embedded in an east–west elongated ridge at 0800 BJT on 1 July 2016. To the southwest, influenced by the South Asian High centered over the eastern Iranian Plateau, the upper air over the Taklimakan Desert was controlled by the westerly jet stream at 100 hPa (Figure 2. d). A low-pressure system at low levels, termed a heat low (Figure 3.), dominated most of southern Xinjiang and resulted in continuous high temperatures over the desert. This situation favored subsidence and served as a triggering mechanism for the deep PBL in the region in the subsequent two to three days (not shown).

3 Results

3.1 Validation of the deep CBL structure

The time series of the surface variables at Tazhong station from the CTRL simulation for 1 July 2016 are presented in Figure 4. a and b. The results show that there are large discrepancies in the thermodynamic surface variables (surface temperature and the sensible and latent heat fluxes) between the model and the observations. The surface sensible heat flux

删除的内容: 2…he)…vertical profiles were measured using ... [51]
删除的内容: °
删除的内容: Figure 2. Figure 2Figure 2
删除的内容: … b and c). The Taklimakan was …esert was ... [52]
带格式的: 字体:12 pt
带格式的: 字体:12 pt
删除的内容: Figure 2. Figure 2Figure 2
带格式的: 字体:12 pt
删除的内容: …). The ... [53]
删除的内容: high
带格式的: 字体:12 pt
删除的内容: which is …ermed of ... [54]
删除的内容: Figure 3.
删除的内容: Figure 3Figure 3
删除的内容: area of …outhern Xinjiang and resulted in ... [55]
删除的内容: .
删除的内容: <#>Sensitive to Lateral Boundary Condition(LBC) .
Simulated d
删除的内容: Simulated d…he time series ofiurnal ... [56]
删除的内容: 0
带格式的
删除的内容: Figure 4. Figure 4
带格式的
删除的内容:
删除的内容: ,…and b. R…he results show that there are ... [57]

is far lower in the observations (maximum 243 W m^{-2}) than in the model (maximum 613 W m^{-2}), indicating that the sensible heat flux from the WRF simulation is 2.5 times than that of the observations when they are both at their maximum. By contrast, the model shows a significant cold bias for the surface temperature, which is much higher in the observations (maximum 70°C) than in the model (maximum 50°C). To further verify the surface variables, the root-mean-square error (RMSE) and mean bias (BIAS) are calculated, including integration hours from 3 to 12 h for Tazhong station (Table 2). The model significantly overestimates the sensible heat flux (RMSE 263.636 W m^{-2}, BIAS:250.14 W m^{-2}) and dramatically underestimates the surface temperature (RMSE 14.65°C, BIAS −13.37°C).

There are two possible reasons for the model sensible heat flux being far greater than that of the observations. First, mismatches in land use between the model and the observations. The WRF models uses land use categories to assign static parameters and initial values to each grid cell (e.g. the albedo and surface roughness; Schicker et al. 2016). However, Figure 1. c shows that station EC is surrounded by a mixture of grass and sand. This complex underlying surface may not be adequately reproduced by the model and may have an impact on the overestimation of the sensible heat flux. Second, the sensible heat flux and the latent heat flux based on the eddy correlation method may be underestimated (LeMone et al. 2013). It has been shown that if the other two terms in the budget (the net radiation and flux into the soil) are accurate, then the data used for the whole experiment to find the sensible and latent heat fluxes for Tazhong station are, on average 75%, of the values required to balance the surface energy budget.

删除的内容: less …ower in the observations [58]
删除的内容: , the
删除的内容: in …Table 2). As mentioned earlier,. he model [59]
删除的内容: Three
删除的内容: result in…or the model SH…ensible heat flux [60]
删除的内容: （
删除的内容: (1）) Tthe…irst, [61]
删除的内容: mismatch
删除的内容: of …n land -…se between the model and the [62]
带格式的: 字体:12 pt
删除的内容: Figure 1. Figure 1
带格式的: 字体:12 pt
删除的内容: ,…shows that the EC …tation EC is surrounded [63]
删除的内容:
删除的内容: (2) Iit is should be noted that…econd, the [64]
批注 [LP3]: Please give ‘E + LE’ in full (no abbreviations).
删除的内容: H…ensible + …nd LE [65]
删除的内容: equal to an…n average of [66]
删除的内容: 70
删除的内容: what would be…he values required for… [67]
删除的内容: (LeMone et al. 2013)

In contrast with the large differences in the surface variables between the model and the observations, the near-surface variables (the 2 m temperature, the relative humidity and the 10 m wind speed; Figure 4. e, f and g) in the model are higher than in the observations. The time series evolution of the 2 m temperatures follow those of the observations (RMSE 1.66, BIAS 1.61), but the model produces a surface warmer by about 3 K at the beginning of integration and 1 K when the model and observations both reach their maximum temperature.

The results indicate that the near-surface relative humidity in the model is close to the initial observations (Figure 4. f). However, the humidity in the model increases during the first few hours of model integration, while the observed humidity decreases. After three hours of spin-up, the model reproduces the evolution of humidity reasonably well, in agreement with the observations (RMSE 1.22), but the values are higher than the observed values (BIAS 1.11).

One reason for this discrepancy is the overestimation of the soil moisture content during the simulation. The soil moisture content can have a strong influence on the near-surface humidity. An overestimation of the soil moisture content in the initial condition of the model may result in a considerable difference in the humidity of the near-surface layer (Talbot et al. 2012). In our simulations, the model produces large overestimates of the soil moisture content. At initialization of the model in the CTRL simulation, the soil moisture content at 5 cm depth at station EC was 0.230 m^3 m^{-3}, whereas the initial value in the model was 0.6 m^3 m^{-3} (Figure 4. d). This large overestimate of the soil moisture content results in a continuing increase in the latent heat in the model (Figure 4. b, f). As a result, the near-surface in the model is far moister than in the observations during the first few hours of model integration. The model

删除的内容: Despite

删除的内容: surface

删除的内容: o…n the surface variables between the model [68]

带格式的

删除的内容: Figure 4. Figure 44

删除的内容: (Figure 6 e)

带格式的

删除的内容: …, f and g) are closer to measurements than [69]

删除的内容: nearly

删除的内容: observations

删除的内容: :…1.66, BIAS:…1.61);… but the model [70]

删除的内容: Results …he results indicate [71]

带格式的

删除的内容: Figure 4. Figure 44

删除的内容: from …n the model keeps …ncreasing [72]

带格式的

删除的内容: observation

删除的内容: :…1.22), but their…values are relatively higher [73]

删除的内容: e…on of the soil moisture content during the [74]

删除的内容: .

删除的内容: the …ur present …imulations, the model results [75]

删除的内容: Figure 4. Figure 44

删除的内容: …). This large overestimate of the soil [76]

删除的内容: Figure 4. Figure 44

删除的内容: …, f) from the model continue to increase [77]

删除的内容: from the model to continue increasing, then forces near-surface far moister than observation at the first few hours of model integration.

删除的内容: An interesting result to note is that t simulation has the ability to correct some of the bias due to the initial conditions of the surface and the results from the CTRL experiment are closer to the observed values after three hours of spin-up.

Figure 5. (solid lines) compares the potential temperatures simulated by the model with the GPS sounding measurements (dash lines) at Tazhong from 0800 to 2000 BJT on 1 July 2016. The radiosonde was about 7 km away from Tazhong when it reached a height of 6 km. The profiles of the model simulations are therefore averaged at a radius of 3.5 km from the measurement station. When the model is initialized at 0800 BJT, the nocturnal inversion reaches 300 m (not shown). This inversion is eroded in the model by 1100 BJT, in agreement with the observations, and both the model results and the observations reach about 300 m at 1100 BJT (Figure 5. a). However, the simulated CBL grows faster in the morning than that in the observations due to a larger sensible heat flux, reaching 3500 m (3000 m in the observations) at 1400 BJT (Figure 5. b). The simulated and observed CBL heights exceed 4000 and 5000 m, respectively, at 1700 BJT (Figure 5. c). This indicates that the simulated CBL increases more slowly in the afternoon than the observed CBL. Compared with the measurements, the model is initially cooler, but with a faster heating rate in the morning. As a result, the model is warmer than the observations in the afternoon, but in agreement with the observations by the end of the day. This may be due to the differences in the potential temperature lapse rate above the top of the mixing layer between the observations and the simulated results. The stronger simulated inversion layer restricts the development of the CBL.

The model initially simulates a cooler and drier CBL at 1100 BJT on July 2016 than the

删除的内容: abilities …bility to correct some of the bias due ... [78]

删除的内容: t

删除的内容: observation …bserved values after 3 hree ... [79]

删除的内容: Figure 5. Figure 5

删除的内容: The model simulated …otential temperatures ... [80]

删除的内容: Figure 5. Figure 5Figure

删除的内容: …). However, the simulated CBL grows faster ... [81]

删除的内容: Figure 5. Figure 5Figure

删除的内容:

删除的内容: ,

删除的内容: At 1700 BJT (Figure 5Figure c),, t he ... [82]

删除的内容: Figure 5. Figure 5

删除的内容: grows …ncreases more slowly in the afternoon ... [83]

删除的内容: The main source of model error is inauthentic cold advection within PBL in the afternoon which will be discussed below. Another

删除的内容: One possible minor reason is…his may be due ... [84]

删除的内容: , … simulated ... [85]

删除的内容: Simulated…he stronger simulated inversion ... [86]

删除的内容: Han et al. (2012)

删除的内容: Moreover, in terms of CBL temperatures, t

删除的内容: P

删除的内容: at

observations (Figure 5. a). Compared with the observed potential temperature profile, the CBL appears earlier in model forecasts due to an obvious warming in the surface layer. The residual layer may play a key part in the deep PBL over the Taklimakan Desert. At 1100 BJT, when the CBLH (Convective Boundary Layer Height) in the observations was about 300 m, the potential temperature was about 317 K in the PBL and 320 K in the residual layer. When the potential temperature in the CBL increased to the value in the residual layer (320 K), the CBL merged with the residual layer and the height of the PBL in the observations reached 3000 m at 1400 BJT. These results are in good agreement with those of Han et al. (2012), who, by analyzing observations from a CBL in the Badanjilin region, found that the CBL developed rapidly after 1200 LST, possible as a result of the disappearance of the inversion layer.

When the sensible heat flux reached its maximum at 1400 BJT (Figure 5. b), the potential temperature profile was closer to the observations than at the initial time and their value was higher than the observed values. By 2000 BJT (Figure 5. d), the height of the CBL in the model reached its maximum value, consistent with the observations, despite being about 0.4 K cooler at lower levels (<2.5 km). One cause of the higher temperatures produced in the model may be the large difference in the surface heat fluxes and we concluded that the surface sensible heat flux from the land surface parameterization was the crucial factor affecting the CBL processes during the daytime in summer. Differences in the surface sensible heat flux create differences in the vertical development of the PBL. Thus the large difference in the surface sensible heat flux between the model and the observations may lead to differences in the growth of the CBL during the daytime and in its peak depth during the

删除的内容: ed…tions,…at 1100 BJT01 JUL [87]

删除的内容: Figure 5. Figure 5Figure 4

删除的内容: to …ith the observed potential temperature [88]

带格式的: 字体:(默认) Times New Roman, (中文) +中文主题正文 (宋体), 字体颜色: 文字 1

删除的内容: was about 300 m …n the observations was [89]

删除的内容: However, w

删除的内容: SH

删除的内容: has …eached [90]

删除的内容: s

删除的内容: extent

删除的内容: Figure 5. Figure 5Figure 4

删除的内容: is …as closer to measurements …he [91]

删除的内容: Figure 5. Figure 5Figure 4

删除的内容: PBL height

删除的内容: H…in the model reaches… its maximum value [92]

删除的内容: , …onsistent with the observations, although [93]

删除的内容: of approximately…eing about 0.4 K cooler on [94] simulation. Fortunately, the surface sensible heat flux computed by the land surface model can artificially be modified to control the calculation of the surface fluxes. Sensitive simulations will be realized and discussed in next section.

Figure 5. also shows vertical profiles of the vapor mixing ratio (dashed lines) at Tazhong station. The simulated profiles with a lower residual layer are much drier than the observations from 1500 to 3500 m at 1100 BJT. Vertical mixing results in a uniform structure of the vapor mixing ratio within the CBL, so the differences between the profiles of the simulated results and the observations are remarkably reduced when the CBL is above 4000 m at 1400 BJT. The differences are generally <1 g kg^{-1} at 1100 BJT, reaching a maximum of 0.3 g kg^{-1} at 1400 BJT. However, the PBL shows an inverse layer at lower levels (<2000 m) with a measured moisture content of 2.8–3.6 g kg^{-1}, which is not captured by the model. As the CBL grows, the inversion moisture structure below 3000 m develops and is maintained below 3000 m from 1400 to 2000 h BJT. By the end of the day, the simulated humidity of the CBL is higher than in the observations, because the model cannot reproduce the inverse moisture layer within the CBL.

The inverse pattern in humidity may be caused by the interactions between the heterogeneous pattern of humidity and large-scale advection over the underlying surface. For instance, the interaction of an oasis with the desert environment may lead to an inverse humidity layer in the PBL above the desert. One possible reason for the discrepancy between the model results and the observations may be an error in the classification of land use type. The USGS land use data in the ARW-WRF model is based on Advanced Very High Resolution Radiometer 1 km resolution satellite data during the time period 1992–1993 and

删除的内容: Fortunately, one can artificially modify t

删除的内容: T

删除的内容: he …urface SH…ensible heat flux computed by ... [95]

删除的内容: modified

删除的内容: ,…which …o controls…the calculation of the ... [96]

删除的内容:

删除的内容: Figure 5. Figure 5Figure

删除的内容: also …hows vV…rtical profiles of the vapor ... [97]

删除的内容: with no …nverse moisture layer within the CBL ... [98]

删除的内容:

删除的内容: Inverse …he inverse pattern in humidity may be ... [99]

this land use data may no longer be accurate in the Taklimakan Desert. Misclassifications have also been found in the USGS land use data, which is the default land use dataset in the WRF model (Schicker et al. 2016). This is confirmed by the discrepancies in land use between the simulation and the observations at Tazhong station. The large-scale advection of dry air can affect the moisture profile. The moisture content is also variable in the horizontal direction, so advection at low levels may contribute to the drier conditions in the lower PBL and more moist conditions in the upper PBL between 1100 and 2000 BJT.

The mismatch between the model results and the observations in terms of moisture content suggest that the effects of land use type and large-scale advection need to be quantified and that more detailed data may be required for the Taklimakan Desert (both land and atmosphere) to realize more realistic results. Extra care should also be taken with the sparse and limited data at the periphery of the Taklimakan Desert (ter Maat et al. 2012).

3.2 Sensitivity to the lateral boundary conditions

After verifying the details of the LES experiments, we assessed the sensitivity of the simulations to the time resolution and domain size of the specified LBCs. For a one-way nest, the specified LBCs are obtained from coarser simulations. The analysis and forecast times from a previously run larger area simulation are used to specify the LBC. The primary cause of the differences in the structure of the PBL was diagnosed as the difference in the domain sizes and frequency provided by the coarser resolution. The aim was to assess the sensitivity of the finer LESs to uncertainties of the specified LBC forcing by model simulations with a larger area.

Figure 5. compares the profiles of the simulated potential temperature and vapor

删除的内容: -…se data may no longer be outdated…ccurate … [100]

删除的内容: at bottom base of the

批注 [LP4]: This sentence has been edited for clarity – please check and confirm meaning is now correct.

删除的内容: moisture …ore moist conditions at …n the … [101]

删除的内容: …nd the observations in terms of moisture … [102]

删除的内容: e…ty to the lateral boundary … [103]

删除的内容: simulation…experimentss … [104]

删除的内容: LES …imulations to the time resolution and … [105]

删除的内容: s

删除的内容: PBL …tructure of the PBL was diagnosed as … [106]

删除的内容: the time frequency and domain size

删除的内容: S…he specified LBC forcing by … [107]

删除的内容: Figure 5. Figure 5Figure 4

带格式的: 检查拼写和语法

mixing ratio profiles from the LBC sensitivity experiments and observations. The results show that there is a distinct relationship between the development of the LBCs and the CBL. The profiles produced by the model are almost all the same at the initial time (not shown). However, the results show that there are large discrepancies in the CBL structure among the different experiments. The results indicate that a larger domain size and higher time frequency for the LBCs leads to a warmer and drier PBL, but a cooler and moister free troposphere. This sensitivity is monotonic with respect to the LBCs (Figure 5.). Over the next three hours, the differences between the sensitivity experiments increase over time (Figure 5. a, b). The potential temperature profiles within the CBL diverge at 1100 BJT. However, the results show a greater convergence in the afternoon as the CBL continues to grow (Figure 5. c), but the largest discrepancies are found at end of the day (Figure 5. d) when the model CBL potential temperature is warmer than the observations by up to 0.7 and 0.9 K in BDY_T2 and BDY_T1, respectively.

Figure 6. shows cross-sections of the horizontal winds along 39.03° N, superposed with theta and the vapor mixing ratio. Less frequent updates of the LBCs are desirable in the cold zone near the LBCs, which results in cold advection of the temperature and moisture to the area of interest (Figure 6. b, c). A larger domain size, which changes the distance of the area of interest from the LBC, is efficient in reducing the influence of large forecast errors near the LBCs on the area of interest (CMP, Figure 6. a, c).

To further examine the impact of the LBCs on the turbulence in the deep Taklimakan Desert CBL, the instantaneous vertical velocity fields are shown in Figure 7. By 1400 BJT, the convection of the CTRL simulation had clearly intensified under strong surface heating

删除的内容: R…he results indicat…howe…that, there is a ... [108]

删除的内容: more moist

删除的内容: er…free troposphere. Such ... [109]

删除的内容: Figure 5. Figure 5Figure 4

带格式的: 检查拼写和语法

删除的内容: Furthermore, in…ver the next three hours, the ... [110]

删除的内容: Figure 5. Figure 5Figure 4

带格式的: 检查拼写和语法

删除的内容: …, b). The potential temperature profiles ... [111]

删除的内容: Figure 5. Figure 5Figure 4

带格式的: 检查拼写和语法

删除的内容: …)….Finally, ... [112]

删除的内容: and

删除的内容: by

删除的内容: Figure 5. Figure 5Figure 4

带格式的: 检查拼写和语法

删除的内容: …) where… the model CBL potential ... [113]

带格式的: 字体:12 pt

删除的内容: Figure 6. Figure 6 6

带格式的: 字体:12 pt

删除的内容: sections…along 39.03°N …f the horizontal ... [114]

带格式的: 字体:12 pt

删除的内容: Figure 6. Figure 6 6

带格式的: 字体:12 pt

删除的内容: …, c). L… larger domain size, which ... [115]

带格式的: 字体:12 pt

删除的内容: Figure 6. Figure 6 6

带格式的: 字体:12 pt

删除的内容:

删除的内容: The results suggest that the model results are sensitive to changes in the time resolution and domain size of Sthe specified LBCs. The mismatch among sensitive experiments is present means that the effect of the LBCs needs to be quantified to realize a more realistic performance in the sub-kilometer-scale simulations.

删除的内容: S… on the turbulence of…n the deep ... [116]

批注 [LP5]: Is Figure 7 correct here?

删除的内容: obviously

(Xu et al. 2018). Thus the maximum vertical velocity reached 9 m s^{-1} and the depth of the mixed layer grew to about 4.3 km (Figure 7 a). The distances between the boundary layer rolls correspondingly increased to about 12 km and the height of the peak up-draft was raised to just under 4 km. The cellular shape of the up- and down-drafts characteristic of the boundary layer rolls is clear in the horizontal view showing the strength of convection. The BDY_T2 and BDY_T3 experiments (Figure 7b, c) both reproduce motions with much weaker maximum and minimum values at the boundary of the domain. In BDY_T3, Tazhong station at the center of the model is directly influenced by the inflow of cold advection produced by the low-frequency LBCs, resulting in much weaker maximum and minimum values of *w* (about 6 m s^{-1}). However, despite the underestimation of the potential temperature, the *w* fields in the BDY_T2 experiment are similar to those in the CTRL experiment in plan view and the horizontal extent of the up-/down-drafts agrees with the CTRL experiment.

To further examine the vertical structure of the desert CBL, Figure 8 presents vertical cross-sections of *w* along Tazhong station (39° N). Wide and regularly spaced up-drafts along A1–A2 split into stronger and more irregular motions in the CTRL and BDY_T2 experiments. The up-drafts are much weaker in experiment BDY_T3 (Figure 8 c). The peak up-drafts in BDY_T3 are about 4 m s^{-1}, much weaker than in the CTRL (9 m s^{-1}) and BDY_T2 (8 m s^{-1}) experiments. The inflow boundary is wider in BDY_T2 and BDY_T3 and the intensity of the convection is weaker at the boundary. The horizontal distribution of the vertical velocity at Tazhong station in BDY_T3 is much weaker than in BDY_T2. The results suggest that the model results are sensitive to changes in the time resolution and domain size of the specified LBCs. The mismatch among sensitive experiments means that the effect of the LBCs needs to

删除的内容: …hus,…the maximum vertical velocity … [117]

批注 [LP6]: Is Figure 7 correct here?

删除的内容: …he distances between the boundary layer … [118]

批注 [LP7]: It is not clear what you mean here by 'boundary layer rolls' – please try to clarify.

批注 [LP8]: Is Figure 7 correct here?

删除的内容: …, c) both reproduce motions with much … [119]

删除的内容: …o further examine the vertical structure of … [120]

带格式的: 字体:(中文) SimSun, 10 pt

删除的内容: Figure 8. Figure 88

带格式的: 字体:(中文) SimSun, 10 pt

删除的内容: …). P…he peak up-drafts io… BDY_T3 are … [121]

be quantified to realize a more realistic performance in sub-kilometer-scale simulations.

3.3 Simulations with different surface sensible heat fluxes and land surface models

An important cause of the differences in the structure of the PBL was determined to be the differences in sensible heat flux predicted by the land surface schemes. The sensible heat flux is a key factor affecting the height of the CBL during daytime in summer. The difference between the models and observations may therefore lead to differences in the growth of the PBL during the day. To further confirm whether this occurs, three additional sensitive simulations were realized based on the CTRL experiment. The Noah land surface model replaced the RUC land surface model in the CTRL experiment and the sensible heat fluxes for HFX-125% and HFX-75% are %125 and %75 that of the CTRL (HFX -100%) experiment while the other parameters remain the same.

The results in Figure 10. and Table 2 show that HFX-75% successively improved the simulation of the sensible heat flux with an RMSE of 151.12 compared with 263.64 and 357.11 in the CTRL and HFX-125% experiments, respectively. The Noah land surface experiment yielded the best performance in terms of the sensible heat flux, the surface temperature and the air temperature. However, the Noah land surface model showed large discrepancies with the observations in terms of the soil moisture content, resulting in a dramatic overestimate of the latent heat flux and relative humidity compared with the CTRL experiment.

A further examination of the potential temperature and vapor mixing ratio (Figure 9.) indicates that a smaller sensible heat flux leads to a cooler, more moist lower PBL and a

- 删除的内容: .
- 删除的内容: (SH) …nd surface-
- 删除的内容: The
- 删除的内容: primary
- 删除的内容: PBL …he structure of the PBL was diagnosed
- 删除的内容: surface sensible heat flux
- 删除的内容: SH…ensible heat flux predicted by the surface
- 删除的内容: surface sensible heat flux
- 删除的内容: SH…ensible heat flux is one of the
- 删除的内容: dominant
- 删除的内容: H
- 删除的内容: depth
- 删除的内容: summer …ay …ime in summer. Thus, this the
- 删除的内容: the
- 删除的内容: PB…he L …rowth of the PBL during the
- 删除的内容: and in its peak depth during the simulated day
- 删除的内容: ;… To further confirm whether this indeed
- 删除的内容: two
- 删除的内容: For Noah experiment…he Noah land
- 删除的内容: For
- 删除的内容: ,…and HFX …75% the surface sensible heat
- 删除的内容:
- 删除的内容: ,…while the other parameters remain the same
- 删除的内容: from
- 删除的内容: Figure 10. Figure 10
- 带格式的: 检查拼写和语法
- 删除的内容: ed…that HFX-75% successively improved the
- 删除的内容: F… further examining
- 带格式的: 字体:12 pt
- 删除的内容: Figure 9. Figure 9
- 带格式的: 字体:12 pt
- 删除的内容: The results …ndicates that ,
- 删除的内容: with… smaller SH
- 删除的内容: and
- 删除的内容: er

warmer, drier free atmosphere. This sensitivity is monotonic with respect to the sensible heat flux. The structure of the CBL from the HFX-75% and Noah experiments matches the GPS radiosonde measurements better than the CTRL (HFX-100%) simulations. The potential temperature profiles from the CTRL (HFX-100%) and HFX-125% experiments are consistently warmer than the observations by about 0.4 and 0.5 K, respectively, whereas the results from the HFX-75% and Noah experiments are within about 0.2 K at 1400 BJT (Figure 9. b). These results suggest that the model is sensitive to changes in the sensible heat flux from the land surface model. The simulations converge at the end of the day, although there are still differences at 2000 BJT (Figure 9. d). The HFX-75% and Noah experiments with a weaker surface sensible heat flux still produce almost the same deep CBL as the CTRL and HFX-125% experiments. This indicates that the sensible heat flux may not the dominant factor in the formation of the deep CBL over the Taklimakan Desert.

The results of the simulations of the desert PBL in the morning agree with previous studies of the sensitivities the land surface model in other areas (Hu et al. 2010; Zhang et al. 2017). However, all the experiments produce nearly the same height of the CBL and moisture content from 1700 to 2000 BJT on 1 July 2016 (Figure 9. b, d), in agreement with the observations in the PBL. The effects of the sensible heat flux on the evolution of the PBL structures in the Taklimakan Desert during this period need to be examined further to determine why the simulations are insensitive to land surface processes at the end of the day. As reported by Stull (1988), the development of the CBL is mainly influenced by the effects of thermodynamic and turbulent entrainment if we do not consider factors such as large-scale advection or subsidence. In addition to the surface sensible heat, the intensity of the

删除的内容: and …rier free troposphere ... [136]
删除的内容: Such …his sensitivity is monotonic with respect ... [137]
删除的内容: determined …rom the HFX-%…5% and Noah ... [138]
删除的内容: (…FX-100%)… simulations. The pP…tential ... [139]
删除的内容: CTRL…nd (…FX-125% experiments) ... [140]
删除的内容: while …hereas the results from the HFX-75% ... [141]
删除的内容: CTRL(HFX-100%)
带格式的: 字体:12 pt
删除的内容: Figure 9. Figure 9Figure
带格式的: 字体:12 pt
删除的内容:
已移动(插入) [2]
删除的内容: results are…s sensitive to changes in the ... [142]
删除的内容: S…mulations results ... [143]
删除的内容: but remain
带格式的: 字体:12 pt
删除的内容: Figure 9. Figure 9Figure
带格式的: 字体:12 pt
删除的内容:
删除的内容:
已上移 [2]: The results suggest that the model results are sensitive to changes SH from land-surface model.
删除的内容: can …till produce almost the samethe deep ... [144]
删除的内容: R…he results of the simulations on the desert ... [145]
删除的内容: Figure 9. Figure 9
删除的内容: SH…ensible heat flux on the evolution of the ... [146]

entrainment process determines the increase in the CBL. Thus the entrainment rate w_e is a valuable indicator of the development of the structure of the PBL. The rate of growth of the CBL is mainly determined by the entrainment rate w_e at the inversion layer without considering large-scale vertical motion. w_e usually has a positive correlation with the amount of heat flux at the inversion layer $\overline{(w'\theta_v')}_h$ and LES experiments show that $\overline{(w'\theta_v')}_h$ is about 0.2 times the surface flux of the buoyancy $\overline{(w'\theta_0')}$. During the period from 1100 to 1400 BJT, a larger sensible heat flux is clearly correlated with stronger turbulent entrainment and warmer air from the free atmosphere entraining into the Mixing Layer (ML) . As a result, the CBL develops rapidly and warms too quickly in the early simulation phase due to the clear increase in temperature and strong vertical mixing in the model. The reduction in the sensible heat flux reproduces the evolution of the desert PBL better in the early simulation phase because the HFX-75% and Noah simulations produce the smallest simulation errors in both temperature and moisture. However, the height of the CBL and the potential temperature for HFX-75% and Noah reach >5000 m and 323.2 K, respectively, at 1700 BJT (Figure 9. a). For the rest of the day, the rate of increase in the height of the CBL slows due to the deep CBL (>5000 m), which requires more heat for the increase in the depth of the PBL. w_e decreases with increasing intensity of the inversion, which inhibits the mixing and entrainment processes. These two factors limit the growth of the CBL when the height is >5000 m in this deep desert event. Therefore increasing the sensible heat flux from 75 to 125% significantly reduced the total time required for the increase in the CBL to a relatively low altitude (<5000 m) at the middle and preliminary stages of the development of the CBL, rather than produces a higher CBL at a later stage. When the height of the CBL over the

删除的内容: ing… in the rate of …CBL. Thus,…the [147]

删除的内容: large

域代码已更改

删除的内容: ,

域代码已更改 [148]

删除的内容: larger SH … larger sensible heat flux is [149]

批注 [LP9]: Please give ‘ML’ in full – no abbreviation.

删除的内容: is …arms too fast…uickly in the early [150]

删除的内容: Figure 9. Figure 9Figure

删除的内容: …). For the rest of the day, the increase…ate [151]

删除的内容: example

删除的内容: ,…increasing the SH…ensible heat flux from [152]

删除的内容: k

删除的内容: the

Taklimakan Desert exceeds 5000 m, it may not change in proportion to the sensible heat flux (Figure 9. d). As a result, the PBL is basically the same in the WRF simulations and is not sensitive to the sensible heat flux at the end of the day.

4 Summary

In this paper, we assessed the performance of the WRF model LES in an example of a deep convective PBL over the Taklimakan Desert. The tests were performed with multiple configurations and sensitivity experiments. The sensitivity tests for the LBCs showed that the model results are sensitive to changes in the size of the time resolution and domain of the specified LBC. A larger domain size changes the distance of the area of interest from the LBC and is efficient in reducing the influence of the large forecast error near the LBC.

The model reproduces the evolution of PBL processes reasonably well with the configuration used in this study. The model shows discrepancies between the main CBL characteristics in the morning, including the thermal and moisture structures. The model simulates the relatively colder and drier morning CBL, underestimating the temperature in the near-surface layer at Tazhong station by up to 1.5 K and the moisture content by 1 g kg^{-1}. The overestimation of the CBL profile may be caused by initial discrepancies between the model and the observations. This indicates that the results are sensitive to the initial conditions of the model, although the simulation seems to be able to correct some of the bias due to the initial conditions. The model correctly reproduces the thermal structure in the afternoon, but the simulations are relatively warmer and moister than the observations. The potential temperature profile at the CBL appears warmer than the observations by about 0.4 K. The model seriously overestimates the moisture content in the afternoon and overestimates the

删除的内容: desert…exceeds 5000 m, it might …ay not [153]

删除的内容: Figure 9. Figure 9

删除的内容: …). As a result, the PBL of WRF simulations [154]

删除的内容: .

删除的内容: This paper assesses

删除的内容: W

删除的内容: Weather Research and Forecasting Model [155]

删除的内容: Whereas, the more frequently updated LBC is desirable to inhibit model error near the LBC. Air variables (air temperature, relative humidity and 10m wind speed) are closer to measurements than at surface, but their values are relative higher than those observed. However, it is found that discrepancies of thermodynamic surface variables (the surface temperature, sensible and latent fluxes) between model and observation are large during 12h simulation.

删除的内容: Consequently, with the configuration used in this study, t…he model reproduces reasonably well [156]

删除的内容: well

删除的内容: it …he temperature in the near-surface layer at [157]

删除的内容: t

删除的内容: y…es between the model and measurement [158]

删除的内容: struggles to …orrectly simulate [159]

删除的内容: more moist

删除的内容: er…than thos… observed [160]

删除的内容: Theta

删除的内容: P

删除的内容: which …t the CBL appears warmer by [161]

删除的内容: by up to about 0.4K compared to…han the [162]

删除的内容: overestimate

删除的内容: afternoon …oisture content in the afternoon [163] vapor mixing ratio in the CBL by about 1–2 g kg^{-1}. The largest discrepancies are found in 0–3 km layer, where the model vapor mixing ratio is twice as moist as that of the observations (up to about 3 g kg^{-1}).

Three additional simulations were realized to confirm whether the large differences in the sensible heat flux lead to differences in growth of the CBL during the daytime relative to the CTRL experiment. The results suggest that the model results are sensitive to changes in the sensible heat flux and different land surface models. The large difference between the model and observations may lead to differences in the growth of the CBL during the daytime. It was concluded the surface sensible heat flux is an important factor affecting the processes of the CBL over the Taklimakan Desert during the daytime in summer. However, its peak depth during the simulation was less sensitive to the sensible heat flux because w_e had decreased by the end of the day. One should note that the CBL of Taklimakan need several days of favorable environment to reach its super depth (> 4000m), and sustained high temperature and SH is the crucial factor for CBL to develop from shallow to deep CBL. The SH is not dominant factor, but still an important factor affecting the deep CBL.

Future work will study several other examples of a deep CBL over the Taklimakan Desert to determine their common features. We hope to use high-resolution models and observations to describe the fine characteristics of a typical deep CBL over the Taklimakan Desert, particularly the turbulent and vertical mixing and its impact on the regional weather forecast. This research aims to improve our understanding of the deep CBL over the Taklimakan Desert and its influence on the regional weather and climate.

Conflict of interests

删除的内容: by about 1 to 2 g/Kg …n the CBL by about 1–2 ... [164]

删除的内容: above AGL

删除的内容: as observed… ... [165]

删除的内容: Furthermore, two t…hree additional ... [166]

批注 [LP11]: Please give 'ABL' in full (no abbreviation).

删除的内容: A

删除的内容: ,…based on…elative to the CTRL ... [167]

删除的内容: from

删除的内容: -…urface models. The large difference between ... [168]

删除的内容: the …n dominant ... [169]

删除的内容: CBL

删除的内容: depth

删除的内容: summer …he day …ime in summer. However ... [170]

删除的内容: Thus, the large difference between the model and observation may lead to differences in CBL growth during daytime and in its peak depth during the simulation.

删除的内容: The f…uture work aimed to…ill study several ... [171]

删除的内容: by,

删除的内容: is aimed …ims to improve the ... [172]

删除的内容: **Interests**

The authors declare that there is no conflict of interests regarding the publication of this paper.

Acknowledgments

This study is supported by the National Natural Science Foundation of China (Grant no. 41575008 and 41775030). The author thanks the reviewers and editors for their professional advice in improving this paper.

删除的内容: s

删除的内容: con

删除的内容: the State Key Program of

删除的内容: would like to

删除的内容: all

删除的内容: to

删除的内容: e

删除的内容: e

Captions:

Figure 1. Simulation domains used in the ARW model with (a) the terrain height (shaded, units:m), (b) the land use categories for domains D03 and D04 and (c) photograph of the area around Tazhong station.

Figure 2. Horizontal distribution of the geopotential height (solid lines, units: da gpm), wind speed (shaded, units: knots) and wind barbs from the NCEP FNL analysis at 0800 BJT on 1 July 2016 at (a) 850, (b) 700, (c) 500 and (d) 100 hPa.Figure 2. Horizontal distribution of the geopotential height (solid lines, units: da gpm), wind speed (shaded, units: knots) and wind barbs from the NCEP FNL analysis at 0800 BJT on 1 July 2016 at (a) 850, (b) 700, (c) 500 and (d) 100 hPa.

Figure 3. NCEP FNL 700 hPa potential temperature (colors) and mean sea level pressure (white lines) at 0800 BJT on 1 July 2016. The black dot shows the location of Tazhong station in Xingjiang province.

Figure 4. Time series of the initial simulated surface variables from the innermost domain of the simulations and the surface observations at Tazhong station (83.63° E, 39.03° N) at 0800 BJT on 1 July 2016: (a) sensible heat flux; (b) latent heat flux; (c) surface temperature; (d) soil moisture content; (e) temperature at 2 m; (f) relative humidity at 2 m; (g) wind speed at 10 m; and (h) wind direction at 10 m.

Figure 5. Vertical profiles of the potential temperature (solid line, units: K) and vapor mixing ratio (dashed line, units: g kg^{-1}) from the innermost domain of the simulations and the observations from GPS sounding at Tazhong station (83.63° E, 39.03° N) at (a) 1100, (b)

删除的内容: Figure 1. Simulation domains used in the ARW model with (a) the terrain height (shaded, units:m), (b) the land use categories for domains D03 and D04 and (c) photograph of the area around Tazhong station.

删除的内容: Figure 2. Horizontal distribution of the geopotential height (solid lines, units: da gpm), wind speed (shaded, units: knots) and wind barbs from the NCEP FNL analysis at 0800 BJT on 1 July 2016 at (a) 850, (b) 700, (c) 500 and (d) 100 hPa.

删除的内容: Figure 2. Horizontal distribution of the geopotential height (solid lines, units: da gpm), wind speed (shaded, units: knots) and wind barbs from the NCEP FNL analysis at 0800 BJT on 1 July 2016 at (a) 850, (b) 700, (c) 500 and (d) 100 hPa.

带格式的: 字体:11 pt

删除的内容: Figure 3. NCEP FNL 700 hPa potential temperature (colors) and mean sea level pressure (white lines) at 0800 BJT on 1 July 2016. The black dot shows the location of Tazhong station in Xingjiang province.

带格式的: 字体:11 pt

删除的内容: Figure 4. Time series of the initial simulated surface variables from the innermost domain of the simulations and the surface observations at Tazhong station (83.63° E, 39.03° N) at 0800 BJT on 1 July 2016: (a) sensible heat flux; (b) latent heat flux; (c) surface temperature; (d) soil moisture content; (e) temperature at 2 m; (f) relative humidity at 2 m; (g) wind speed at 10 m; and (h) wind direction at 10 m.

1400, (c) 1700 and (d) 2000 BJT on 1 July 2016. The profiles of the model output are averaged over a radius of 3.5 km.

Figure 6. Cross-sections along 39.03° N of the horizontal winds (barbs, units: m s^{-1}) at intervals of 5 m s^{-1} superposed with theta (shaded, units: K) and the vapor mixing ratio (contours, units: g kg^{-1}) from the (a) BDY_T1, (c) BDY_T2 and (e) BDY_T3 experiments at 1400 BJT on 1 July 2016 and the (b) BDY_T1, (d) BDY_T2 and (f) BDY_T3 experiments at 2000 BJT on 1 July 2016.

Figure 7. Instantaneous vertical velocity fields (shading: m s^{-1}) at 3000 m for the (a) BDY_T1 (CTRL), (b) BDY_T2, (c) BDY_T3 and (d) Noah experiments at 1400 BJT on 1 July 2016.

Figure 8. Vertical cross-sections of the instantaneous vertical velocity fields (shading: m s^{-1}) along A1–A2 in for the (a) BDY_T1 (CTRL), (b) BDY_T2, (c) BDY_T3 and (d) Noah experiments at 1400 BJT on 1 July 2016.

Figure 9. Vertical profiles of the potential temperature (solid line, units: K) and vapor mixing ratio (dashed line, units: g kg^{-1}) for the sensible heat flux sensitivity and Noah land surface experiments at (a) 1100, (b) 1400, (c) 1700 and (d) 2000 BJT on 1 July 2016. The profiles of the model output are averaged over a radius of 3.5 km.

Figure 10. Time series of the initial simulated surface variables for the sensible heat flux sensitivity and Noah land surface experiments: (a) sensible heat flux; (b) latent heat flux; (c) surface temperature; (d) soil moisture content; (e) temperature at 2 m; (f) relative humidity at 2 m; (g) wind speed at 10 m; and (h) wind direction at 10 m.

删除的内容: Figure 5. Vertical profiles of the potential temperature (solid line, units: K) and vapor mixing ratio (dashed line, units: g kg^{-1}) from the innermost domain of the simulations and the observations from GPS sounding at Tazhong station (83.63° E, 39.03° N) at (a) 1100, (b) 1400, (c) 1700 and (d) 2000 BJT on 1 July 2016. The profiles of the model output are averaged over a radius of 3.5 km.

删除的内容: Figure 6. Cross-sections along 39.03° N of the horizontal winds (barbs, units: m s^{-1}) at intervals of 5 m s^{-1} superposed with theta (shaded, units: K) and the vapor mixing ratio (contours, units: g kg^{-1}) from the (a) BDY_T1, (c) BDY_T2 and (e) BDY_T3 experiments at 1400 BJT on 1 July 2016 and the (b) BDY_T1, (d) BDY_T2 and (f) BDY_T3 experiments at 2000 BJT on 1 July 2016.

带格式的: 字体:11 pt

删除的内容: Figure 7. Instantaneous vertical velocity fields (shading: m s^{-1}) at 3000 m for the (a) BDY_T1 (CTRL), (b) BDY_T2, (c) BDY_T3 and (d) Noah experiments at 1400 BJT on 1 July 2016.

带格式的: 字体:11 pt

带格式的: 字体:11 pt

删除的内容: Figure 8. Vertical cross-sections of the instantaneous vertical velocity fields (shading: m s^{-1}) along A1–A2 in for the (a) BDY_T1 (CTRL), (b) BDY_T2, (c) BDY_T3 and (d) Noah experiments at 1400 BJT on 1 July 2016.

带格式的: 字体:11 pt

带格式的: 字体:11 pt

删除的内容: Figure 9. Vertical profiles of the potential temperature (solid line, units: K) and vapor mixing ratio (dashed line, units: g kg^{-1}) for the sensible heat flux sensitivity and Noah land surface experiments at (a) 1100, (b) 1400, (c) 1700 and (d) 2000 BJT on 1 July 2016. The profiles of the model output are averaged over a radius of 3.5 km.

带格式的: 字体:11 pt

带格式的: 字体:12 pt

删除的内容: Figure 10. Time series of the initial simulated surface variables for the sensible heat flux sensitivity and ... [173]

带格式的: 字体:12 pt

删除的内容: Figure 1. Simulation domains used in the ARW model with (a) the terrain height (shaded, units: m) ... [174]

带格式的: s1, 字体:(默认) +主题正文 (Calibri), 11 pt, 字体颜色: 自动

带格式的: 两端对齐

带格式的 ... [175]

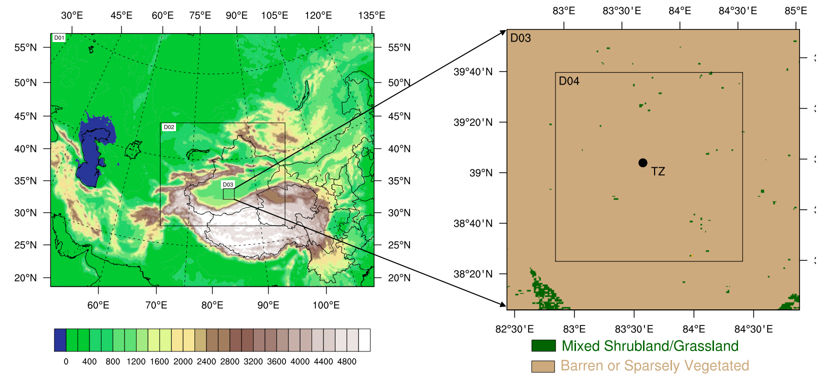

（a） （b）

（c）

Figure 1. Simulation domains used in the ARW model with (a) the terrain height (shaded, units:m), (b) the land use categories for domains D03 and D04 and (c) photograph of the area around Tazhong station.

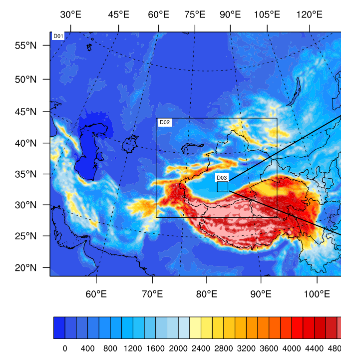

删除的内容:

带格式的: 字体:(默认) Times New Roman, 11 pt, 字体颜色: 文字 1

带格式的: 字体:Times, 11 pt, 字体颜色: 文字 1

带格式的: 字体:(默认) Times, 11 pt, 字体颜色: 文字 1

删除的内容: （a）

（b） ... [176]

删除的内容: Figure 1.

带格式的: 字体:11 pt

带格式的: 字体:11 pt, 检查拼写和语法

带格式的: 字体:11 pt

删除的内容: ;

删除的内容: ;

批注 [LP12]: Please check that all lettering is clearly visible on the original artwork.

带格式的: 字体:11 pt

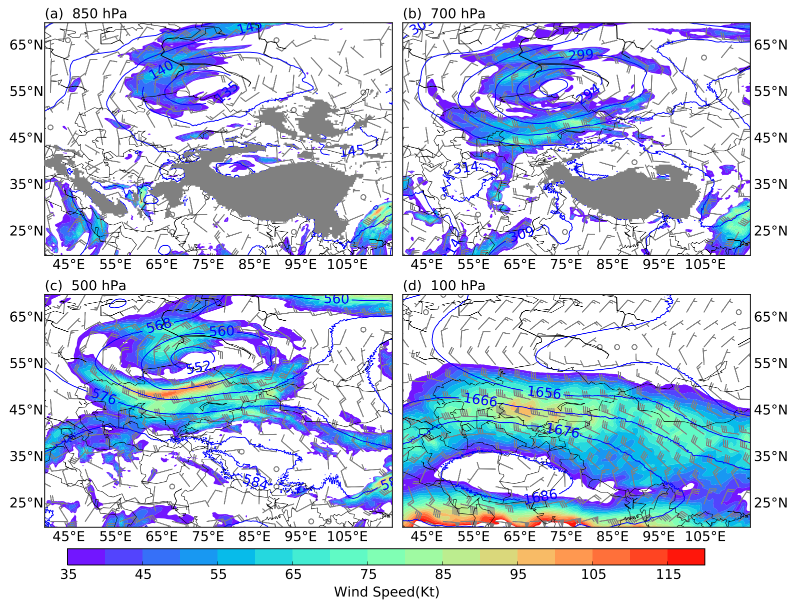

Figure 2. Horizontal distribution of the geopotential height (solid lines, units: da gpm), wind speed (shaded, units: knots) and wind barbs from the NCEP FNL analysis at 0800 BJT on 1 July 2016 at (a) 850, (b) 700, (c) 500 and (d) 100 hPa.

带格式的: 字体:(默认) Times, 11 pt, 字体颜色: 文字 1

批注 [LP13]: Are units for geopotential height correct?

删除的内容: Figure 2.

带格式的: 字体:11 pt

带格式的: 字体:11 pt, 检查拼写和语法

带格式的: 字体:11 pt

带格式的: 字体:11 pt

删除的内容: ,

删除的内容: hPa

删除的内容: c

删除的内容: hPa

删除的内容: e

删除的内容: hPa,

带格式的: 字体:11 pt

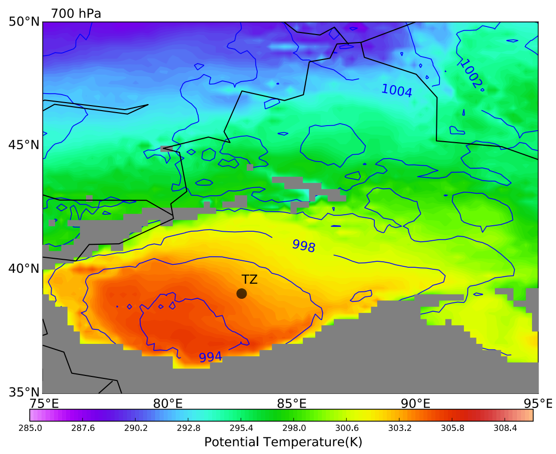

Figure 3. NCEP FNL 700 hPa potential temperature (colors) and mean sea level pressure (white lines) at 0800 BJT on 1 July 2016. The black dot shows the location of Tazhong station in Xingjiang province.

已移动(插入) [3]

带格式的: 字体:(默认) Times, 11 pt, 字体颜色: 文字 1

带格式的: 居中

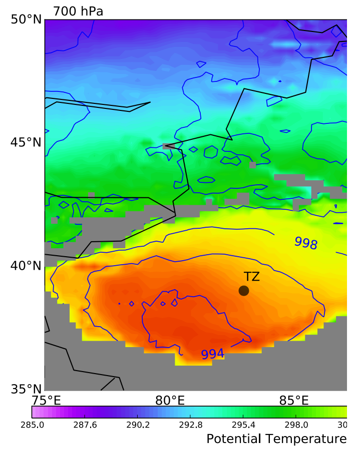

已上移 [3]:

删除的内容:

带格式的: 字体:(默认) Times, 11 pt, 字体颜色: 文字 1

带格式的: 字体:(默认) +主题正文 (Calibri), 字体颜色: 自动

带格式的: 正文

删除的内容: Figure 3.

带格式的 ... [177]

删除的内容: fnl

批注 [LP14]: Is 'white lines' correct here?

带格式的 ... [178]

删除的内容: at

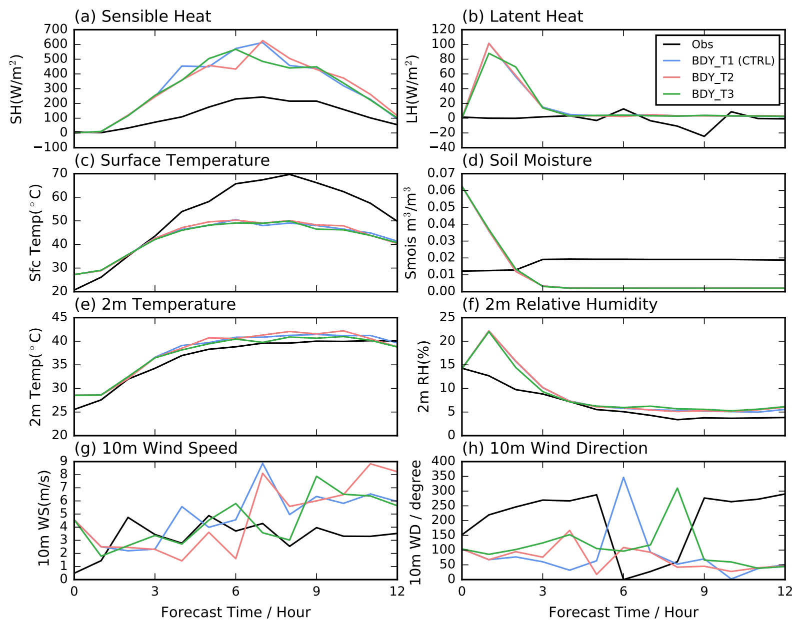

Figure 4. Time series of the initial simulated surface variables from the innermost domain of the simulations and the surface observations at Tazhong station (83.63° E, 39.03° N) at 0800 BJT on 1 July 2016: (a) sensible heat flux; (b) latent heat flux; (c) surface temperature; (d) soil moisture content; (e) temperature at 2 m; (f) relative humidity at 2 m; (g) wind speed at 10 m; and (h) wind direction at 10 m.

带格式的：字体颜色：文字 1

带格式的：居中

删除的内容：Figure 4.

删除的内容：initial

删除的内容：0

删除的内容：(W/m^2),

删除的内容：(W/m^2),

删除的内容：2-m

删除的内容：(∘C),

删除的内容：(d) surface temperature (∘C),

删除的内容：e

删除的内容：2-m

删除的内容：(%) and

删除的内容：f

删除的内容：10-m

删除的内容：

批注 [LP15]: The caption has been amended to match the graphs in Fig. 4 – please check and confirm that the parts are now labelled correctly Please also check all text citation of the parts of Fig. 4 and confirm that these are correct.

删除的内容：(m/s)

删除的内容：with corresponding observations

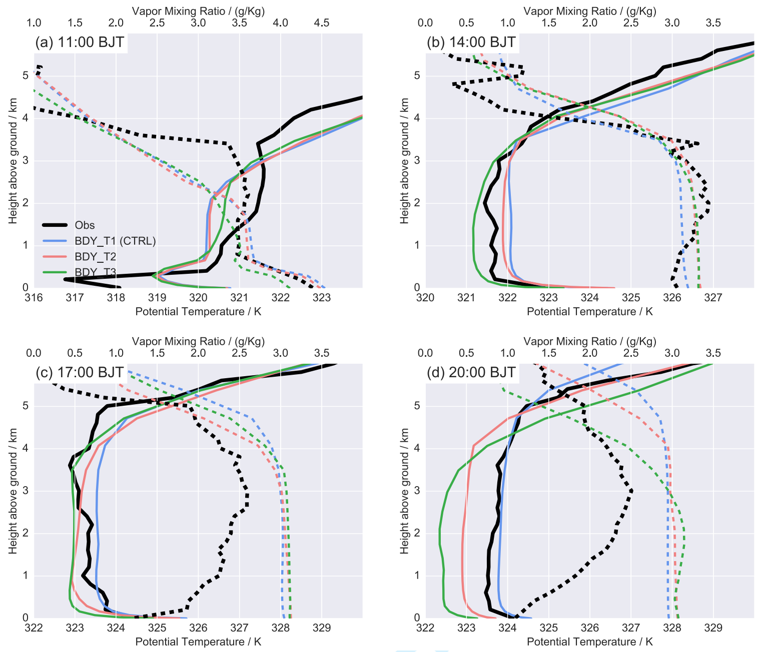

Figure 5. Vertical profiles of the potential temperature (solid line, units: K) and vapor mixing ratio (dashed line, units: g kg^{-1}) from the innermost domain of the simulations and the observations from GPS sounding at Tazhong station (83.63° E, 39.03° N) at (a) 1100, (b) 1400, (c) 1700 and (d) 2000 BJT on 1 July 2016. The profiles of the model output are averaged over a radius of 3.5 km.

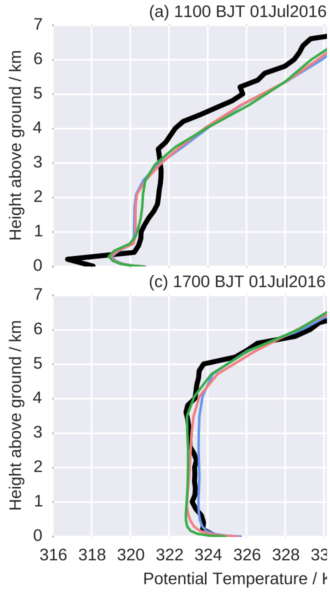

删除的内容:

带格式的: 字体:(默认) Times, 11 pt, 字体颜色: 文字 1

带格式的: 字体:(默认) Times New Roman, 11 pt, 字体颜色: 文字 1

带格式的: 行距: 1.5 倍行距

删除的内容: Figure 54.

删除的内容: /K

删除的内容: of

删除的内容: 0

删除的内容: in

删除的内容: ,

删除的内容: 分页

带格式的: 字体:11 pt, 字体颜色: 文字 1

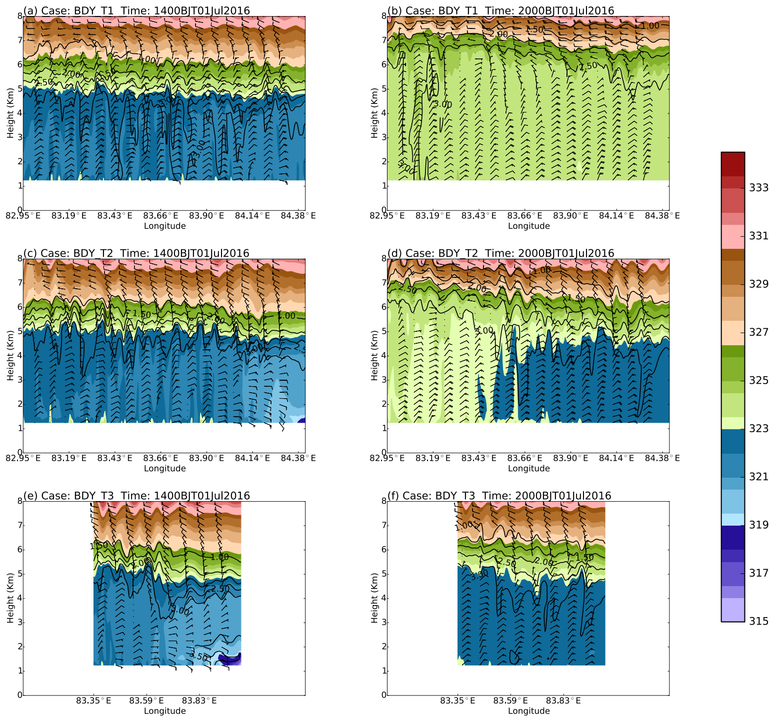

Figure 6. Cross-sections along 39.03° N of the horizontal winds (barbs, units: m s^{-1}) at intervals of 5 m s^{-1} superposed with theta (shaded, units: K) and the vapor mixing ratio (contours, units: g kg^{-1}) from the (a) BDY_T1, (c) BDY_T2 and (e) BDY_T3 experiments at 1400 BJT on 1 July 2016 and the (b) BDY_T1, (d) BDY_T2 and (f) BDY_T3 experiments at 2000 BJT on 1 July 2016

带格式的: 字体:(默认) Times, 11 pt, 字体颜色: 文字 1

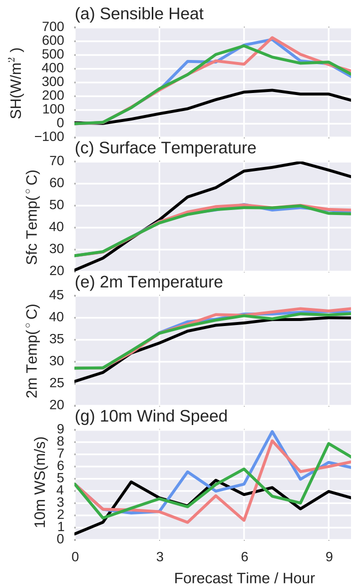

删除的内容: ... [179]

带格式的 ... [180]

带格式的: 行距: 1.5 倍行距

删除的内容: Figure 6.

带格式的 ... [181]

删除的内容: Figure 7

删除的内容: c…oss-sections sections…along 39.03° N of ... [182]

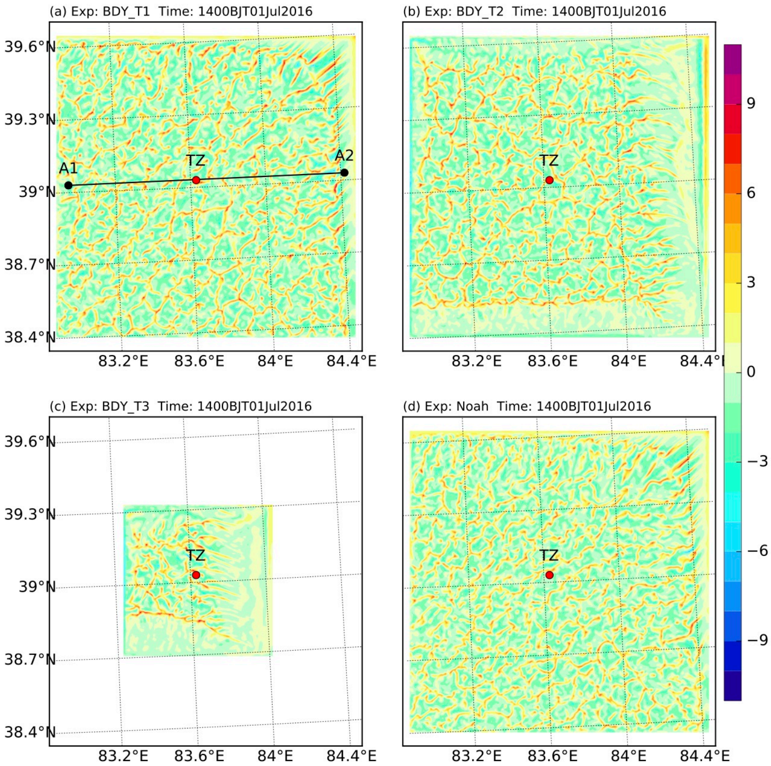

Figure 7. Instantaneous vertical velocity fields (shading: m s^{-1}) at 3000 m for the (a) BDY_T1 (CTRL), (b) BDY_T2, (c) BDY_T3 and (d) Noah experiments at 1400 BJT on 1 July 2016.

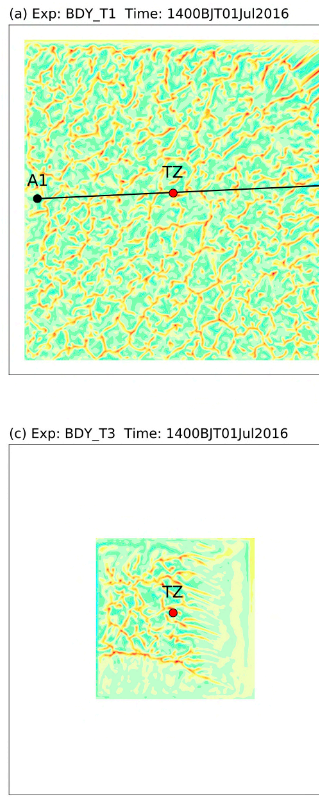

删除的内容:

带格式的: 字体颜色: 文字 1

带格式的: 字体:(默认) +主题正文 (Calibri), 10.5 pt, 字体颜色: 自动

带格式的: 正文

删除的内容: Figure 7.

带格式的: 字体:11 pt

删除的内容: /

删除的内容: ,

删除的内容: ,

删除的内容:

带格式的: 字体:11 pt

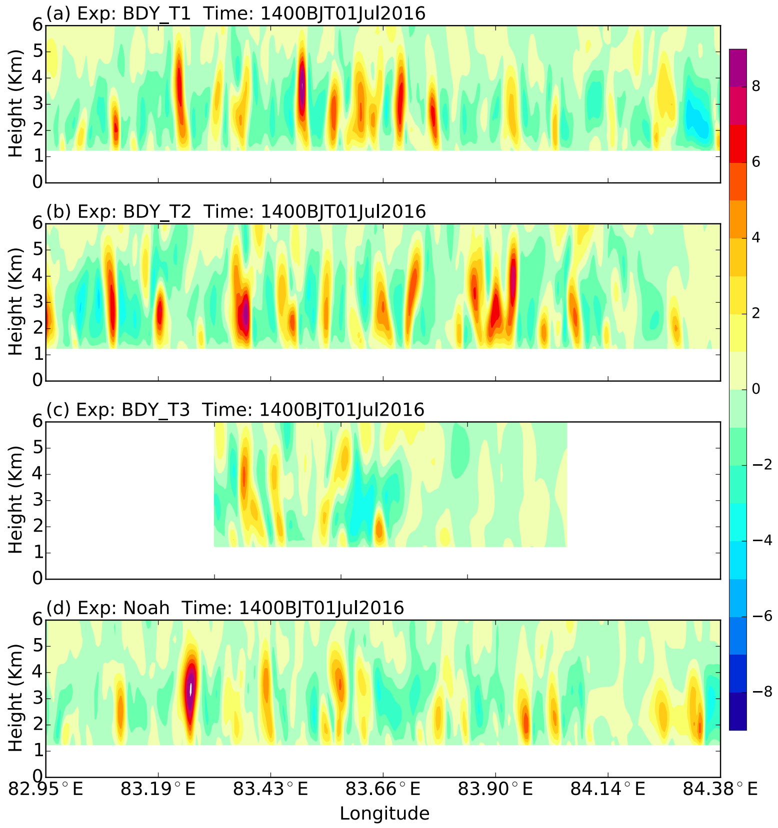

Figure 8. Vertical cross-sections of the instantaneous vertical velocity fields (shading: m s^{-1}) along A1–A2 in for the (a) BDY_T1 (CTRL), (b) BDY_T2, (c) BDY_T3 and (d) Noah experiments at 1400 BJT on 1 July 2016.

带格式的：字体:(默认) Times, 12 pt, 字体颜色: 文字 1

带格式的：字体:11 pt

带格式的：行距： 1.5 倍行距

删除的内容: Figure 8.

带格式的：字体:11 pt

带格式的：字体:11 pt

删除的内容: /

删除的内容: -

删除的内容: for

删除的内容: ,

删除的内容: ,

删除的内容: .

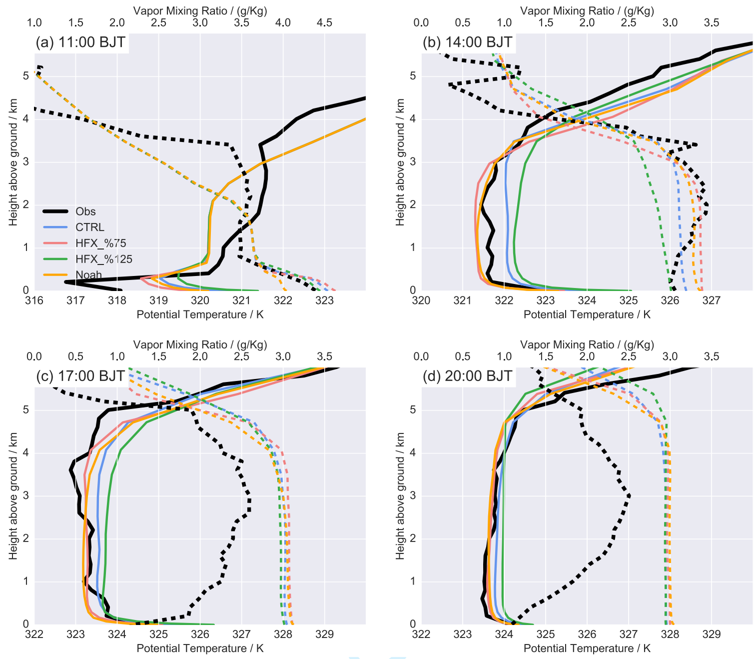

Figure 9. Vertical profiles of the potential temperature (solid line, units: K) and vapor mixing ratio (dashed line, units: g kg^{-1}) for the sensible heat flux sensitivity and Noah land surface experiments at (a) 1100, (b) 1400, (c) 1700 and (d) 2000 BJT on 1 July 2016. The profiles of the model output are averaged over a radius of 3.5 km.

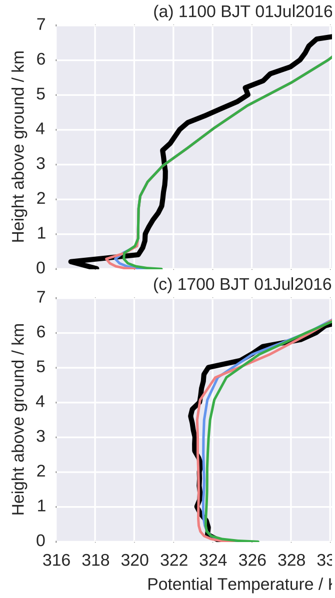

删除的内容:

带格式的: 字体:(默认) Times New Roman, (中文) SimSun, 11 pt, 字体颜色: 文字 1

带格式的: 字体:(默认) Times, 11 pt, 字体颜色: 文字 1

删除的内容: Figure 98

带格式的: 字体:11 pt

带格式的: 字体:11 pt

批注 [LP16]: This caption has been edited for clarity – please check and confirm meaning is now correct.

带格式的: 字体:11 pt

删除的内容: The same as Figure 5Figure 4, but for SH flux sensitive and Noah land-surface experiment

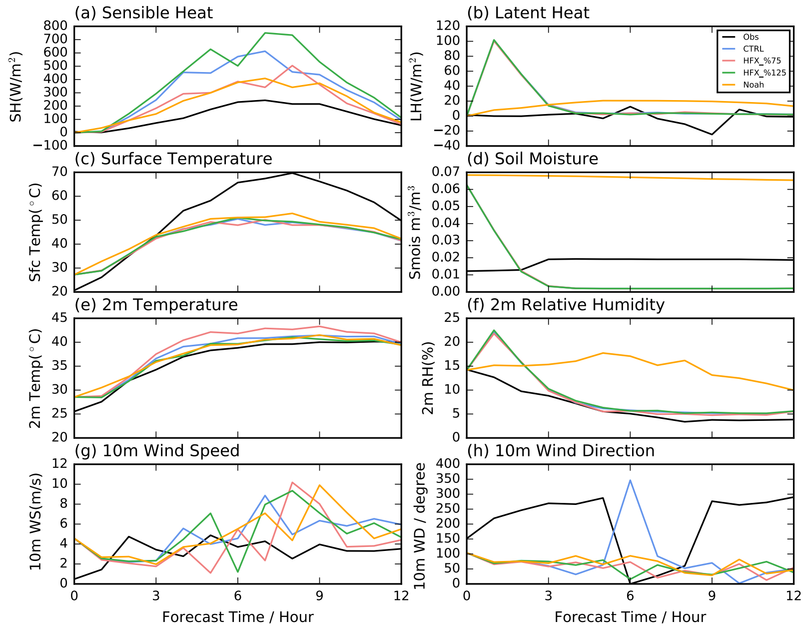

Figure 10. Time series of the initial simulated surface variables for the sensible heat flux sensitivity and Noah land surface experiments: (a) sensible heat flux; (b) latent heat flux; (c) surface temperature; (d) soil moisture content; (e) temperature at 2 m; (f) relative humidity at 2 m; (g) wind speed at 10 m; and (h) wind direction at 10 m.

带格式的：字体颜色：文字 1

删除的内容: Figure 108.

带格式的：字体:12 pt

带格式的：字体:12 pt，检查拼写和语法

带格式的：字体:12 pt

批注 [LP17]: The caption has been amended to match the graphs in Fig. 10 – please check and confirm that the parts are now labelled correctly. Please also check all text citation of the parts of Fig. 10 and confirm that these are correct. This caption has been edited for clarity – please check and confirm meaning is now correct.

带格式的：字体:12 pt

带格式的：字体:12 pt

删除的内容: The same as Figure 4, but for SH flux sensitive and Noah land-surface experiment.

Experiment	Name	Remarks
1	BDY_T1(CTRL)	LBC of D04 is provided by d03 every one hour with 403 × 406 model grids
2	BDY_T2	As BDY_T1, but LBC of D04 is provided by d03 every six hours
3	BDY_T3	As BDY_T2, but with 205 ×208 model grids
4	HFX_%75	As CTRL_T2, but with a sensible heat flux of 75%
5	HFX_%125	As CTRL_T2, but with a sensible heat flux of 125%
6	Noah	As CTRL_T2, but with the Noah land surface model

Table 1. List of designed experiments.

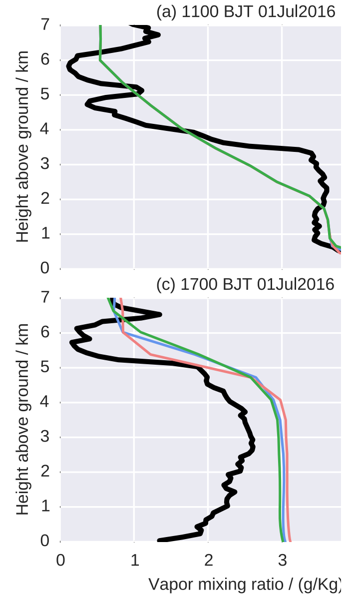

删除的内容: [183]

带格式的: 字体:(默认) Times New Roman, 11 pt, 字体颜色: 文字 1

删除的内容: 1 …ne hour with model grids [184]

删除的内容: 403X406

删除的内容: x

删除的内容: 6

删除的内容: model grids …05 ×x …08. [185]

删除的内容: SH… sensible heat flux of 75%. [186]

删除的内容: SH …25% . [187]

删除的内容: 3

删除的内容: BDY_T3

删除的内容: surface-…and surface model. [188]

删除的内容: As BDY_T2, but with model grids 205 X 208.

Experiments	Sensible heat flux		Latent heat flux		Surface temperature		Soil moisture content		Temperature at 2 m		Relative humidity at 2 m		Wind speed at 2 m	
	RMSE	BIAS	RMSE	BIAS	RMSE	BIAS	RMSE	BIAS	RMSE	BIAS	RMSE	BIAS	RMSE	BIAS
CTRL	263.636	250.140	12.398	6.674	14.654	−13.373	0.017	−0.017	1.666	1.613	1.220	1.109	2.579	1.864
BDY_T2	249.395	240.660	12.383	6.253	14.116	−12.853	0.017	−0.017	1.912	1.817	1.275	1.162	2.943	1.307
BDY_T3	241.681	232.705	12.251	6.328	14.929	−13.737	0.017	−0.017	1.227	1.046	1.483	1.280	2.118	1.287
HFX_%75	151.119	134.594	12.544	6.354	14.740	−13.426	0.017	−0.017	3.078	3.016	0.956	0.826	3.335	0.874
HFX_%125	357.711	335.556	12.439	6.152	14.244	−13.043	0.017	−0.017	1.026	0.860	1.303	1.231	3.265	2.052
Noah	125.695	120.313	23.350	20.664	12.757	−11.502	0.048	0.048	1.046	0.983	10.116	9.904	2.788	1.795

Table 2. Summary of the verification of surface and air variables including the integration hours from 3 to 12 h for Tazhong station.

删除的内容: H
删除的内容: H…eat fluxt ... [189]
删除的内容: T
删除的内容: M
删除的内容: 2m
删除的内容: 2m …elative H ... [190]
删除的内容: 10m …ind S ... [191]
删除的内容:
删除的内容: …63.636 ... [192]
删除的内容:
删除的内容:
删除的内容: ….674 ... [193]
删除的内容:
删除的内容: -…13.373 ... [194]
删除的内容: ….017 ... [195]
删除的内容: -…0.017 ... [196]
删除的内容: ….666 ... [197]
删除的内容: ….613 ... [198]
删除的内容: ….220 ... [199]
删除的内容: ….109 ... [200]
删除的内容: ….579 ... [201]
删除的内容: ….864 ... [202]
删除的内容:
删除的内容: …49.395 ... [203]
删除的内容:
删除的内容:
删除的内容: ….253 ... [204]
删除的内容:
删除的内容: -…12.853 ... [205]
删除的内容: ….017 ... [206]
... [207]
... [208]
... [209]
... [210]
... [211]

Reference:

Chen, F., and J. Dudhia, 2001a: Coupling an Advanced Land Surface–Hydrology Model with the Penn State–NCAR MM5 Modeling System. Part II: Preliminary Model Validation. *Monthly Weather Review*, **129,** 587-604.

——, 2001b: Coupling an advanced land surface-hydrology model with the Penn State-NCAR MM5 modeling system. Part I: Model implementation and sensitivity. *Monthly Weather Review*, **129,** 569-585.

Dudhia, J., 1989: Numerical study of convection observed during the winter monsoon experiment using a mesoscale two-dimensional model. *J. Atmos. Sci.*, **46,** 3077-3107.

Engelstaedter, S., R. Washington, C. Flamant, D. J. Parker, C. J. T. Allen, and M. C. Todd, 2015: The Saharan heat low and moisture transport pathways in the central Sahara—Multiaircraft observations and Africa-LAM evaluation. *Journal of Geophysical Research: Atmospheres*, **120,** 2015JD023123.

Garcia-Carreras, L., and Coauthors, 2015: The Turbulent Structure and Diurnal Growth of the Saharan Atmospheric Boundary Layer. *Journal of the Atmospheric Sciences*, **72,** 693-713.

Han, B., S. Lü, and Y. Ao, 2012: Development of the convective boundary layer capping with a thick neutral layer in Badanjilin: Observations and simulations. *Adv. Atmos. Sci.*, **29,** 177-192.

Heinold, B., P. Knippertz, and J. H. Marsham, 2013: Large Eddy Simulations of Nocturnal Low-Level Jets over Desert Regions and Implications for Dust Emission. *EGU General Assembly Conference*.

Heinold, B., P. Knippertz, and R. J. Beare, 2015: Idealized large-eddy simulations of nocturnal low-level jets over subtropical desert regions and implications for dust-generating winds. *Quarterly Journal of the Royal Meteorological Society*, **141,** 1740–1752.

Heinze, R., D. Mironov, and S. Raasch, 2015: Second-moment budgets in cloud topped boundary layers: A large-eddy simulation study. *Journal of Advances in Modeling Earth Systems*, **7,** 510-536.

Hong, S.-Y., and H.-L. Pan, 1996: Nonlocal boundary layer vertical diffusion in a medium-range forecast model. *Monthly weather review*, **124,** 2322-2339.

Hong, S.-Y., and J.-O. J. Lim, 2006: The WRF single-moment 6-class microphysics scheme (WSM6). *J. Korean Meteor. Soc*, **42,** 129-151.

Hu, X.-M., J. W. Nielsen-Gammon, and F. Zhang, 2010: Evaluation of Three Planetary Boundary Layer Schemes in the WRF Model. *Journal of Applied Meteorology and Climatology*, **49,** 1831-1844.

Kain, J. S., 1993: Convective parameterization for mesoscale models: The Kain-Fritsch scheme. *The representation of cumulus convection in numerical models, Meteor. Monogr*, **46,** 165-170.

Kain, J. S., 2004: The Kain–Fritsch Convective Parameterization: An Update. *JOURNAL OF APPLIED METEOROLOGY*, **43,** 170-181.

LeMone, M. A., M. Tewari, F. Chen, and J. Dudhia, 2013: Objectively Determined Fair-Weather CBL Depths in the ARW-WRF Model and Their Comparison to CASES-97 Observations. *Monthly Weather Review*, **141,** 30-54.

Liu, Y., Q. He, H. Zhang, and A. Mamtimin, 2012: Improving the CoLM in Taklimakan Desert hinterland with accurate key parameters and an appropriate parameterization scheme. *Adv. Atmos. Sci.*, **29,** 381-390.

Liu, Y., and Coauthors, 2011: Simultaneous nested modeling from the synoptic scale to the LES scale for wind energy applications. *Journal of Wind Engineering and Industrial Aerodynamics*, **99,** 308-319.

Marsham, J. H., P. Knippertz, N. Dixon, D. J. Parker, and G. M. S. Lister, 2011: The importance of the representation of deep convection for modeled dust- generating winds over West Africa during summer. *Geophysical Research Letters*, **38**.

删除的内容: ... [257]

Mlawer, E. J., S. J. Taubman, P. D. Brown, M. J. Iacono, and S. A. Clough, 1997: Radiative transfer for inhomogeneous atmospheres: RRTM, a validated correlated-k model for the longwave. *J. Geophys. Res.*, **102,** 16663-16682.

Moeng, C.-H., J. Dudhia, J. Klemp, and P. Sullivan, 2007: Examining Two-Way Grid Nesting for Large Eddy Simulation of the PBL Using the WRF Model. *Monthly Weather Review*, **135,** 2295-2311.

National Centers for Environmental Prediction, N. W. S. N. U. S. D. o. C., 2015: NCEP GDAS/FNL 0.25 Degree Global Tropospheric Analyses and Forecast Grids. Research Data Archive at the National Center for Atmospheric Research, Computational and Information Systems Laboratory.

Rai, R. K., L. K. Berg, B. Kosović, J. D. Mirocha, M. S. Pekour, and W. J. Shaw, 2017: Comparison of Measured and Numerically Simulated Turbulence Statistics in a Convective Boundary Layer Over Complex Terrain. *Boundary-Layer Meteorology*, **163,** 69-89.

Schicker, I., D. Arnold Arias, and P. Seibert, 2016: Influences of updated land-use datasets on WRF simulations for two Austrian regions. *Meteorology and Atmospheric Physics*, **128,** 279-301.

Shin, H. H., and S. Y. Hong, 2011: Intercomparison of Planetary Boundary-Layer Parametrizations in the WRF Model for a Single Day from CASES-99. *Boundary-Layer Meteorology*, **139,** 261-281.

Shin, H. H., and S.-Y. Hong, 2015: Representation of the Subgrid-Scale Turbulent Transport in Convective Boundary Layers at Gray-Zone Resolutions. *Monthly Weather Review*, **143,** 250-271.

Skamarock, W. C., and Coauthors, 2008: A Description of the Advanced Research WRF Version 3. . *NCAR/TN–475+STR, NCAR TECHNICAL NOTE*.

Smirnova Tatiana, G., M. Brown John, G. Benjamin Stanley, and D. Kim, 2000: Parameterization of cold- season processes in the MAPS land- surface scheme. *Journal of Geophysical Research: Atmospheres*, **105,** 4077-4086.

Smirnova, T. G., J. M. Brown, and S. G. Benjamin, 1997: Performance of Different Soil Model Configurations in Simulating Ground Surface Temperature and Surface Fluxes. *Monthly Weather Review*, **125,** 1870-1884.

Stull, R. B., 1988: An Introduction to Boundary Layer Meteorology. *Atmospheric Sciences Library*, **8,** 89.

Sun, J., and Q. Xu, 2009: Parameterization of Sheared Convective Entrainment in the First-Order Jump Model: Evaluation Through Large-Eddy Simulation. *Boundary-Layer Meteorology*, **132,** 279-288.

Talbot, C., E. Bou-Zeid, and J. Smith, 2012: Nested Mesoscale Large-Eddy Simulations with WRF: Performance in Real Test Cases. *Journal of Hydrometeorology*, **13,** 1421-1441.

ter Maat, H. W., E. J. Moors, R. W. A. Hutjes, A. A. M. Holtslag, and A. J. Dolman, 2012: Exploring the Impact of Land Cover and Topography on Rainfall Maxima in the Netherlands. *Journal of Hydrometeorology*, **14,** 524-542.

WANG, and Coauthors, 2016a: Summer atmospheric boundary layer structure in the hinterland of Taklimakan Desert, China. *Journal of Arid Land*, **8,** 846-860.

Wang, M., X. Xu, and H. Xu: The possible influence of the summertime deep atmospheric boundary layer process over the Taklimakan Desert on the regional weather. *(submitted to Quarterly Journal of the Royal Meteorological Society)*.

Wang, M. Z., H. Lu, H. Ming, and J. Zhang, 2016b: Vertical structure of summer clear-sky atmospheric boundary layer over the hinterland and southern margin of Taklamakan Desert: The deep convective boundary layer of Taklamakan Desert. *Meteorological Applications*, **23,** 438-447.

Zhang, F., Z. Pu, and C. Wang, 2017: Effects of Boundary Layer Vertical Mixing on the Evolution of Hurricanes over Land. *Monthly Weather Review*, **145,** 2343-2361.

删除的内容: .

删除的内容: ... [258]

页 1: [1] 删除的内容	LucidPapers	2018/6/20 PM2:01:00

页 1: [2] 删除的内容	LucidPapers	2018/6/20 PM2:00:00

页 1: [3] 删除的内容	Microsoft Office User	2018/4/14 AM10:39:00

页 2: [4] 删除的内容	LucidPapers	2018/6/19 PM3:49:00

During the summer season over Taklimakan Desert, the

页 2: [4] 删除的内容	LucidPapers	2018/6/19 PM3:49:00

During the summer season over Taklimakan Desert, the

页 2: [4] 删除的内容	LucidPapers	2018/6/19 PM3:49:00

During the summer season over Taklimakan Desert, the

页 2: [4] 删除的内容 LucidPapers 2018/6/19 PM3:49:00

During the summer season over Taklimakan Desert, the

页 2: [4] 删除的内容 LucidPapers 2018/6/19 PM3:49:00

During the summer season over Taklimakan Desert, the

页 2: [4] 删除的内容 LucidPapers 2018/6/19 PM3:49:00

During the summer season over Taklimakan Desert, the

页 2: [4] 删除的内容 LucidPapers 2018/6/19 PM3:49:00

During the summer season over Taklimakan Desert, the

页 2: [4] 删除的内容 LucidPapers 2018/6/19 PM3:49:00

During the summer season over Taklimakan Desert, the

页 2: [4] 删除的内容 LucidPapers 2018/6/19 PM3:49:00

During the summer season over Taklimakan Desert, the

页 2: [4] 删除的内容 LucidPapers 2018/6/19 PM3:49:00

During the summer season over Taklimakan Desert, the

页 2: [4] 删除的内容	LucidPapers	2018/6/19 PM3:49:00

During the summer season over Taklimakan Desert, the

页 2: [4] 删除的内容	LucidPapers	2018/6/19 PM3:49:00

During the summer season over Taklimakan Desert, the

页 2: [4] 删除的内容	LucidPapers	2018/6/19 PM3:49:00

During the summer season over Taklimakan Desert, the

页 2: [4] 删除的内容	LucidPapers	2018/6/19 PM3:49:00

During the summer season over Taklimakan Desert, the

页 2: [4] 删除的内容	LucidPapers	2018/6/19 PM3:49:00

During the summer season over Taklimakan Desert, the

页 2: [5] 删除的内容	Microsoft Office 用户	2018/6/22 AM9:39:00

p

页 2: [5] 删除的内容	Microsoft Office 用户	2018/6/22 AM9:39:00

p

页 2: [6] 删除的内容	LucidPapers	2018/6/19 PM3:50:00

)

页 2: [6] 删除的内容	LucidPapers	2018/6/19 PM3:50:00

)

页 2: [6] 删除的内容	LucidPapers	2018/6/19 PM3:50:00

)

页 2: [6] 删除的内容	LucidPapers	2018/6/19 PM3:50:00

)

页 2: [6] 删除的内容	LucidPapers	2018/6/19 PM3:50:00

)

页 2: [6] 删除的内容	LucidPapers	2018/6/19 PM3:50:00

)

页 2: [6] 删除的内容	LucidPapers	2018/6/19 PM3:50:00

)

页 2: [6] 删除的内容	LucidPapers	2018/6/19 PM3:50:00

)

页 2: [6] 删除的内容	LucidPapers	2018/6/19 PM3:50:00

)

页 2: [6] 删除的内容	LucidPapers	2018/6/19 PM3:50:00

)

页 2: [6] 删除的内容	LucidPapers	2018/6/19 PM3:50:00

)

页 2: [6] 删除的内容	LucidPapers	2018/6/19 PM3:50:00

)

页 2: [6] 删除的内容	LucidPapers	2018/6/19 PM3:50:00

)

页 2: [6] 删除的内容	LucidPapers	2018/6/19 PM3:50:00

)

页 2: [6] 删除的内容	LucidPapers	2018/6/19 PM3:50:00

)

页 2: [6] 删除的内容	LucidPapers	2018/6/19 PM3:50:00

)

页 2: [6] 删除的内容	LucidPapers	2018/6/19 PM3:50:00

)

页 2: [6] 删除的内容	LucidPapers	2018/6/19 PM3:50:00

)

页 2: [6] 删除的内容	LucidPapers	2018/6/19 PM3:50:00

)

页 2: [6] 删除的内容	LucidPapers	2018/6/19 PM3:50:00

)

页 2: [6] 删除的内容	LucidPapers	2018/6/19 PM3:50:00

)

页 2: [6] 删除的内容	LucidPapers	2018/6/19 PM3:50:00

)

页 2: [6] 删除的内容	LucidPapers	2018/6/19 PM3:50:00

)

页 2: [6] 删除的内容	LucidPapers	2018/6/19 PM3:50:00

)

页 2: [6] 删除的内容	LucidPapers	2018/6/19 PM3:50:00

)

页 2: [6] 删除的内容	LucidPapers	2018/6/19 PM3:50:00

)

页 2: [6] 删除的内容	LucidPapers	2018/6/19 PM3:50:00

)

页 2: [6] 删除的内容	LucidPapers	2018/6/19 PM3:50:00

)

页 2: [6] 删除的内容	LucidPapers	2018/6/19 PM3:50:00

)

页 2: [6] 删除的内容	LucidPapers	2018/6/19 PM3:50:00

)

页 2: [7] 删除的内容	LucidPapers	2018/6/19 PM3:54:00

c

页 2: [7] 删除的内容	LucidPapers	2018/6/19 PM3:54:00

c

页 2: [7] 删除的内容 LucidPapers 2018/6/19 PM3:54:00

c

页 2: [7] 删除的内容 LucidPapers 2018/6/19 PM3:54:00

c

页 2: [7] 删除的内容 LucidPapers 2018/6/19 PM3:54:00

c

页 2: [7] 删除的内容 LucidPapers 2018/6/19 PM3:54:00

c

页 2: [7] 删除的内容 LucidPapers 2018/6/19 PM3:54:00

c

页 2: [8] 删除的内容 Microsoft Office User 2018/4/14 AM10:48:00

a reduction(increment) in SH decreases(increases) maximum PBL by roughly 15% over desert.

页 2: [8] 删除的内容 Microsoft Office User 2018/4/14 AM10:48:00

a reduction(increment) in SH decreases(increases) maximum PBL by roughly 15% over desert.

页 2: [9] 删除的内容	LucidPapers	2018/6/19 PM3:55:00

very

页 2: [9] 删除的内容	LucidPapers	2018/6/19 PM3:55:00

very

页 2: [9] 删除的内容	LucidPapers	2018/6/19 PM3:55:00

very

页 2: [9] 删除的内容	LucidPapers	2018/6/19 PM3:55:00

very

页 2: [9] 删除的内容	LucidPapers	2018/6/19 PM3:55:00

very

页 2: [9] 删除的内容	LucidPapers	2018/6/19 PM3:55:00

very

页 2: [9] 删除的内容	LucidPapers	2018/6/19 PM3:55:00

very

页 2: [10] 删除的内容	LucidPapers	2018/6/19 AM10:59:00

SH

页 2: [10] 删除的内容	LucidPapers	2018/6/19 AM10:59:00

SH

页 2: [10] 删除的内容	LucidPapers	2018/6/19 AM10:59:00

SH

页 2: [10] 删除的内容	LucidPapers	2018/6/19 AM10:59:00

SH

页 2: [10] 删除的内容	LucidPapers	2018/6/19 AM10:59:00

SH

页 2: [10] 删除的内容	LucidPapers	2018/6/19 AM10:59:00

SH

页 2: [10] 删除的内容	LucidPapers	2018/6/19 AM10:59:00

SH

页 2: [10] 删除的内容	LucidPapers	2018/6/19 AM10:59:00

SH

页 3: [11] 删除的内容	LucidPapers	2018/6/19 AM9:48:00

,

页 3: [11] 删除的内容	LucidPapers	2018/6/19 AM9:48:00

,

页 3: [11] 删除的内容	LucidPapers	2018/6/19 AM9:48:00

,

页 3: [11] 删除的内容	LucidPapers	2018/6/19 AM9:48:00

,

页 3: [11] 删除的内容	LucidPapers	2018/6/19 AM9:48:00

,

页 3: [11] 删除的内容	LucidPapers	2018/6/19 AM9:48:00

,

页 3: [11] 删除的内容	LucidPapers	2018/6/19 AM9:48:00

,

页 3: [11] 删除的内容	LucidPapers	2018/6/19 AM9:48:00

,

页 3: [11] 删除的内容	LucidPapers	2018/6/19 AM9:48:00

,

页 3: [12] 删除的内容	LucidPapers	2018/6/19 AM9:58:00

making it probably

页 3: [12] 删除的内容	LucidPapers	2018/6/19 AM9:58:00

making it probably

页 3: [12] 删除的内容	LucidPapers	2018/6/19 AM9:58:00

making it probably

页 3: [12] 删除的内容	LucidPapers	2018/6/19 AM9:58:00

making it probably

页 3: [12] 删除的内容 LucidPapers 2018/6/19 AM9:58:00

making it probably

页 3: [12] 删除的内容 LucidPapers 2018/6/19 AM9:58:00

making it probably

页 3: [13] 删除的内容 LucidPapers 2018/6/19 AM9:59:00

o

页 3: [13] 删除的内容 LucidPapers 2018/6/19 AM9:59:00

o

页 3: [13] 删除的内容 LucidPapers 2018/6/19 AM9:59:00

o

页 3: [13] 删除的内容 LucidPapers 2018/6/19 AM9:59:00

o

页 3: [14] 删除的内容 LucidPapers 2018/6/19 AM10:13:00

,

页 3: [14] 删除的内容	LucidPapers	2018/6/19 AM10:13:00

,

页 3: [14] 删除的内容	LucidPapers	2018/6/19 AM10:13:00

,

页 3: [14] 删除的内容	LucidPapers	2018/6/19 AM10:13:00

,

页 3: [14] 删除的内容	LucidPapers	2018/6/19 AM10:13:00

,

页 3: [14] 删除的内容	LucidPapers	2018/6/19 AM10:13:00

,

页 3: [14] 删除的内容	LucidPapers	2018/6/19 AM10:13:00

,

页 3: [14] 删除的内容	LucidPapers	2018/6/19 AM10:13:00

,

页 3: [14] 删除的内容	LucidPapers	2018/6/19 AM10:13:00

,

页 3: [14] 删除的内容	LucidPapers	2018/6/19 AM10:13:00

,

页 3: [14] 删除的内容	LucidPapers	2018/6/19 AM10:13:00

,

页 3: [14] 删除的内容	LucidPapers	2018/6/19 AM10:13:00

,

页 3: [14] 删除的内容	LucidPapers	2018/6/19 AM10:13:00

,

页 3: [14] 删除的内容	LucidPapers	2018/6/19 AM10:13:00

,

页 3: [14] 删除的内容	LucidPapers	2018/6/19 AM10:13:00

,

页 3: [14] 删除的内容	LucidPapers	2018/6/19 AM10:13:00

,

页 3: [14] 删除的内容	LucidPapers	2018/6/19 AM10:13:00

,

页 3: [14] 删除的内容	LucidPapers	2018/6/19 AM10:13:00

,

页 3: [14] 删除的内容	LucidPapers	2018/6/19 AM10:13:00

,

页 3: [14] 删除的内容	LucidPapers	2018/6/19 AM10:13:00

,

页 3: [15] 删除的内容	LucidPapers	2018/6/19 AM10:18:00

fundamentally

页 3: [15] 删除的内容	LucidPapers	2018/6/19 AM10:18:00

fundamentally

页 3: [15] 删除的内容	LucidPapers	2018/6/19 AM10:18:00

fundamentally

页 3: [15] 删除的内容	LucidPapers	2018/6/19 AM10:18:00

fundamentally

页 3: [15] 删除的内容	LucidPapers	2018/6/19 AM10:18:00

fundamentally

页 3: [15] 删除的内容	LucidPapers	2018/6/19 AM10:18:00

fundamentally

页 3: [15] 删除的内容	LucidPapers	2018/6/19 AM10:18:00

fundamentally

页 3: [15] 删除的内容	LucidPapers	2018/6/19 AM10:18:00

fundamentally

页 3: [15] 删除的内容	LucidPapers	2018/6/19 AM10:18:00

fundamentally

页 3: [15] 删除的内容	LucidPapers	2018/6/19 AM10:18:00

fundamentally

页 3: [15] 删除的内容	LucidPapers	2018/6/19 AM10:18:00

fundamentally

页 3: [15] 删除的内容	LucidPapers	2018/6/19 AM10:18:00

fundamentally

页 3: [16] 删除的内容 LucidPapers 2018/6/20 PM2:13:00

页 3: [16] 删除的内容 LucidPapers 2018/6/20 PM2:13:00

页 3: [16] 删除的内容 LucidPapers 2018/6/20 PM2:13:00

页 3: [16] 删除的内容 LucidPapers 2018/6/20 PM2:13:00

页 3: [16] 删除的内容 LucidPapers 2018/6/20 PM2:13:00

页 3: [16] 删除的内容 LucidPapers 2018/6/20 PM2:13:00

页 3: [16] 删除的内容 LucidPapers 2018/6/20 PM2:13:00

页 3: [16] 删除的内容	LucidPapers	2018/6/20 PM2:13:00

页 3: [16] 删除的内容	LucidPapers	2018/6/20 PM2:13:00

页 3: [16] 删除的内容	LucidPapers	2018/6/20 PM2:13:00

页 3: [17] 删除的内容	LucidPapers	2018/6/19 AM10:22:00

,

页 3: [17] 删除的内容	LucidPapers	2018/6/19 AM10:22:00

,

页 3: [17] 删除的内容	LucidPapers	2018/6/19 AM10:22:00

,

页 4: [18] 删除的内容	LucidPapers	2018/6/19 AM10:23:00

(CMA)

页 4: [18] 删除的内容	LucidPapers	2018/6/19 AM10:23:00

(CMA)

页 4: [18] 删除的内容	LucidPapers	2018/6/19 AM10:23:00

(CMA)

页 4: [18] 删除的内容	LucidPapers	2018/6/19 AM10:23:00

(CMA)

页 4: [18] 删除的内容	LucidPapers	2018/6/19 AM10:23:00

(CMA)

页 4: [19] 删除的内容	LucidPapers	2018/6/19 AM10:24:00

On the other hand, a

页 4: [19] 删除的内容	LucidPapers	2018/6/19 AM10:24:00

On the other hand, a

页 4: [19] 删除的内容	LucidPapers	2018/6/19 AM10:24:00

On the other hand, a

页 4: [19] 删除的内容	LucidPapers	2018/6/19 AM10:24:00

On the other hand, a

页 4: [19] 删除的内容	LucidPapers	2018/6/19 AM10:24:00

On the other hand, a

页 4: [19] 删除的内容	LucidPapers	2018/6/19 AM10:24:00

On the other hand, a

页 4: [19] 删除的内容	LucidPapers	2018/6/19 AM10:24:00

On the other hand, a

页 4: [19] 删除的内容	LucidPapers	2018/6/19 AM10:24:00

On the other hand, a

页 4: [19] 删除的内容 LucidPapers 2018/6/19 AM10:24:00

On the other hand, a

页 4: [20] 删除的内容 LucidPapers 2018/6/19 AM10:26:00

explicitly

页 4: [20] 删除的内容 LucidPapers 2018/6/19 AM10:26:00

explicitly

页 4: [20] 删除的内容 LucidPapers 2018/6/19 AM10:26:00

explicitly

页 4: [20] 删除的内容 LucidPapers 2018/6/19 AM10:26:00

explicitly

页 4: [20] 删除的内容 LucidPapers 2018/6/19 AM10:26:00

explicitly

页 4: [20] 删除的内容	LucidPapers	2018/6/19 AM10:26:00

explicitly

页 4: [20] 删除的内容	LucidPapers	2018/6/19 AM10:26:00

explicitly

页 4: [20] 删除的内容	LucidPapers	2018/6/19 AM10:26:00

explicitly

页 4: [20] 删除的内容	LucidPapers	2018/6/19 AM10:26:00

explicitly

页 4: [20] 删除的内容	LucidPapers	2018/6/19 AM10:26:00

explicitly

页 4: [21] 删除的内容	Microsoft Office User	2018/4/16 AM9:18:00

planetary boundary layer (

页 4: [21] 删除的内容	Microsoft Office User	2018/4/16 AM9:18:00

planetary boundary layer (

页 4: [22] 删除的内容	LucidPapers	2018/6/19 AM10:28:00

heavily

页 4: [22] 删除的内容	LucidPapers	2018/6/19 AM10:28:00

heavily

页 4: [22] 删除的内容	LucidPapers	2018/6/19 AM10:28:00

heavily

页 4: [22] 删除的内容	LucidPapers	2018/6/19 AM10:28:00

heavily

页 4: [23] 删除的内容	LucidPapers	2018/6/19 AM10:28:00

One way to tackle c

页 4: [23] 删除的内容	LucidPapers	2018/6/19 AM10:28:00

One way to tackle c

页 4: [23] 删除的内容	LucidPapers	2018/6/19 AM10:28:00

One way to tackle c

页 4: [23] 删除的内容	LucidPapers	2018/6/19 AM10:28:00

One way to tackle c

页 4: [23] 删除的内容	LucidPapers	2018/6/19 AM10:28:00

One way to tackle c

页 4: [23] 删除的内容	LucidPapers	2018/6/19 AM10:28:00

One way to tackle c

页 4: [23] 删除的内容	LucidPapers	2018/6/19 AM10:28:00

One way to tackle c

页 4: [23] 删除的内容	LucidPapers	2018/6/19 AM10:28:00

One way to tackle c

页 4: [23] 删除的内容 LucidPapers 2018/6/19 AM10:28:00

One way to tackle c

页 4: [23] 删除的内容 LucidPapers 2018/6/19 AM10:28:00

One way to tackle c

页 4: [23] 删除的内容 LucidPapers 2018/6/19 AM10:28:00

One way to tackle c

页 4: [23] 删除的内容 LucidPapers 2018/6/19 AM10:28:00

One way to tackle c

页 4: [23] 删除的内容 LucidPapers 2018/6/19 AM10:28:00

One way to tackle c

页 4: [23] 删除的内容 LucidPapers 2018/6/19 AM10:28:00

One way to tackle c

页 4: [23] 删除的内容	LucidPapers	2018/6/19 AM10:28:00

One way to tackle c

页 4: [23] 删除的内容	LucidPapers	2018/6/19 AM10:28:00

One way to tackle c

页 4: [24] 删除的内容	LucidPapers	2018/6/19 AM10:31:00

LES

页 4: [24] 删除的内容	LucidPapers	2018/6/19 AM10:31:00

LES

页 4: [24] 删除的内容	LucidPapers	2018/6/19 AM10:31:00

LES

页 4: [24] 删除的内容	LucidPapers	2018/6/19 AM10:31:00

LES

页 4: [24] 删除的内容	LucidPapers	2018/6/19 AM10:31:00

LES

页 4: [24] 删除的内容	LucidPapers	2018/6/19 AM10:31:00

LES

页 4: [24] 删除的内容	LucidPapers	2018/6/19 AM10:31:00

LES

页 4: [24] 删除的内容	LucidPapers	2018/6/19 AM10:31:00

LES

页 4: [24] 删除的内容	LucidPapers	2018/6/19 AM10:31:00

LES

页 4: [25] 删除的内容	LucidPapers	2018/6/20 PM2:16:00

LES

页 4: [25] 删除的内容	LucidPapers	2018/6/20 PM2:16:00

LES

页 4: [25] 删除的内容	LucidPapers	2018/6/20 PM2:16:00

LES

页 4: [25] 删除的内容	LucidPapers	2018/6/20 PM2:16:00

LES

页 4: [25] 删除的内容	LucidPapers	2018/6/20 PM2:16:00

LES

页 4: [25] 删除的内容	LucidPapers	2018/6/20 PM2:16:00

LES

页 4: [25] 删除的内容	LucidPapers	2018/6/20 PM2:16:00

LES

页 4: [25] 删除的内容	LucidPapers	2018/6/20 PM2:16:00

LES

页 5: [26] 删除的内容	LucidPapers	2018/6/19 AM9:41:00

-

页 5: [26] 删除的内容	LucidPapers	2018/6/19 AM9:41:00

-

页 5: [26] 删除的内容	LucidPapers	2018/6/19 AM9:41:00

-

页 5: [26] 删除的内容	LucidPapers	2018/6/19 AM9:41:00

-

页 5: [26] 删除的内容	LucidPapers	2018/6/19 AM9:41:00

-

页 5: [26] 删除的内容	LucidPapers	2018/6/19 AM9:41:00

-

页 5: [26] 删除的内容	LucidPapers	2018/6/19 AM9:41:00

-

页 5: [26] 删除的内容 LucidPapers 2018/6/19 AM9:41:00

-

页 5: [27] 删除的内容 LucidPapers 2018/6/19 AM10:34:00

of

页 5: [27] 删除的内容 LucidPapers 2018/6/19 AM10:34:00

of

页 5: [28] 删除的内容 Microsoft Office User 2018/4/14 AM11:09:00

WRF land-surface model

页 5: [28] 删除的内容 Microsoft Office User 2018/4/14 AM11:09:00

WRF land-surface model

页 5: [29] 删除的内容 LucidPapers 2018/6/20 PM2:17:00

However, m

页 5: [29] 删除的内容	LucidPapers	2018/6/20 PM2:17:00

However, m

页 5: [29] 删除的内容	LucidPapers	2018/6/20 PM2:17:00

However, m

页 5: [30] 删除的内容	LucidPapers	2018/6/19 AM10:35:00

is the first attempt to

页 5: [30] 删除的内容	LucidPapers	2018/6/19 AM10:35:00

is the first attempt to

页 5: [30] 删除的内容	LucidPapers	2018/6/19 AM10:35:00

is the first attempt to

页 5: [30] 删除的内容	LucidPapers	2018/6/19 AM10:35:00

is the first attempt to

页 5: [31] 删除的内容 LucidPapers 2018/6/19 AM10:36:00

the ongoing

页 5: [31] 删除的内容 LucidPapers 2018/6/19 AM10:36:00

the ongoing

页 5: [32] 删除的内容 LucidPapers 2018/6/19 AM10:37:00

cases

页 5: [32] 删除的内容 LucidPapers 2018/6/19 AM10:37:00

cases

页 5: [33] 删除的内容 LucidPapers 2018/6/19 AM10:38:00

First w

页 5: [33] 删除的内容 LucidPapers 2018/6/19 AM10:38:00

First w

页 5: [33] 删除的内容 LucidPapers 2018/6/19 AM10:38:00

First w

页 5: [33] 删除的内容	LucidPapers	2018/6/19 AM10:38:00

First w

页 5: [33] 删除的内容	LucidPapers	2018/6/19 AM10:38:00

First w

页 5: [33] 删除的内容	LucidPapers	2018/6/19 AM10:38:00

First w

页 5: [33] 删除的内容	LucidPapers	2018/6/19 AM10:38:00

First w

页 5: [33] 删除的内容	LucidPapers	2018/6/19 AM10:38:00

First w

页 5: [34] 删除的内容	LucidPapers	2018/6/19 AM10:40:00

the

页 5: [34] 删除的内容	LucidPapers	2018/6/19 AM10:40:00

the

页 5: [34] 删除的内容	LucidPapers	2018/6/19 AM10:40:00

the

页 5: [34] 删除的内容	LucidPapers	2018/6/19 AM10:40:00

the

页 5: [34] 删除的内容	LucidPapers	2018/6/19 AM10:40:00

the

页 5: [34] 删除的内容	LucidPapers	2018/6/19 AM10:40:00

the

页 5: [35] 删除的内容	LucidPapers	2018/6/19 AM10:41:00

,

页 5: [35] 删除的内容	LucidPapers	2018/6/19 AM10:41:00

，

页 5: [35] 删除的内容	LucidPapers	2018/6/19 AM10:41:00

，

页 5: [35] 删除的内容	LucidPapers	2018/6/19 AM10:41:00

，

页 5: [35] 删除的内容	LucidPapers	2018/6/19 AM10:41:00

，

页 5: [35] 删除的内容	LucidPapers	2018/6/19 AM10:41:00

，

页 5: [35] 删除的内容	LucidPapers	2018/6/19 AM10:41:00

，

页 5: [36] 删除的内容	LucidPapers	2018/6/19 AM10:42:00

.

页 5: [36] 删除的内容 LucidPapers 2018/6/19 AM10:42:00

.

页 5: [36] 删除的内容 LucidPapers 2018/6/19 AM10:42:00

.

页 5: [36] 删除的内容 LucidPapers 2018/6/19 AM10:42:00

.

页 5: [36] 删除的内容 LucidPapers 2018/6/19 AM10:42:00

.

页 5: [37] 删除的内容 Microsoft Office User 2018/4/7 AM9:10:00

Data

In this study, model simulations compared for 12 hours from the Tazhong field experiment, from 0800 BJT 01 July to 2000 BJT 01 July 2016. The field observation experiment was held during the month of July 2016 in Tazhong, by the Institute of Desert Meteorology (IDM), Chinese Meteorological Administration (CMA), Urumqi. The main station was located at 86.63°E, 39.03°N. The location is relatively flat with few hills and covered by sand combined with grass (Figure 1), and the 12-h period of our simulation was under a cloudless sky and dry environment. We conducted one way nest WRF from mesoscale(12km) down to LES-scales(0.33km) and compare its results to various instruments including:

1) surface fluxes: The eddy correlation system was a R3-50 supersonic anemometer developed by Gill Company, UK, deployed at a height of 10 m. The data acquisition frequency was 20 Hz, and the surface sensible heat flux was calculated by the eddy-covariance method.

2) vertical profiles measured using soundings: Upper air soundings of temperature, pressure, humidity, and wind speed and direction were conducted 3-6 times per day with the GPS sounding system developed by No. 23 Institute of China Aerospace Science & Industry Corp. (CASIC23). The sounding times were 01:15, 07:15, 10:15, 13:15, 16:15 and 19:15 respectively.

页 6: [38] 删除的内容	LucidPapers	2018/6/19 AM11:00:00

s

页 6: [38] 删除的内容	LucidPapers	2018/6/19 AM11:00:00

s

页 6: [39] 删除的内容	LucidPapers	2018/6/20 PM2:19:00

event in

页 6: [39] 删除的内容	LucidPapers	2018/6/20 PM2:19:00

event in

页 6: [39] 删除的内容	LucidPapers	2018/6/20 PM2:19:00

event in

页 6: [40] 删除的内容	LucidPapers	2018/6/19 AM11:02:00

A

页 6: [40] 删除的内容	LucidPapers	2018/6/19 AM11:02:00

A

页 6: [40] 删除的内容	LucidPapers	2018/6/19 AM11:02:00

A

页 6: [40] 删除的内容	LucidPapers	2018/6/19 AM11:02:00

A

页 6: [40] 删除的内容	LucidPapers	2018/6/19 AM11:02:00

A

页 6: [40] 删除的内容	LucidPapers	2018/6/19 AM11:02:00

A

页 6: [40] 删除的内容	LucidPapers	2018/6/19 AM11:02:00

A

页 6: [40] 删除的内容	LucidPapers	2018/6/19 AM11:02:00

A

页 6: [40] 删除的内容	LucidPapers	2018/6/19 AM11:02:00

A

页 6: [40] 删除的内容	LucidPapers	2018/6/19 AM11:02:00

A

页 6: [40] 删除的内容	LucidPapers	2018/6/19 AM11:02:00

A

页 6: [40] 删除的内容	LucidPapers	2018/6/19 AM11:02:00

A

页 6: [40] 删除的内容	LucidPapers	2018/6/19 AM11:02:00

A

页 6: [40] 删除的内容	LucidPapers	2018/6/19 AM11:02:00

A

页 6: [40] 删除的内容	LucidPapers	2018/6/19 AM11:02:00

A

页 6: [41] 删除的内容	LucidPapers	2018/6/19 AM11:05:00

for

页 6: [41] 删除的内容	LucidPapers	2018/6/19 AM11:05:00

for

页 6: [41] 删除的内容	LucidPapers	2018/6/19 AM11:05:00

for

页 6: [41] 删除的内容	LucidPapers	2018/6/19 AM11:05:00

for

页 6: [41] 删除的内容	LucidPapers	2018/6/19 AM11:05:00

for

页 6: [42] 删除的内容	LucidPapers	2018/6/20 PM2:22:00

ized condition

页 6: [42] 删除的内容	LucidPapers	2018/6/20 PM2:22:00

ized condition

页 6: [42] 删除的内容	LucidPapers	2018/6/20 PM2:22:00

ized condition

页 6: [42] 删除的内容	LucidPapers	2018/6/20 PM2:22:00

ized condition

页 6: [43] 删除的内容	LucidPapers	2018/6/19 AM11:07:00

-degree by

页 6: [43] 删除的内容	LucidPapers	2018/6/19 AM11:07:00

-degree by

页 6: [43] 删除的内容	LucidPapers	2018/6/19 AM11:07:00

-degree by

页 6: [43] 删除的内容	LucidPapers	2018/6/19 AM11:07:00

-degree by

页 6: [44] 删除的内容	LucidPapers	2018/6/19 AM11:07:00

millibars

页 6: [44] 删除的内容	LucidPapers	2018/6/19 AM11:07:00

millibars

页 6: [44] 删除的内容	LucidPapers	2018/6/19 AM11:07:00

millibars

页 6: [45] 删除的内容	LucidPapers	2018/6/19 AM11:08:00

model

页 6: [45] 删除的内容	LucidPapers	2018/6/19 AM11:08:00

model

页 6: [45] 删除的内容	LucidPapers	2018/6/19 AM11:08:00

model

页 6: [45] 删除的内容	LucidPapers	2018/6/19 AM11:08:00

model

页 6: [45] 删除的内容	LucidPapers	2018/6/19 AM11:08:00

model

页 6: [45] 删除的内容	LucidPapers	2018/6/19 AM11:08:00

model

页 6: [45] 删除的内容	LucidPapers	2018/6/19 AM11:08:00

model

页 7: [46] 删除的内容	LucidPapers	2018/6/19 AM11:09:00

.

页 7: [46] 删除的内容	LucidPapers	2018/6/19 AM11:09:00

.

页 7: [46] 删除的内容 LucidPapers 2018/6/19 AM11:09:00

.

页 7: [46] 删除的内容 LucidPapers 2018/6/19 AM11:09:00

.

页 7: [47] 删除的内容 LucidPapers 2018/6/19 AM11:10:00

shows the

页 7: [47] 删除的内容 LucidPapers 2018/6/19 AM11:10:00

shows the

页 7: [47] 删除的内容 LucidPapers 2018/6/19 AM11:10:00

shows the

页 7: [47] 删除的内容 LucidPapers 2018/6/19 AM11:10:00

shows the

页 7: [47] 删除的内容	LucidPapers	2018/6/19 AM11:10:00

shows the

页 7: [47] 删除的内容	LucidPapers	2018/6/19 AM11:10:00

shows the

页 7: [47] 删除的内容	LucidPapers	2018/6/19 AM11:10:00

shows the

页 7: [47] 删除的内容	LucidPapers	2018/6/19 AM11:10:00

shows the

页 7: [47] 删除的内容	LucidPapers	2018/6/19 AM11:10:00

shows the

页 7: [47] 删除的内容	LucidPapers	2018/6/19 AM11:10:00

shows the

页 7: [47] 删除的内容	LucidPapers	2018/6/19 AM11:10:00

shows the

页 7: [47] 删除的内容	LucidPapers	2018/6/19 AM11:10:00

shows the

页 7: [47] 删除的内容	LucidPapers	2018/6/19 AM11:10:00

shows the

页 7: [47] 删除的内容	LucidPapers	2018/6/19 AM11:10:00

shows the

页 7: [47] 删除的内容	LucidPapers	2018/6/19 AM11:10:00

shows the

页 7: [47] 删除的内容	LucidPapers	2018/6/19 AM11:10:00

shows the

页 7: [47] 删除的内容	LucidPapers	2018/6/19 AM11:10:00

shows the

页 7: [47] 删除的内容	LucidPapers	2018/6/19 AM11:10:00

shows the

页 7: [47] 删除的内容	LucidPapers	2018/6/19 AM11:10:00

shows the

页 7: [47] 删除的内容	LucidPapers	2018/6/19 AM11:10:00

shows the

页 7: [47] 删除的内容	LucidPapers	2018/6/19 AM11:10:00

shows the

页 7: [47] 删除的内容	LucidPapers	2018/6/19 AM11:10:00

shows the

页 7: [47] 删除的内容	LucidPapers	2018/6/19 AM11:10:00

shows the

页 7: [47] 删除的内容	LucidPapers	2018/6/19 AM11:10:00

shows the

页 7: [48] 删除的内容	LucidPapers	2018/6/19 PM12:14:00

to

页 7: [48] 删除的内容	LucidPapers	2018/6/19 PM12:14:00

to

页 7: [48] 删除的内容	LucidPapers	2018/6/19 PM12:14:00

to

页 7: [48] 删除的内容	LucidPapers	2018/6/19 PM12:14:00

to

页 7: [48] 删除的内容	LucidPapers	2018/6/19 PM12:14:00

to

页 7: [48] 删除的内容	LucidPapers	2018/6/19 PM12:14:00

to

页 7: [48] 删除的内容	LucidPapers	2018/6/19 PM12:14:00

to

页 7: [48] 删除的内容	LucidPapers	2018/6/19 PM12:14:00

to

页 7: [49] 删除的内容	LucidPapers	2018/6/19 PM12:16:00

,

页 7: [49] 删除的内容	LucidPapers	2018/6/19 PM12:16:00

,

页 7: [49] 删除的内容	LucidPapers	2018/6/19 PM12:16:00

,

页 7: [49] 删除的内容	LucidPapers	2018/6/19 PM12:16:00

,

页 7: [49] 删除的内容	LucidPapers	2018/6/19 PM12:16:00

,

页 7: [50] 删除的内容	LucidPapers	2018/6/19 PM12:16:00

1)

页 7: [50] 删除的内容	LucidPapers	2018/6/19 PM12:16:00

1)

页 7: [50] 删除的内容	LucidPapers	2018/6/19 PM12:16:00

1)

页 7: [50] 删除的内容	LucidPapers	2018/6/19 PM12:16:00

1)

页 7: [50] 删除的内容	LucidPapers	2018/6/19 PM12:16:00

1)

页 7: [50] 删除的内容	LucidPapers	2018/6/19 PM12:16:00

1)

页 7: [50] 删除的内容	LucidPapers	2018/6/19 PM12:16:00

1)

页 7: [50] 删除的内容	LucidPapers	2018/6/19 PM12:16:00

1)

页 7: [50] 删除的内容	LucidPapers	2018/6/19 PM12:16:00

1)

页 7: [50] 删除的内容	LucidPapers	2018/6/19 PM12:16:00

1)

页 8: [51] 删除的内容	LucidPapers	2018/6/19 PM12:17:00

2

页 8: [51] 删除的内容	LucidPapers	2018/6/19 PM12:17:00

2

页 8: [51] 删除的内容	LucidPapers	2018/6/19 PM12:17:00

2

页 8: [51] 删除的内容	LucidPapers	2018/6/19 PM12:17:00

2

页 8: [51] 删除的内容	LucidPapers	2018/6/19 PM12:17:00

2

页 8: [51] 删除的内容	LucidPapers	2018/6/19 PM12:17:00

2

页 8: [51] 删除的内容	LucidPapers	2018/6/19 PM12:17:00

2

页 8: [51] 删除的内容	LucidPapers	2018/6/19 PM12:17:00

2

页 8: [52] 删除的内容	LucidPapers	2018/6/19 PM12:20:00

页 8: [52] 删除的内容	LucidPapers	2018/6/19 PM12:20:00

页 8: [52] 删除的内容	LucidPapers	2018/6/19 PM12:20:00

页 8: [52] 删除的内容	LucidPapers	2018/6/19 PM12:20:00

页 8: [52] 删除的内容	LucidPapers	2018/6/19 PM12:20:00

页 8: [53] 删除的内容	LucidPapers	2018/6/19 PM12:21:00

页 8: [53] 删除的内容	LucidPapers	2018/6/19 PM12:21:00

页 8: [54] 删除的内容	LucidPapers	2018/6/19 PM12:21:00

which is

页 8: [54] 删除的内容	LucidPapers	2018/6/19 PM12:21:00

which is

页 8: [55] 删除的内容	LucidPapers	2018/6/19 PM12:21:00

area of

页 8: [55] 删除的内容	LucidPapers	2018/6/19 PM12:21:00

area of

页 8: [55] 删除的内容	LucidPapers	2018/6/19 PM12:21:00

area of

页 8: [55] 删除的内容	LucidPapers	2018/6/19 PM12:21:00

area of

页 8: [56] 删除的内容	Microsoft Office User	2018/4/14 AM11:37:00

Simulated d

页 8: [56] 删除的内容	Microsoft Office User	2018/4/14 AM11:37:00

Simulated d

页 8: [57] 删除的内容	LucidPapers	2018/6/19 PM12:22:00

,

页 8: [57] 删除的内容	LucidPapers	2018/6/19 PM12:22:00

,

页 8: [57] 删除的内容	LucidPapers	2018/6/19 PM12:22:00

,

页 8: [57] 删除的内容	LucidPapers	2018/6/19 PM12:22:00

,

页 8: [57] 删除的内容	LucidPapers	2018/6/19 PM12:22:00

,

页 8: [57] 删除的内容	LucidPapers	2018/6/19 PM12:22:00

,

页 8: [57] 删除的内容	LucidPapers	2018/6/19 PM12:22:00

,

页 8: [57] 删除的内容	LucidPapers	2018/6/19 PM12:22:00

,

页 9: [58] 删除的内容	LucidPapers	2018/6/19 PM12:24:00

less

页 9: [58] 删除的内容	LucidPapers	2018/6/19 PM12:24:00

less

页 9: [58] 删除的内容	LucidPapers	2018/6/19 PM12:24:00

less

页 9: [58] 删除的内容	LucidPapers	2018/6/19 PM12:24:00

less

页 9: [58] 删除的内容	LucidPapers	2018/6/19 PM12:24:00

less

页 9: [58] 删除的内容	LucidPapers	2018/6/19 PM12:24:00

less

页 9: [58] 删除的内容	LucidPapers	2018/6/19 PM12:24:00

less

页 9: [58] 删除的内容	LucidPapers	2018/6/19 PM12:24:00

less

页 9: [58] 删除的内容	LucidPapers	2018/6/19 PM12:24:00

less

页 9: [58] 删除的内容	LucidPapers	2018/6/19 PM12:24:00

less

页 9: [58] 删除的内容	LucidPapers	2018/6/19 PM12:24:00

less

页 9: [58] 删除的内容	LucidPapers	2018/6/19 PM12:24:00

less

页 9: [58] 删除的内容	LucidPapers	2018/6/19 PM12:24:00

less

页 9: [58] 删除的内容	LucidPapers	2018/6/19 PM12:24:00

less

页 9: [58] 删除的内容	LucidPapers	2018/6/19 PM12:24:00

less

页 9: [58] 删除的内容	LucidPapers	2018/6/19 PM12:24:00

less

页 9: [58] 删除的内容	LucidPapers	2018/6/19 PM12:24:00

less

页 9: [58] 删除的内容	LucidPapers	2018/6/19 PM12:24:00

less

页 9: [58] 删除的内容	LucidPapers	2018/6/19 PM12:24:00

less

页 9: [58] 删除的内容	LucidPapers	2018/6/19 PM12:24:00

less

页 9: [58] 删除的内容	LucidPapers	2018/6/19 PM12:24:00

less

页 9: [58] 删除的内容	LucidPapers	2018/6/19 PM12:24:00

less

页 9: [58] 删除的内容	LucidPapers	2018/6/19 PM12:24:00

less

页 9: [59] 删除的内容	LucidPapers	2018/6/19 PM12:26:00

in

页 9: [59] 删除的内容	LucidPapers	2018/6/19 PM12:26:00

in

页 9: [59] 删除的内容	LucidPapers	2018/6/19 PM12:26:00

in

页 9: [59] 删除的内容	LucidPapers	2018/6/19 PM12:26:00

in

页 9: [59] 删除的内容	LucidPapers	2018/6/19 PM12:26:00

in

页 9: [59] 删除的内容	LucidPapers	2018/6/19 PM12:26:00

in

页 9: [59] 删除的内容	LucidPapers	2018/6/19 PM12:26:00

in

页 9: [59] 删除的内容	LucidPapers	2018/6/19 PM12:26:00

in

页 9: [59] 删除的内容	LucidPapers	2018/6/19 PM12:26:00

in

页 9: [59] 删除的内容	LucidPapers	2018/6/19 PM12:26:00

in

页 9: [59] 删除的内容	LucidPapers	2018/6/19 PM12:26:00

in

页 9: [59] 删除的内容	LucidPapers	2018/6/19 PM12:26:00

in

页 9: [59] 删除的内容	LucidPapers	2018/6/19 PM12:26:00

in

页 9: [59] 删除的内容	LucidPapers	2018/6/19 PM12:26:00

in

页 9: [60] 删除的内容	LucidPapers	2018/6/19 PM12:28:00

result in

页 9: [60] 删除的内容	LucidPapers	2018/6/19 PM12:28:00

result in

页 9: [60] 删除的内容	LucidPapers	2018/6/19 PM12:28:00

result in

页 9: [60] 删除的内容	LucidPapers	2018/6/19 PM12:28:00

result in

页 9: [61] 删除的内容	LucidPapers	2018/6/19 PM12:28:00

(1）) Tthe

页 9: [61] 删除的内容	LucidPapers	2018/6/19 PM12:28:00

(1）) Tthe

页 9: [62] 删除的内容	LucidPapers	2018/6/20 PM2:26:00

of

页 9: [62] 删除的内容	LucidPapers	2018/6/20 PM2:26:00

of

页 9: [62] 删除的内容	LucidPapers	2018/6/20 PM2:26:00

of

页 9: [62] 删除的内容	LucidPapers	2018/6/20 PM2:26:00

of

页 9: [62] 删除的内容	LucidPapers	2018/6/20 PM2:26:00

of

页 9: [62] 删除的内容	LucidPapers	2018/6/20 PM2:26:00

of

页 9: [62] 删除的内容	LucidPapers	2018/6/20 PM2:26:00

of

页 9: [62] 删除的内容	LucidPapers	2018/6/20 PM2:26:00

of

页 9: [62] 删除的内容	LucidPapers	2018/6/20 PM2:26:00

of

页 9: [62] 删除的内容	LucidPapers	2018/6/20 PM2:26:00

of

页 9: [62] 删除的内容	LucidPapers	2018/6/20 PM2:26:00

of

页 9: [63] 删除的内容	LucidPapers	2018/6/19 PM12:29:00

,

页 9: [63] 删除的内容	LucidPapers	2018/6/19 PM12:29:00

,

页 9: [63] 删除的内容	LucidPapers	2018/6/19 PM12:29:00

,

页 9: [63] 删除的内容	LucidPapers	2018/6/19 PM12:29:00

,

页 9: [63] 删除的内容	LucidPapers	2018/6/19 PM12:29:00

,

页 9: [63] 删除的内容	LucidPapers	2018/6/19 PM12:29:00

,

页 9: [63] 删除的内容	LucidPapers	2018/6/19 PM12:29:00

,

页 9: [63] 删除的内容	LucidPapers	2018/6/19 PM12:29:00

,

页 9: [63] 删除的内容	LucidPapers	2018/6/19 PM12:29:00

,

页 9: [63] 删除的内容	LucidPapers	2018/6/19 PM12:29:00

,

页 9: [63] 删除的内容	LucidPapers	2018/6/19 PM12:29:00

,

页 9: [64] 删除的内容	LucidPapers	2018/6/19 PM12:30:00

(2) Iit is should be noted that

页 9: [64] 删除的内容	LucidPapers	2018/6/19 PM12:30:00

(2) Iit is should be noted that

页 9: [64] 删除的内容	LucidPapers	2018/6/19 PM12:30:00

(2) Iit is should be noted that

页 9: [64] 删除的内容	LucidPapers	2018/6/19 PM12:30:00

(2) Iit is should be noted that

页 9: [64] 删除的内容	LucidPapers	2018/6/19 PM12:30:00

(2) Iit is should be noted that

页 9: [64] 删除的内容	LucidPapers	2018/6/19 PM12:30:00

(2) Iit is should be noted that

页 9: [64] 删除的内容	LucidPapers	2018/6/19 PM12:30:00

(2) Iit is should be noted that

页 9: [64] 删除的内容	LucidPapers	2018/6/19 PM12:30:00

(2) Iit is should be noted that

页 9: [64] 删除的内容	LucidPapers	2018/6/19 PM12:30:00

(2) Iit is should be noted that

页 9: [65] 删除的内容	Microsoft Office 用户	2018/6/22 AM9:57:00

H

页 9: [65] 删除的内容	Microsoft Office 用户	2018/6/22 AM9:57:00

H

页 9: [65] 删除的内容	Microsoft Office 用户	2018/6/22 AM9:57:00

H

页 9: [66] 删除的内容	LucidPapers	2018/6/19 PM12:32:00

equal to an

页 9: [66] 删除的内容	LucidPapers	2018/6/19 PM12:32:00

equal to an

页 9: [67] 删除的内容	LucidPapers	2018/6/19 PM12:32:00

what would be

页 9: [67] 删除的内容	LucidPapers	2018/6/19 PM12:32:00

what would be

页 9: [67] 删除的内容	LucidPapers	2018/6/19 PM12:32:00

what would be

页 10: [68] 删除的内容	LucidPapers	2018/6/19 PM12:33:00

o

页 10: [68] 删除的内容	LucidPapers	2018/6/19 PM12:33:00

o

页 10: [69] 删除的内容 LucidPapers 2018/6/19 PM12:33:00

页 10: [69] 删除的内容 LucidPapers 2018/6/19 PM12:33:00

页 10: [69] 删除的内容 LucidPapers 2018/6/19 PM12:33:00

页 10: [69] 删除的内容 LucidPapers 2018/6/19 PM12:33:00

页 10: [70] 删除的内容 LucidPapers 2018/6/19 PM12:35:00

:

页 10: [70] 删除的内容 LucidPapers 2018/6/19 PM12:35:00

:

页 10: [70] 删除的内容 LucidPapers 2018/6/19 PM12:35:00

:

页 10: [70] 删除的内容 LucidPapers 2018/6/19 PM12:35:00

:

页 10: [70] 删除的内容 LucidPapers 2018/6/19 PM12:35:00

:

页 10: [70] 删除的内容 LucidPapers 2018/6/19 PM12:35:00

:

页 10: [70] 删除的内容 LucidPapers 2018/6/19 PM12:35:00

:

页 10: [70] 删除的内容 LucidPapers 2018/6/19 PM12:35:00

:

页 10: [70] 删除的内容 LucidPapers 2018/6/19 PM12:35:00

:

页 10: [71] 删除的内容 LucidPapers 2018/6/19 PM12:36:00

Results

页 10: [71] 删除的内容 LucidPapers 2018/6/19 PM12:36:00

Results

页 10: [71] 删除的内容 LucidPapers 2018/6/19 PM12:36:00

Results

页 10: [71] 删除的内容 LucidPapers 2018/6/19 PM12:36:00

Results

页 10: [72] 删除的内容 LucidPapers 2018/6/19 PM12:36:00

from

页 10: [72] 删除的内容 LucidPapers 2018/6/19 PM12:36:00

from

页 10: [72] 删除的内容	LucidPapers	2018/6/19 PM12:36:00

from

页 10: [72] 删除的内容	LucidPapers	2018/6/19 PM12:36:00

from

页 10: [72] 删除的内容	LucidPapers	2018/6/19 PM12:36:00

from

页 10: [72] 删除的内容	LucidPapers	2018/6/19 PM12:36:00

from

页 10: [72] 删除的内容	LucidPapers	2018/6/19 PM12:36:00

from

页 10: [72] 删除的内容	LucidPapers	2018/6/19 PM12:36:00

from

页 10: [72] 删除的内容	LucidPapers	2018/6/19 PM12:36:00

from

页 10: [72] 删除的内容 LucidPapers 2018/6/19 PM12:36:00

from

页 10: [73] 删除的内容 LucidPapers 2018/6/19 PM12:37:00

:

页 10: [73] 删除的内容 LucidPapers 2018/6/19 PM12:37:00

:

页 10: [73] 删除的内容 LucidPapers 2018/6/19 PM12:37:00

:

页 10: [73] 删除的内容 LucidPapers 2018/6/19 PM12:37:00

:

页 10: [73] 删除的内容 LucidPapers 2018/6/19 PM12:37:00

:

页 10: [74] 删除的内容 LucidPapers 2018/6/19 PM12:38:00

e

页 10: [74] 删除的内容 LucidPapers 2018/6/19 PM12:38:00

e

页 10: [74] 删除的内容 LucidPapers 2018/6/19 PM12:38:00

e

页 10: [74] 删除的内容 LucidPapers 2018/6/19 PM12:38:00

e

页 10: [74] 删除的内容 LucidPapers 2018/6/19 PM12:38:00

e

页 10: [74] 删除的内容 LucidPapers 2018/6/19 PM12:38:00

e

页 10: [74] 删除的内容	LucidPapers	2018/6/19 PM12:38:00

e

页 10: [74] 删除的内容	LucidPapers	2018/6/19 PM12:38:00

e

页 10: [74] 删除的内容	LucidPapers	2018/6/19 PM12:38:00

e

页 10: [74] 删除的内容	LucidPapers	2018/6/19 PM12:38:00

e

页 10: [75] 删除的内容	LucidPapers	2018/6/19 PM12:39:00

the

页 10: [75] 删除的内容	LucidPapers	2018/6/19 PM12:39:00

the

页 10: [75] 删除的内容	LucidPapers	2018/6/19 PM12:39:00

the

页 10: [75] 删除的内容	LucidPapers	2018/6/19 PM12:39:00

the

页 10: [75] 删除的内容	LucidPapers	2018/6/19 PM12:39:00

the

页 10: [75] 删除的内容	LucidPapers	2018/6/19 PM12:39:00

the

页 10: [75] 删除的内容	LucidPapers	2018/6/19 PM12:39:00

the

页 10: [75] 删除的内容	LucidPapers	2018/6/19 PM12:39:00

the

页 10: [75] 删除的内容	LucidPapers	2018/6/19 PM12:39:00

the

页 10: [75] 删除的内容	LucidPapers	2018/6/19 PM12:39:00

the

页 10: [75] 删除的内容	LucidPapers	2018/6/19 PM12:39:00

the

页 10: [75] 删除的内容	LucidPapers	2018/6/19 PM12:39:00

the

页 10: [75] 删除的内容	LucidPapers	2018/6/19 PM12:39:00

the

页 10: [75] 删除的内容	LucidPapers	2018/6/19 PM12:39:00

the

页 10: [76] 删除的内容	LucidPapers	2018/6/20 PM2:29:00

页 10: [76] 删除的内容	LucidPapers	2018/6/20 PM2:29:00

页 10: [77] 删除的内容	LucidPapers	2018/6/19 PM12:43:00

页 10: [77] 删除的内容	LucidPapers	2018/6/19 PM12:43:00

页 10: [77] 删除的内容	LucidPapers	2018/6/19 PM12:43:00

页 10: [77] 删除的内容	LucidPapers	2018/6/19 PM12:43:00

页 10: [77] 删除的内容	LucidPapers	2018/6/19 PM12:43:00

页 10: [77] 删除的内容	LucidPapers	2018/6/19 PM12:43:00

页 11: [78] 删除的内容	LucidPapers	2018/6/19 PM12:44:00

abilities

页 11: [78] 删除的内容	LucidPapers	2018/6/19 PM12:44:00

abilities

页 11: [78] 删除的内容	LucidPapers	2018/6/19 PM12:44:00

abilities

页 11: [79] 删除的内容	LucidPapers	2018/6/19 PM12:44:00

observation

页 11: [79] 删除的内容	LucidPapers	2018/6/19 PM12:44:00

observation

页 11: [79] 删除的内容	LucidPapers	2018/6/19 PM12:44:00

observation

页 11: [79] 删除的内容 LucidPapers 2018/6/19 PM12:44:00

observation

页 11: [80] 删除的内容 LucidPapers 2018/6/19 PM12:53:00

The model simulated

页 11: [80] 删除的内容 LucidPapers 2018/6/19 PM12:53:00

The model simulated

页 11: [80] 删除的内容 LucidPapers 2018/6/19 PM12:53:00

The model simulated

页 11: [80] 删除的内容 LucidPapers 2018/6/19 PM12:53:00

The model simulated

页 11: [80] 删除的内容 LucidPapers 2018/6/19 PM12:53:00

The model simulated

页 11: [80] 删除的内容	LucidPapers	2018/6/19 PM12:53:00

The model simulated

页 11: [80] 删除的内容	LucidPapers	2018/6/19 PM12:53:00

The model simulated

页 11: [80] 删除的内容	LucidPapers	2018/6/19 PM12:53:00

The model simulated

页 11: [80] 删除的内容	LucidPapers	2018/6/19 PM12:53:00

The model simulated

页 11: [80] 删除的内容	LucidPapers	2018/6/19 PM12:53:00

The model simulated

页 11: [80] 删除的内容	LucidPapers	2018/6/19 PM12:53:00

The model simulated

页 11: [80] 删除的内容	LucidPapers	2018/6/19 PM12:53:00

The model simulated

页 11: [80] 删除的内容	LucidPapers	2018/6/19 PM12:53:00

The model simulated

页 11: [80] 删除的内容	LucidPapers	2018/6/19 PM12:53:00

The model simulated

页 11: [80] 删除的内容	LucidPapers	2018/6/19 PM12:53:00

The model simulated

页 11: [80] 删除的内容	LucidPapers	2018/6/19 PM12:53:00

The model simulated

页 11: [80] 删除的内容	LucidPapers	2018/6/19 PM12:53:00

The model simulated

页 11: [80] 删除的内容	LucidPapers	2018/6/19 PM12:53:00

The model simulated

页 11: [80] 删除的内容	LucidPapers	2018/6/19 PM12:53:00

The model simulated

页 11: [80] 删除的内容	LucidPapers	2018/6/19 PM12:53:00

The model simulated

页 11: [80] 删除的内容	LucidPapers	2018/6/19 PM12:53:00

The model simulated

页 11: [81] 删除的内容	LucidPapers	2018/6/19 PM12:55:00

页 11: [81] 删除的内容	LucidPapers	2018/6/19 PM12:55:00

页 11: [81] 删除的内容	LucidPapers	2018/6/19 PM12:55:00

页 11: [82] 删除的内容 LucidPapers 2018/6/19 PM12:56:00

At 1700 BJT (Figure 5Figure c),, t

页 11: [82] 删除的内容 LucidPapers 2018/6/19 PM12:56:00

At 1700 BJT (Figure 5Figure c),, t

页 11: [83] 删除的内容 LucidPapers 2018/6/19 PM12:56:00

grows

页 11: [83] 删除的内容 LucidPapers 2018/6/19 PM12:56:00

grows

页 11: [83] 删除的内容 LucidPapers 2018/6/19 PM12:56:00

grows

页 11: [83] 删除的内容 LucidPapers 2018/6/19 PM12:56:00

grows

页 11: [83] 删除的内容 LucidPapers 2018/6/19 PM12:56:00

grows

页 11: [83] 删除的内容 LucidPapers 2018/6/19 PM12:56:00

grows

页 11: [83] 删除的内容 LucidPapers 2018/6/19 PM12:56:00

grows

页 11: [83] 删除的内容 LucidPapers 2018/6/19 PM12:56:00

grows

页 11: [84] 删除的内容 LucidPapers 2018/6/19 PM12:57:00

One possible minor reason is

页 11: [84] 删除的内容 LucidPapers 2018/6/19 PM12:57:00

One possible minor reason is

页 11: [84] 删除的内容 LucidPapers 2018/6/19 PM12:57:00

One possible minor reason is

页 11: [85] 删除的内容	Microsoft Office User	2018/4/10 PM3:47:00

,

页 11: [85] 删除的内容	Microsoft Office User	2018/4/10 PM3:47:00

,

页 11: [86] 删除的内容	LucidPapers	2018/6/19 PM12:58:00

Simulated

页 11: [86] 删除的内容	LucidPapers	2018/6/19 PM12:58:00

Simulated

页 11: [86] 删除的内容	LucidPapers	2018/6/19 PM12:58:00

Simulated

页 12: [87] 删除的内容	LucidPapers	2018/6/19 PM12:59:00

ed

页 12: [87] 删除的内容	LucidPapers	2018/6/19 PM12:59:00

ed

页 12: [87] 删除的内容	LucidPapers	2018/6/19 PM12:59:00

ed

页 12: [88] 删除的内容	LucidPapers	2018/6/19 PM12:59:00

to

页 12: [88] 删除的内容	LucidPapers	2018/6/19 PM12:59:00

to

页 12: [88] 删除的内容	LucidPapers	2018/6/19 PM12:59:00

to

页 12: [88] 删除的内容	LucidPapers	2018/6/19 PM12:59:00

to

页 12: [88] 删除的内容	LucidPapers	2018/6/19 PM12:59:00

to

页 12: [88] 删除的内容	LucidPapers	2018/6/19 PM12:59:00

to

页 12: [88] 删除的内容	LucidPapers	2018/6/19 PM12:59:00

to

页 12: [88] 删除的内容	LucidPapers	2018/6/19 PM12:59:00

to

页 12: [88] 删除的内容	LucidPapers	2018/6/19 PM12:59:00

to

页 12: [88] 删除的内容	LucidPapers	2018/6/19 PM12:59:00

to

页 12: [89] 删除的内容	LucidPapers	2018/6/19 PM1:01:00

was about 300 m

页 12: [89] 删除的内容	LucidPapers	2018/6/19 PM1:01:00

was about 300 m

页 12: [89] 删除的内容	LucidPapers	2018/6/19 PM1:01:00

was about 300 m

页 12: [89] 删除的内容	LucidPapers	2018/6/19 PM1:01:00

was about 300 m

页 12: [89] 删除的内容	LucidPapers	2018/6/19 PM1:01:00

was about 300 m

页 12: [89] 删除的内容	LucidPapers	2018/6/19 PM1:01:00

was about 300 m

页 12: [89] 删除的内容	LucidPapers	2018/6/19 PM1:01:00

was about 300 m

页 12: [89] 删除的内容	LucidPapers	2018/6/19 PM1:01:00

was about 300 m

页 12: [89] 删除的内容	LucidPapers	2018/6/19 PM1:01:00

was about 300 m

页 12: [89] 删除的内容	LucidPapers	2018/6/19 PM1:01:00

was about 300 m

页 12: [89] 删除的内容	LucidPapers	2018/6/19 PM1:01:00

was about 300 m

页 12: [89] 删除的内容	LucidPapers	2018/6/19 PM1:01:00

was about 300 m

页 12: [89] 删除的内容	LucidPapers	2018/6/19 PM1:01:00

was about 300 m

页 12: [89] 删除的内容	LucidPapers	2018/6/19 PM1:01:00

was about 300 m

页 12: [89] 删除的内容	LucidPapers	2018/6/19 PM1:01:00

was about 300 m

页 12: [89] 删除的内容	LucidPapers	2018/6/19 PM1:01:00

was about 300 m

页 12: [89] 删除的内容	LucidPapers	2018/6/19 PM1:01:00

was about 300 m

页 12: [89] 删除的内容	LucidPapers	2018/6/19 PM1:01:00

was about 300 m

页 12: [89] 删除的内容	LucidPapers	2018/6/19 PM1:01:00

was about 300 m

页 12: [89] 删除的内容	LucidPapers	2018/6/19 PM1:01:00

was about 300 m

页 12: [89] 删除的内容	LucidPapers	2018/6/19 PM1:01:00

was about 300 m

页 12: [89] 删除的内容	LucidPapers	2018/6/19 PM1:01:00

was about 300 m

页 12: [89] 删除的内容	LucidPapers	2018/6/19 PM1:01:00

was about 300 m

页 12: [90] 删除的内容	Microsoft Office User	2018/4/14 PM11:06:00

has

页 12: [90] 删除的内容	Microsoft Office User	2018/4/14 PM11:06:00

has

页 12: [91] 删除的内容	LucidPapers	2018/6/19 PM1:03:00

is

页 12: [91] 删除的内容	LucidPapers	2018/6/19 PM1:03:00

is

页 12: [91] 删除的内容	LucidPapers	2018/6/19 PM1:03:00

is

页 12: [91] 删除的内容	LucidPapers	2018/6/19 PM1:03:00

is

页 12: [91] 删除的内容	LucidPapers	2018/6/19 PM1:03:00

is

页 12: [91] 删除的内容	LucidPapers	2018/6/19 PM1:03:00

is

页 12: [91] 删除的内容	LucidPapers	2018/6/19 PM1:03:00

is

页 12: [92] 删除的内容	LucidPapers	2018/6/19 PM1:04:00

H

页 12: [92] 删除的内容	LucidPapers	2018/6/19 PM1:04:00

H

页 12: [92] 删除的内容	LucidPapers	2018/6/19 PM1:04:00

H

页 12: [93] 删除的内容	Microsoft Office User	2018/4/14 PM11:08:00

,

页 12: [93] 删除的内容	Microsoft Office User	2018/4/14 PM11:08:00

,

页 12: [94] 删除的内容	LucidPapers	2018/6/19 PM1:04:00

of approximately

页 12: [94] 删除的内容	LucidPapers	2018/6/19 PM1:04:00

of approximately

页 12: [94] 删除的内容 LucidPapers 2018/6/19 PM1:04:00

of approximately

页 12: [94] 删除的内容 LucidPapers 2018/6/19 PM1:04:00

of approximately

页 12: [94] 删除的内容 LucidPapers 2018/6/19 PM1:04:00

of approximately

页 12: [94] 删除的内容 LucidPapers 2018/6/19 PM1:04:00

of approximately

页 12: [94] 删除的内容 LucidPapers 2018/6/19 PM1:04:00

of approximately

页 12: [94] 删除的内容 LucidPapers 2018/6/19 PM1:04:00

of approximately

页 12: [94] 删除的内容 LucidPapers 2018/6/19 PM1:04:00

of approximately

页 12: [94] 删除的内容 LucidPapers 2018/6/19 PM1:04:00

of approximately

页 12: [94] 删除的内容 LucidPapers 2018/6/19 PM1:04:00

of approximately

页 12: [94] 删除的内容 LucidPapers 2018/6/19 PM1:04:00

of approximately

页 12: [94] 删除的内容 LucidPapers 2018/6/19 PM1:04:00

of approximately

页 12: [94] 删除的内容 LucidPapers 2018/6/19 PM1:04:00

of approximately

页 12: [94] 删除的内容 LucidPapers 2018/6/19 PM1:04:00

of approximately

页 12: [94] 删除的内容	LucidPapers	2018/6/19 PM1:04:00

of approximately

页 13: [95] 删除的内容	LucidPapers	2018/6/19 PM1:06:00

he

页 13: [95] 删除的内容	LucidPapers	2018/6/19 PM1:06:00

he

页 13: [95] 删除的内容	LucidPapers	2018/6/19 PM1:06:00

he

页 13: [96] 删除的内容	LucidPapers	2018/6/19 PM1:07:00

,

页 13: [96] 删除的内容	LucidPapers	2018/6/19 PM1:07:00

,

页 13: [96] 删除的内容	LucidPapers	2018/6/19 PM1:07:00

,

页 13: [96] 删除的内容	LucidPapers	2018/6/19 PM1:07:00

,

页 13: [97] 删除的内容	LucidPapers	2018/6/19 PM1:07:00

also

页 13: [97] 删除的内容	LucidPapers	2018/6/19 PM1:07:00

also

页 13: [97] 删除的内容	LucidPapers	2018/6/19 PM1:07:00

also

页 13: [97] 删除的内容	LucidPapers	2018/6/19 PM1:07:00

also

页 13: [97] 删除的内容	LucidPapers	2018/6/19 PM1:07:00

also

页 13: [97] 删除的内容	LucidPapers	2018/6/19 PM1:07:00

also

页 13: [97] 删除的内容	LucidPapers	2018/6/19 PM1:07:00

also

页 13: [97] 删除的内容	LucidPapers	2018/6/19 PM1:07:00

also

页 13: [97] 删除的内容	LucidPapers	2018/6/19 PM1:07:00

also

页 13: [97] 删除的内容	LucidPapers	2018/6/19 PM1:07:00

also

页 13: [97] 删除的内容	LucidPapers	2018/6/19 PM1:07:00

also

页 13: [97] 删除的内容	LucidPapers	2018/6/19 PM1:07:00

also

页 13: [97] 删除的内容	LucidPapers	2018/6/19 PM1:07:00

also

页 13: [97] 删除的内容	LucidPapers	2018/6/19 PM1:07:00

also

页 13: [97] 删除的内容	LucidPapers	2018/6/19 PM1:07:00

also

页 13: [97] 删除的内容	LucidPapers	2018/6/19 PM1:07:00

also

页 13: [97] 删除的内容	LucidPapers	2018/6/19 PM1:07:00

also

页 13: [97] 删除的内容	LucidPapers	2018/6/19 PM1:07:00

also

页 13: [97] 删除的内容	LucidPapers	2018/6/19 PM1:07:00

also

页 13: [97] 删除的内容	LucidPapers	2018/6/19 PM1:07:00

also

页 13: [97] 删除的内容	LucidPapers	2018/6/19 PM1:07:00

also

页 13: [97] 删除的内容	LucidPapers	2018/6/19 PM1:07:00

also

页 13: [97] 删除的内容	LucidPapers	2018/6/19 PM1:07:00

also

页 13: [97] 删除的内容	LucidPapers	2018/6/19 PM1:07:00

also

页 13: [97] 删除的内容	LucidPapers	2018/6/19 PM1:07:00

also

页 13: [97] 删除的内容	LucidPapers	2018/6/19 PM1:07:00

also

页 13: [97] 删除的内容	LucidPapers	2018/6/19 PM1:07:00

also

页 13: [97] 删除的内容	LucidPapers	2018/6/19 PM1:07:00

also

页 13: [97] 删除的内容	LucidPapers	2018/6/19 PM1:07:00

also

页 13: [97] 删除的内容	LucidPapers	2018/6/19 PM1:07:00

also

页 13: [97] 删除的内容	LucidPapers	2018/6/19 PM1:07:00

also

页 13: [97] 删除的内容	LucidPapers	2018/6/19 PM1:07:00

also

页 13: [98] 删除的内容	Microsoft Office User	2018/4/14 PM11:13:00

with no

页 13: [98] 删除的内容	Microsoft Office User	2018/4/14 PM11:13:00

with no

页 13: [99] 删除的内容	LucidPapers	2018/6/19 PM2:03:00

Inverse

页 13: [99] 删除的内容	LucidPapers	2018/6/19 PM2:03:00

Inverse

页 13: [99] 删除的内容	LucidPapers	2018/6/19 PM2:03:00

Inverse

页 13: [99] 删除的内容	LucidPapers	2018/6/19 PM2:03:00

Inverse

页 13: [99] 删除的内容	LucidPapers	2018/6/19 PM2:03:00

Inverse

页 13: [99] 删除的内容	LucidPapers	2018/6/19 PM2:03:00

Inverse

页 13: [99] 删除的内容	LucidPapers	2018/6/19 PM2:03:00

Inverse

页 13: [99] 删除的内容	LucidPapers	2018/6/19 PM2:03:00

Inverse

页 13: [99] 删除的内容	LucidPapers	2018/6/19 PM2:03:00

Inverse

页 13: [99] 删除的内容	LucidPapers	2018/6/19 PM2:03:00

Inverse

页 13: [99] 删除的内容	LucidPapers	2018/6/19 PM2:03:00

Inverse

页 13: [99] 删除的内容	LucidPapers	2018/6/19 PM2:03:00

Inverse

页 13: [99] 删除的内容	LucidPapers	2018/6/19 PM2:03:00

Inverse

页 13: [99] 删除的内容	LucidPapers	2018/6/19 PM2:03:00

Inverse

页 13: [99] 删除的内容	LucidPapers	2018/6/19 PM2:03:00

Inverse

页 13: [99] 删除的内容	LucidPapers	2018/6/19 PM2:03:00

Inverse

页 14: [100] 删除的内容	LucidPapers	2018/6/19 AM9:39:00

-

页 14: [100] 删除的内容	LucidPapers	2018/6/19 AM9:39:00

-

页 14: [100] 删除的内容	LucidPapers	2018/6/19 AM9:39:00

-

页 14: [100] 删除的内容	LucidPapers	2018/6/19 AM9:39:00

-

页 14: [100] 删除的内容	LucidPapers	2018/6/19 AM9:39:00

-

页 14: [100] 删除的内容	LucidPapers	2018/6/19 AM9:39:00

-

页 14: [100] 删除的内容	LucidPapers	2018/6/19 AM9:39:00

-

页 14: [100] 删除的内容	LucidPapers	2018/6/19 AM9:39:00

-

页 14: [100] 删除的内容	LucidPapers	2018/6/19 AM9:39:00

-

页 14: [100] 删除的内容	LucidPapers	2018/6/19 AM9:39:00

-

页 14: [100] 删除的内容	LucidPapers	2018/6/19 AM9:39:00

-

页 14: [100] 删除的内容	LucidPapers	2018/6/19 AM9:39:00

-

页 14: [100] 删除的内容	LucidPapers	2018/6/19 AM9:39:00

-

页 14: [100] 删除的内容	LucidPapers	2018/6/19 AM9:39:00

-

页 14: [100] 删除的内容	LucidPapers	2018/6/19 AM9:39:00

-

页 14: [100] 删除的内容	LucidPapers	2018/6/19 AM9:39:00

-

页 14: [100] 删除的内容	LucidPapers	2018/6/19 AM9:39:00

-

页 14: [100] 删除的内容	LucidPapers	2018/6/19 AM9:39:00

-

页 14: [100] 删除的内容	LucidPapers	2018/6/19 AM9:39:00

-

页 14: [100] 删除的内容	LucidPapers	2018/6/19 AM9:39:00

-

页 14: [101] 删除的内容	LucidPapers	2018/6/19 PM2:08:00

moisture

页 14: [101] 删除的内容	LucidPapers	2018/6/19 PM2:08:00

moisture

页 14: [101] 删除的内容	LucidPapers	2018/6/19 PM2:08:00

moisture

页 14: [101] 删除的内容	LucidPapers	2018/6/19 PM2:08:00

moisture

页 14: [102] 删除的内容	LucidPapers	2018/6/19 PM2:10:00

页 14: [102] 删除的内容	LucidPapers	2018/6/19 PM2:10:00

页 14: [102] 删除的内容	LucidPapers	2018/6/19 PM2:10:00

页 14: [102] 删除的内容	LucidPapers	2018/6/19 PM2:10:00

页 14: [102] 删除的内容	LucidPapers	2018/6/19 PM2:10:00

页 14: [102] 删除的内容	LucidPapers	2018/6/19 PM2:10:00

页 14: [102] 删除的内容	LucidPapers	2018/6/19 PM2:10:00

页 14: [102] 删除的内容	LucidPapers	2018/6/19 PM2:10:00

页 14: [102] 删除的内容	LucidPapers	2018/6/19 PM2:10:00

页 14: [102] 删除的内容	LucidPapers	2018/6/19 PM2:10:00

页 14: [102] 删除的内容	LucidPapers	2018/6/19 PM2:10:00

页 14: [103] 删除的内容	LucidPapers	2018/6/19 PM2:11:00

e

1.1

页 14: [103] 删除的内容	LucidPapers	2018/6/19 PM2:11:00

e

1.2

页 14: [104] 删除的内容 Microsoft Office 用户 2018/7/14 AM10:58:00

simulation

页 14: [104] 删除的内容 Microsoft Office 用户 2018/7/14 AM10:58:00

simulation

页 14: [105] 删除的内容 LucidPapers 2018/6/19 PM2:12:00

LES

页 14: [105] 删除的内容 LucidPapers 2018/6/19 PM2:12:00

LES

页 14: [105] 删除的内容 LucidPapers 2018/6/19 PM2:12:00

LES

页 14: [105] 删除的内容 LucidPapers 2018/6/19 PM2:12:00

LES

页 14: [105] 删除的内容	LucidPapers	2018/6/19 PM2:12:00

LES

页 14: [105] 删除的内容	LucidPapers	2018/6/19 PM2:12:00

LES

页 14: [105] 删除的内容	LucidPapers	2018/6/19 PM2:12:00

LES

页 14: [105] 删除的内容	LucidPapers	2018/6/19 PM2:12:00

LES

页 14: [105] 删除的内容	LucidPapers	2018/6/19 PM2:12:00

LES

页 14: [106] 删除的内容	LucidPapers	2018/6/19 PM2:12:00

PBL

页 14: [106] 删除的内容	LucidPapers	2018/6/19 PM2:12:00

PBL

页 14: [106] 删除的内容	LucidPapers	2018/6/19 PM2:12:00

PBL

页 14: [106] 删除的内容	LucidPapers	2018/6/19 PM2:12:00

PBL

页 14: [107] 删除的内容	LucidPapers	2018/6/19 PM2:13:00

S

页 14: [107] 删除的内容	LucidPapers	2018/6/19 PM2:13:00

S

页 14: [107] 删除的内容	LucidPapers	2018/6/19 PM2:13:00

S

页 14: [107] 删除的内容	LucidPapers	2018/6/19 PM2:13:00

S

页 15: [108] 删除的内容 LucidPapers 2018/6/19 PM2:14:00

R

页 15: [108] 删除的内容 LucidPapers 2018/6/19 PM2:14:00

R

页 15: [108] 删除的内容 LucidPapers 2018/6/19 PM2:14:00

R

页 15: [108] 删除的内容 LucidPapers 2018/6/19 PM2:14:00

R

页 15: [108] 删除的内容 LucidPapers 2018/6/19 PM2:14:00

R

页 15: [108] 删除的内容 LucidPapers 2018/6/19 PM2:14:00

R

页 15: [108] 删除的内容	LucidPapers	2018/6/19 PM2:14:00

R

页 15: [108] 删除的内容	LucidPapers	2018/6/19 PM2:14:00

R

页 15: [108] 删除的内容	LucidPapers	2018/6/19 PM2:14:00

R

页 15: [108] 删除的内容	LucidPapers	2018/6/19 PM2:14:00

R

页 15: [108] 删除的内容	LucidPapers	2018/6/19 PM2:14:00

R

页 15: [109] 删除的内容	LucidPapers	2018/6/19 PM2:16:00

er

页 15: [109] 删除的内容	LucidPapers	2018/6/19 PM2:16:00

er

页 15: [110] 删除的内容	LucidPapers	2018/6/19 PM2:17:00

Furthermore, in

页 15: [110] 删除的内容	LucidPapers	2018/6/19 PM2:17:00

Furthermore, in

页 15: [110] 删除的内容	LucidPapers	2018/6/19 PM2:17:00

Furthermore, in

页 15: [110] 删除的内容	LucidPapers	2018/6/19 PM2:17:00

Furthermore, in

页 15: [110] 删除的内容	LucidPapers	2018/6/19 PM2:17:00

Furthermore, in

页 15: [111] 删除的内容	LucidPapers	2018/6/19 PM2:17:00

页 15: [111] 删除的内容	LucidPapers	2018/6/19 PM2:17:00

页 15: [111] 删除的内容	LucidPapers	2018/6/19 PM2:17:00

页 15: [111] 删除的内容	LucidPapers	2018/6/19 PM2:17:00

页 15: [111] 删除的内容	LucidPapers	2018/6/19 PM2:17:00

页 15: [112] 删除的内容	LucidPapers	2018/6/19 PM2:17:00

页 15: [112] 删除的内容	LucidPapers	2018/6/19 PM2:17:00

页 15: [112] 删除的内容 LucidPapers 2018/6/19 PM2:17:00

页 15: [113] 删除的内容 LucidPapers 2018/6/19 PM2:18:00

页 15: [113] 删除的内容 LucidPapers 2018/6/19 PM2:18:00

页 15: [113] 删除的内容 LucidPapers 2018/6/19 PM2:18:00

页 15: [113] 删除的内容 LucidPapers 2018/6/19 PM2:18:00

页 15: [113] 删除的内容 LucidPapers 2018/6/19 PM2:18:00

页 15: [114] 删除的内容	LucidPapers	2018/6/19 AM9:39:00

sections

页 15: [114] 删除的内容	LucidPapers	2018/6/19 AM9:39:00

sections

页 15: [114] 删除的内容	LucidPapers	2018/6/19 AM9:39:00

sections

页 15: [114] 删除的内容	LucidPapers	2018/6/19 AM9:39:00

sections

页 15: [114] 删除的内容	LucidPapers	2018/6/19 AM9:39:00

sections

页 15: [114] 删除的内容	LucidPapers	2018/6/19 AM9:39:00

sections

页 15: [114] 删除的内容	LucidPapers	2018/6/19 AM9:39:00

sections

页 15: [114] 删除的内容 LucidPapers 2018/6/19 AM9:39:00

sections

页 15: [115] 删除的内容 LucidPapers 2018/6/19 PM2:19:00

页 15: [115] 删除的内容 LucidPapers 2018/6/19 PM2:19:00

页 15: [115] 删除的内容 LucidPapers 2018/6/19 PM2:19:00

页 15: [115] 删除的内容 LucidPapers 2018/6/19 PM2:19:00

页 15: [115] 删除的内容 LucidPapers 2018/6/19 PM2:19:00

页 15: [115] 删除的内容	LucidPapers	2018/6/19 PM2:19:00

页 15: [115] 删除的内容	LucidPapers	2018/6/19 PM2:19:00

页 15: [116] 删除的内容	LucidPapers	2018/6/19 PM2:21:00

S

页 15: [116] 删除的内容	LucidPapers	2018/6/19 PM2:21:00

S

页 15: [116] 删除的内容	LucidPapers	2018/6/19 PM2:21:00

S

页 15: [116] 删除的内容	LucidPapers	2018/6/19 PM2:21:00

S

页 15: [116] 删除的内容	LucidPapers	2018/6/19 PM2:21:00

S

页 16: [117] 删除的内容	LucidPapers	2018/6/19 PM2:24:00

页 16: [117] 删除的内容	LucidPapers	2018/6/19 PM2:24:00

页 16: [117] 删除的内容	LucidPapers	2018/6/19 PM2:24:00

页 16: [117] 删除的内容	LucidPapers	2018/6/19 PM2:24:00

页 16: [117] 删除的内容	LucidPapers	2018/6/19 PM2:24:00

页 16: [117] 删除的内容	LucidPapers	2018/6/19 PM2:24:00

页 16: [118] 删除的内容	LucidPapers	2018/6/19 PM2:25:00

页 16: [118] 删除的内容	LucidPapers	2018/6/19 PM2:25:00

页 16: [118] 删除的内容	LucidPapers	2018/6/19 PM2:25:00

页 16: [118] 删除的内容	LucidPapers	2018/6/19 PM2:25:00

页 16: [118] 删除的内容	LucidPapers	2018/6/19 PM2:25:00

页 16: [118] 删除的内容	LucidPapers	2018/6/19 PM2:25:00

页 16: [118] 删除的内容	LucidPapers	2018/6/19 PM2:25:00

页 16: [118] 删除的内容	LucidPapers	2018/6/19 PM2:25:00

页 16: [118] 删除的内容	LucidPapers	2018/6/19 PM2:25:00

页 16: [119] 删除的内容	LucidPapers	2018/6/19 PM2:26:00

页 16: [119] 删除的内容	LucidPapers	2018/6/19 PM2:26:00

页 16: [119] 删除的内容	LucidPapers	2018/6/19 PM2:26:00

页 16: [119] 删除的内容 LucidPapers 2018/6/19 PM2:26:00

页 16: [119] 删除的内容 LucidPapers 2018/6/19 PM2:26:00

页 16: [119] 删除的内容 LucidPapers 2018/6/19 PM2:26:00

页 16: [119] 删除的内容 LucidPapers 2018/6/19 PM2:26:00

页 16: [119] 删除的内容 LucidPapers 2018/6/19 PM2:26:00

页 16: [119] 删除的内容 LucidPapers 2018/6/19 PM2:26:00

页 16: [119] 删除的内容 LucidPapers 2018/6/19 PM2:26:00

页 16: [119] 删除的内容	LucidPapers	2018/6/19 PM2:26:00

页 16: [119] 删除的内容	LucidPapers	2018/6/19 PM2:26:00

页 16: [119] 删除的内容	LucidPapers	2018/6/19 PM2:26:00

页 16: [119] 删除的内容	LucidPapers	2018/6/19 PM2:26:00

页 16: [119] 删除的内容	LucidPapers	2018/6/19 PM2:26:00

页 16: [119] 删除的内容	LucidPapers	2018/6/19 PM2:26:00

页 16: [119] 删除的内容	LucidPapers	2018/6/19 PM2:26:00

页 16: [120] 删除的内容	LucidPapers	2018/6/19 PM2:29:00

页 16: [120] 删除的内容	LucidPapers	2018/6/19 PM2:29:00

页 16: [120] 删除的内容	LucidPapers	2018/6/19 PM2:29:00

页 16: [120] 删除的内容	LucidPapers	2018/6/19 PM2:29:00

页 16: [120] 删除的内容	LucidPapers	2018/6/19 PM2:29:00

页 16: [120] 删除的内容 LucidPapers 2018/6/19 PM2:29:00

页 16: [120] 删除的内容 LucidPapers 2018/6/19 PM2:29:00

页 16: [120] 删除的内容 LucidPapers 2018/6/19 PM2:29:00

页 16: [120] 删除的内容 LucidPapers 2018/6/19 PM2:29:00

页 16: [121] 删除的内容 LucidPapers 2018/6/19 PM2:30:00

页 16: [121] 删除的内容 LucidPapers 2018/6/19 PM2:30:00

页 16: [121] 删除的内容 LucidPapers 2018/6/19 PM2:30:00

页 16: [121] 删除的内容	LucidPapers	2018/6/19 PM2:30:00

页 16: [121] 删除的内容	LucidPapers	2018/6/19 PM2:30:00

页 16: [121] 删除的内容	LucidPapers	2018/6/19 PM2:30:00

页 16: [121] 删除的内容	LucidPapers	2018/6/19 PM2:30:00

页 16: [121] 删除的内容	LucidPapers	2018/6/19 PM2:30:00

页 16: [121] 删除的内容	LucidPapers	2018/6/19 PM2:30:00

页 16: [121] 删除的内容	LucidPapers	2018/6/19 PM2:30:00

页 16: [121] 删除的内容	LucidPapers	2018/6/19 PM2:30:00

页 16: [121] 删除的内容	LucidPapers	2018/6/19 PM2:30:00

页 17: [122] 删除的内容	LucidPapers	2018/6/19 AM10:57:00

(SH)

1.3

页 17: [122] 删除的内容	LucidPapers	2018/6/19 AM10:57:00

(SH)

1.4

页 17: [123] 删除的内容	LucidPapers	2018/6/19 PM2:33:00

PBL

页 17: [123] 删除的内容	LucidPapers	2018/6/19 PM2:33:00

PBL

页 17: [123] 删除的内容	LucidPapers	2018/6/19 PM2:33:00

PBL

页 17: [124] 删除的内容	LucidPapers	2018/6/19 AM10:58:00

SH

页 17: [124] 删除的内容	LucidPapers	2018/6/19 AM10:58:00

SH

页 17: [125] 删除的内容	LucidPapers	2018/6/19 AM10:58:00

SH

页 17: [125] 删除的内容	LucidPapers	2018/6/19 AM10:58:00

SH

页 17: [126] 删除的内容	LucidPapers	2018/6/19 PM2:34:00

summer

页 17: [126] 删除的内容 LucidPapers 2018/6/19 PM2:34:00

summer

页 17: [126] 删除的内容 LucidPapers 2018/6/19 PM2:34:00

summer

页 17: [127] 删除的内容 LucidPapers 2018/6/19 PM2:35:00

PB

页 17: [127] 删除的内容 LucidPapers 2018/6/19 PM2:35:00

PB

页 17: [127] 删除的内容 LucidPapers 2018/6/19 PM2:35:00

PB

页 17: [128] 删除的内容 LucidPapers 2018/6/19 PM2:35:00

;

页 17: [128] 删除的内容	LucidPapers	2018/6/19 PM2:35:00

;

页 17: [129] 删除的内容	LucidPapers	2018/6/19 PM2:35:00

For Noah experiment

页 17: [129] 删除的内容	LucidPapers	2018/6/19 PM2:35:00

For Noah experiment

页 17: [129] 删除的内容	LucidPapers	2018/6/19 PM2:35:00

For Noah experiment

页 17: [129] 删除的内容	LucidPapers	2018/6/19 PM2:35:00

For Noah experiment

页 17: [129] 删除的内容	LucidPapers	2018/6/19 PM2:35:00

For Noah experiment

页 17: [130] 删除的内容	LucidPapers	2018/6/19 PM2:36:00

,

页 17: [130] 删除的内容	LucidPapers	2018/6/19 PM2:36:00

,

页 17: [130] 删除的内容	LucidPapers	2018/6/19 PM2:36:00

,

页 17: [130] 删除的内容	LucidPapers	2018/6/19 PM2:36:00

,

页 17: [130] 删除的内容	LucidPapers	2018/6/19 PM2:36:00

,

页 17: [131] 删除的内容	LucidPapers	2018/6/19 PM2:36:00

,

页 17: [131] 删除的内容	LucidPapers	2018/6/19 PM2:36:00

,

页 17: [132] 删除的内容	LucidPapers	2018/6/19 PM2:37:00

ed

页 17: [132] 删除的内容	LucidPapers	2018/6/19 PM2:37:00

ed

页 17: [132] 删除的内容	LucidPapers	2018/6/19 PM2:37:00

ed

页 17: [132] 删除的内容	LucidPapers	2018/6/19 PM2:37:00

ed

页 17: [132] 删除的内容	LucidPapers	2018/6/19 PM2:37:00

ed

页 17: [132] 删除的内容	LucidPapers	2018/6/19 PM2:37:00

ed

页 17: [132] 删除的内容	LucidPapers	2018/6/19 PM2:37:00

ed

页 17: [132] 删除的内容	LucidPapers	2018/6/19 PM2:37:00

ed

页 17: [132] 删除的内容	LucidPapers	2018/6/19 PM2:37:00

ed

页 17: [132] 删除的内容	LucidPapers	2018/6/19 PM2:37:00

ed

页 17: [132] 删除的内容	LucidPapers	2018/6/19 PM2:37:00

ed

页 17: [132] 删除的内容	LucidPapers	2018/6/19 PM2:37:00

ed

页 17: [132] 删除的内容	LucidPapers	2018/6/19 PM2:37:00

ed

页 17: [132] 删除的内容	LucidPapers	2018/6/19 PM2:37:00

ed

页 17: [132] 删除的内容	LucidPapers	2018/6/19 PM2:37:00

ed

页 17: [132] 删除的内容	LucidPapers	2018/6/19 PM2:37:00

ed

页 17: [132] 删除的内容	LucidPapers	2018/6/19 PM2:37:00

ed

页 17: [132] 删除的内容	LucidPapers	2018/6/19 PM2:37:00

ed

页 17: [132] 删除的内容	LucidPapers	2018/6/19 PM2:37:00

ed

页 17: [133] 删除的内容	LucidPapers	2018/6/19 PM2:48:00

F

页 17: [133] 删除的内容	LucidPapers	2018/6/19 PM2:48:00

F

页 17: [134] 删除的内容	Microsoft Office User	2018/4/7 PM4:34:00

The results

页 17: [134] 删除的内容	Microsoft Office User	2018/4/7 PM4:34:00

The results

页 17: [135] 删除的内容	LucidPapers	2018/6/19 PM2:49:00

with

页 17: [135] 删除的内容	LucidPapers	2018/6/19 PM2:49:00

with

页 18: [136] 删除的内容	Microsoft Office User	2018/4/15 AM9:25:00

and

页 18: [136] 删除的内容	Microsoft Office User	2018/4/15 AM9:25:00

and

页 18: [137] 删除的内容	LucidPapers	2018/6/19 PM2:49:00

Such

页 18: [137] 删除的内容	LucidPapers	2018/6/19 PM2:49:00

Such

页 18: [137] 删除的内容	LucidPapers	2018/6/19 PM2:49:00

Such

页 18: [137] 删除的内容	LucidPapers	2018/6/19 PM2:49:00

Such

页 18: [138] 删除的内容	Microsoft Office User	2018/4/7 PM4:35:00

determined

页 18: [138] 删除的内容	Microsoft Office User	2018/4/7 PM4:35:00

determined

页 18: [138] 删除的内容	Microsoft Office User	2018/4/7 PM4:35:00

determined

页 18: [139] 删除的内容	LucidPapers	2018/6/19 PM2:49:00

（

页 18: [139] 删除的内容	LucidPapers	2018/6/19 PM2:49:00

（

页 18: [139] 删除的内容	LucidPapers	2018/6/19 PM2:49:00

（

页 18: [139] 删除的内容	LucidPapers	2018/6/19 PM2:49:00

（

页 18: [139] 删除的内容	LucidPapers	2018/6/19 PM2:49:00

（

页 18: [140] 删除的内容	Microsoft Office User	2018/4/7 PM4:36:00

CTRL

页 18: [140] 删除的内容	Microsoft Office User	2018/4/7 PM4:36:00

CTRL

页 18: [140] 删除的内容	Microsoft Office User	2018/4/7 PM4:36:00

CTRL

页 18: [141] 删除的内容	LucidPapers	2018/6/19 PM2:50:00

while

页 18: [141] 删除的内容	LucidPapers	2018/6/19 PM2:50:00

while

页 18: [142] 删除的内容 LucidPapers 2018/6/19 PM2:50:00

results are

页 18: [142] 删除的内容 LucidPapers 2018/6/19 PM2:50:00

results are

页 18: [142] 删除的内容 LucidPapers 2018/6/19 PM2:50:00

results are

页 18: [142] 删除的内容 LucidPapers 2018/6/19 PM2:50:00

results are

页 18: [143] 删除的内容 Microsoft Office User 2018/4/15 AM9:26:00

S

页 18: [143] 删除的内容 Microsoft Office User 2018/4/15 AM9:26:00

S

页 18: [144] 删除的内容	LucidPapers	2018/6/19 PM2:51:00

can

页 18: [144] 删除的内容	LucidPapers	2018/6/19 PM2:51:00

can

页 18: [144] 删除的内容	LucidPapers	2018/6/19 PM2:51:00

can

页 18: [144] 删除的内容	LucidPapers	2018/6/19 PM2:51:00

can

页 18: [144] 删除的内容	LucidPapers	2018/6/19 PM2:51:00

can

页 18: [144] 删除的内容	LucidPapers	2018/6/19 PM2:51:00

can

页 18: [145] 删除的内容	LucidPapers	2018/6/19 PM2:52:00

R

页 18: [145] 删除的内容	LucidPapers	2018/6/19 PM2:52:00

R

页 18: [145] 删除的内容	LucidPapers	2018/6/19 PM2:52:00

R

页 18: [145] 删除的内容	LucidPapers	2018/6/19 PM2:52:00

R

页 18: [145] 删除的内容	LucidPapers	2018/6/19 PM2:52:00

R

页 18: [145] 删除的内容	LucidPapers	2018/6/19 PM2:52:00

R

页 18: [145] 删除的内容	LucidPapers	2018/6/19 PM2:52:00

R

页 18: [146] 删除的内容	LucidPapers	2018/6/19 AM10:58:00

SH

页 18: [146] 删除的内容	LucidPapers	2018/6/19 AM10:58:00

SH

页 18: [146] 删除的内容	LucidPapers	2018/6/19 AM10:58:00

SH

页 18: [146] 删除的内容	LucidPapers	2018/6/19 AM10:58:00

SH

页 18: [146] 删除的内容	LucidPapers	2018/6/19 AM10:58:00

SH

页 18: [146] 删除的内容	LucidPapers	2018/6/19 AM10:58:00

SH

页 18: [146] 删除的内容	LucidPapers	2018/6/19 AM10:58:00

SH

页 18: [146] 删除的内容	LucidPapers	2018/6/19 AM10:58:00

SH

页 18: [146] 删除的内容	LucidPapers	2018/6/19 AM10:58:00

SH

页 18: [146] 删除的内容	LucidPapers	2018/6/19 AM10:58:00

SH

页 18: [146] 删除的内容	LucidPapers	2018/6/19 AM10:58:00

SH

页 18: [146] 删除的内容	LucidPapers	2018/6/19 AM10:58:00

SH

页 18: [146] 删除的内容	LucidPapers	2018/6/19 AM10:58:00

SH

页 18: [146] 删除的内容	LucidPapers	2018/6/19 AM10:58:00

SH

页 18: [146] 删除的内容	LucidPapers	2018/6/19 AM10:58:00

SH

页 18: [146] 删除的内容	LucidPapers	2018/6/19 AM10:58:00

SH

页 19: [147] 删除的内容	LucidPapers	2018/6/19 PM2:55:00

ing

页 19: [147] 删除的内容	LucidPapers	2018/6/19 PM2:55:00

ing

页 19: [147] 删除的内容	LucidPapers	2018/6/19 PM2:55:00

ing

页 19: [147] 删除的内容	LucidPapers	2018/6/19 PM2:55:00

ing

页 19: [147] 删除的内容	LucidPapers	2018/6/19 PM2:55:00

ing

页 19: [147] 删除的内容	LucidPapers	2018/6/19 PM2:55:00

ing

页 19: [147] 删除的内容	LucidPapers	2018/6/19 PM2:55:00

ing

页 19: [147] 删除的内容	LucidPapers	2018/6/19 PM2:55:00

ing

页 19: [147] 删除的内容	LucidPapers	2018/6/19 PM2:55:00

ing

页 19: [147] 删除的内容 LucidPapers 2018/6/19 PM2:55:00

ing

页 19: [148] 修订 Unknown

域代码已更改

页 19: [148] 修订 Unknown

域代码已更改

页 19: [149] 删除的内容 LucidPapers 2018/6/20 PM2:45:00

larger SH

页 19: [149] 删除的内容 LucidPapers 2018/6/20 PM2:45:00

larger SH

页 19: [149] 删除的内容 LucidPapers 2018/6/20 PM2:45:00

larger SH

页 19: [150] 删除的内容 LucidPapers 2018/6/19 PM2:59:00

is

页 19: [150] 删除的内容 LucidPapers 2018/6/19 PM2:59:00

is

页 19: [150] 删除的内容 LucidPapers 2018/6/19 PM2:59:00

is

页 19: [150] 删除的内容 LucidPapers 2018/6/19 PM2:59:00

is

页 19: [150] 删除的内容 LucidPapers 2018/6/19 PM2:59:00

is

页 19: [150] 删除的内容 LucidPapers 2018/6/19 PM2:59:00

is

页 19: [150] 删除的内容 LucidPapers 2018/6/19 PM2:59:00

is

页 19: [150] 删除的内容 LucidPapers 2018/6/19 PM2:59:00

is

页 19: [150] 删除的内容	LucidPapers	2018/6/19 PM2:59:00

is

页 19: [150] 删除的内容	LucidPapers	2018/6/19 PM2:59:00

is

页 19: [150] 删除的内容	LucidPapers	2018/6/19 PM2:59:00

is

页 19: [150] 删除的内容	LucidPapers	2018/6/19 PM2:59:00

is

页 19: [150] 删除的内容	LucidPapers	2018/6/19 PM2:59:00

is

页 19: [150] 删除的内容	LucidPapers	2018/6/19 PM2:59:00

is

页 19: [150] 删除的内容	LucidPapers	2018/6/19 PM2:59:00

is

页 19: [150] 删除的内容	LucidPapers	2018/6/19 PM2:59:00

is

页 19: [150] 删除的内容	LucidPapers	2018/6/19 PM2:59:00

is

页 19: [150] 删除的内容	LucidPapers	2018/6/19 PM2:59:00

is

页 19: [150] 删除的内容	LucidPapers	2018/6/19 PM2:59:00

is

页 19: [150] 删除的内容	LucidPapers	2018/6/19 PM2:59:00

is

页 19: [150] 删除的内容	LucidPapers	2018/6/19 PM2:59:00

is

页 19: [150] 删除的内容	LucidPapers	2018/6/19 PM2:59:00

is

页 19: [151] 删除的内容	LucidPapers	2018/6/19 PM3:01:00

页 19: [151] 删除的内容	LucidPapers	2018/6/19 PM3:01:00

页 19: [151] 删除的内容	LucidPapers	2018/6/19 PM3:01:00

页 19: [151] 删除的内容	LucidPapers	2018/6/19 PM3:01:00

页 19: [151] 删除的内容	LucidPapers	2018/6/19 PM3:01:00

页 19: [151] 删除的内容 LucidPapers 2018/6/19 PM3:01:00

页 19: [151] 删除的内容 LucidPapers 2018/6/19 PM3:01:00

页 19: [151] 删除的内容 LucidPapers 2018/6/19 PM3:01:00

页 19: [151] 删除的内容 LucidPapers 2018/6/19 PM3:01:00

页 19: [151] 删除的内容 LucidPapers 2018/6/19 PM3:01:00

页 19: [151] 删除的内容 LucidPapers 2018/6/19 PM3:01:00

页 19: [151] 删除的内容	LucidPapers	2018/6/19 PM3:01:00

页 19: [151] 删除的内容	LucidPapers	2018/6/19 PM3:01:00

页 19: [151] 删除的内容	LucidPapers	2018/6/19 PM3:01:00

页 19: [152] 删除的内容	LucidPapers	2018/6/19 PM3:02:00

，

页 19: [152] 删除的内容	LucidPapers	2018/6/19 PM3:02:00

，

页 19: [152] 删除的内容	LucidPapers	2018/6/19 PM3:02:00

，

页 19: [152] 删除的内容	LucidPapers	2018/6/19 PM3:02:00

,

页 19: [152] 删除的内容	LucidPapers	2018/6/19 PM3:02:00

,

页 19: [152] 删除的内容	LucidPapers	2018/6/19 PM3:02:00

,

页 20: [153] 删除的内容	LucidPapers	2018/6/19 AM9:45:00

desert

页 20: [153] 删除的内容	LucidPapers	2018/6/19 AM9:45:00

desert

页 20: [153] 删除的内容	LucidPapers	2018/6/19 AM9:45:00

desert

页 20: [153] 删除的内容	LucidPapers	2018/6/19 AM9:45:00

desert

页 20: [153] 删除的内容	LucidPapers	2018/6/19 AM9:45:00

desert

页 20: [154] 删除的内容	LucidPapers	2018/6/19 PM3:04:00

页 20: [154] 删除的内容	LucidPapers	2018/6/19 PM3:04:00

页 20: [154] 删除的内容	LucidPapers	2018/6/19 PM3:04:00

页 20: [154] 删除的内容	LucidPapers	2018/6/19 PM3:04:00

页 20: [154] 删除的内容	LucidPapers	2018/6/19 PM3:04:00

页 20: [155] 删除的内容	LucidPapers	2018/6/19 PM3:05:00

Weather Research and Forecasting Model (

页 20: [155] 删除的内容	LucidPapers	2018/6/19 PM3:05:00

Weather Research and Forecasting Model (

页 20: [155] 删除的内容	LucidPapers	2018/6/19 PM3:05:00

Weather Research and Forecasting Model (

页 20: [155] 删除的内容	LucidPapers	2018/6/19 PM3:05:00

Weather Research and Forecasting Model (

页 20: [155] 删除的内容	LucidPapers	2018/6/19 PM3:05:00

Weather Research and Forecasting Model (

页 20: [155] 删除的内容	LucidPapers	2018/6/19 PM3:05:00

Weather Research and Forecasting Model (

页 20: [155] 删除的内容	LucidPapers	2018/6/19 PM3:05:00

Weather Research and Forecasting Model (

页 20: [155] 删除的内容	LucidPapers	2018/6/19 PM3:05:00

Weather Research and Forecasting Model (

页 20: [155] 删除的内容	LucidPapers	2018/6/19 PM3:05:00

Weather Research and Forecasting Model (

页 20: [155] 删除的内容	LucidPapers	2018/6/19 PM3:05:00

Weather Research and Forecasting Model (

页 20: [155] 删除的内容	LucidPapers	2018/6/19 PM3:05:00

Weather Research and Forecasting Model (

页 20: [155] 删除的内容	LucidPapers	2018/6/19 PM3:05:00

Weather Research and Forecasting Model (

页 20: [155] 删除的内容	LucidPapers	2018/6/19 PM3:05:00

Weather Research and Forecasting Model (

页 20: [155] 删除的内容	LucidPapers	2018/6/19 PM3:05:00

Weather Research and Forecasting Model (

页 20: [155] 删除的内容	LucidPapers	2018/6/19 PM3:05:00

Weather Research and Forecasting Model (

页 20: [155] 删除的内容	LucidPapers	2018/6/19 PM3:05:00

Weather Research and Forecasting Model (

页 20: [155] 删除的内容	LucidPapers	2018/6/19 PM3:05:00

Weather Research and Forecasting Model (

页 20: [155] 删除的内容	LucidPapers	2018/6/19 PM3:05:00

Weather Research and Forecasting Model (

页 20: [155] 删除的内容	LucidPapers	2018/6/19 PM3:05:00

Weather Research and Forecasting Model (

页 20: [155] 删除的内容	LucidPapers	2018/6/19 PM3:05:00

Weather Research and Forecasting Model (

页 20: [156] 删除的内容	LucidPapers	2018/6/19 PM3:07:00

Consequently, with the configuration used in this study, t

页 20: [156] 删除的内容	LucidPapers	2018/6/19 PM3:07:00

Consequently, with the configuration used in this study, t

页 20: [157] 删除的内容	LucidPapers	2018/6/19 PM3:08:00

it

页 20: [157] 删除的内容	LucidPapers	2018/6/19 PM3:08:00

it

页 20: [157] 删除的内容	LucidPapers	2018/6/19 PM3:08:00

it

页 20: [158] 删除的内容	LucidPapers	2018/6/19 PM3:09:00

y

页 20: [158] 删除的内容	LucidPapers	2018/6/19 PM3:09:00

y

页 20: [158] 删除的内容	LucidPapers	2018/6/19 PM3:09:00

y

页 20: [158] 删除的内容	LucidPapers	2018/6/19 PM3:09:00

y

页 20: [158] 删除的内容	LucidPapers	2018/6/19 PM3:09:00

y

页 20: [158] 删除的内容	LucidPapers	2018/6/19 PM3:09:00

y

页 20: [158] 删除的内容	LucidPapers	2018/6/19 PM3:09:00

y

页 20: [159] 删除的内容 Microsoft Office User 2018/4/7 PM4:50:00

struggles to

页 20: [159] 删除的内容 Microsoft Office User 2018/4/7 PM4:50:00

struggles to

页 20: [160] 删除的内容 LucidPapers 2018/6/19 PM3:10:00

er

页 20: [160] 删除的内容 LucidPapers 2018/6/19 PM3:10:00

er

页 20: [160] 删除的内容 LucidPapers 2018/6/19 PM3:10:00

er

页 20: [161] 删除的内容 Microsoft Office User 2018/4/7 PM4:50:00

which

页 20: [161] 删除的内容	Microsoft Office User	2018/4/7 PM4:50:00

which

页 20: [162] 删除的内容	LucidPapers	2018/6/20 PM2:47:00

by up to about 0.4K compared to

页 20: [162] 删除的内容	LucidPapers	2018/6/20 PM2:47:00

by up to about 0.4K compared to

页 20: [162] 删除的内容	LucidPapers	2018/6/20 PM2:47:00

by up to about 0.4K compared to

页 20: [163] 删除的内容	LucidPapers	2018/6/19 PM3:11:00

afternoon

页 20: [163] 删除的内容	LucidPapers	2018/6/19 PM3:11:00

afternoon

页 20: [163] 删除的内容	LucidPapers	2018/6/19 PM3:11:00

afternoon

页 21: [164] 删除的内容	LucidPapers	2018/6/19 PM3:12:00

by about 1 to 2 g/Kg

页 21: [164] 删除的内容	LucidPapers	2018/6/19 PM3:12:00

by about 1 to 2 g/Kg

页 21: [164] 删除的内容	LucidPapers	2018/6/19 PM3:12:00

by about 1 to 2 g/Kg

页 21: [164] 删除的内容	LucidPapers	2018/6/19 PM3:12:00

by about 1 to 2 g/Kg

页 21: [164] 删除的内容	LucidPapers	2018/6/19 PM3:12:00

by about 1 to 2 g/Kg

页 21: [164] 删除的内容	LucidPapers	2018/6/19 PM3:12:00

by about 1 to 2 g/Kg

页 21: [165] 删除的内容	LucidPapers	2018/6/19 PM3:13:00

as observed

页 21: [165] 删除的内容	LucidPapers	2018/6/19 PM3:13:00

as observed

页 21: [166] 删除的内容	LucidPapers	2018/6/19 PM3:13:00

Furthermore, two t

页 21: [166] 删除的内容	LucidPapers	2018/6/19 PM3:13:00

Furthermore, two t

页 21: [166] 删除的内容	LucidPapers	2018/6/19 PM3:13:00

Furthermore, two t

页 21: [166] 删除的内容	LucidPapers	2018/6/19 PM3:13:00

Furthermore, two t

页 21: [166] 删除的内容	LucidPapers	2018/6/19 PM3:13:00

Furthermore, two t

页 21: [166] 删除的内容	LucidPapers	2018/6/19 PM3:13:00

Furthermore, two t

页 21: [167] 删除的内容	LucidPapers	2018/6/19 PM3:14:00

,

页 21: [167] 删除的内容	LucidPapers	2018/6/19 PM3:14:00

,

页 21: [167] 删除的内容	LucidPapers	2018/6/19 PM3:14:00

,

页 21: [167] 删除的内容	LucidPapers	2018/6/19 PM3:14:00

,

页 21: [168] 删除的内容	LucidPapers	2018/6/19 AM9:39:00

-

页 21: [168] 删除的内容	LucidPapers	2018/6/19 AM9:39:00

-

页 21: [168] 删除的内容	LucidPapers	2018/6/19 AM9:39:00

-

页 21: [169] 删除的内容	Microsoft Office User	2018/4/12 PM6:00:00

the

页 21: [169] 删除的内容	Microsoft Office User	2018/4/12 PM6:00:00

the

页 21: [170] 删除的内容	LucidPapers	2018/6/19 PM3:15:00

summer

页 21: [170] 删除的内容	LucidPapers	2018/6/19 PM3:15:00

summer

页 21: [170] 删除的内容	LucidPapers	2018/6/19 PM3:15:00

summer

页 21: [170] 删除的内容	LucidPapers	2018/6/19 PM3:15:00

summer

页 21: [170] 删除的内容	LucidPapers	2018/6/19 PM3:15:00

summer

页 21: [170] 删除的内容	LucidPapers	2018/6/19 PM3:15:00

summer

页 21: [171] 删除的内容	LucidPapers	2018/6/19 PM3:16:00

The f

页 21: [171] 删除的内容	LucidPapers	2018/6/19 PM3:16:00

The f

页 21: [171] 删除的内容	LucidPapers	2018/6/19 PM3:16:00

The f

页 21: [171] 删除的内容	LucidPapers	2018/6/19 PM3:16:00

The f

页 21: [171] 删除的内容	LucidPapers	2018/6/19 PM3:16:00

The f

页 21: [171] 删除的内容	LucidPapers	2018/6/19 PM3:16:00

The f

页 21: [171] 删除的内容	LucidPapers	2018/6/19 PM3:16:00

The f

页 21: [171] 删除的内容	LucidPapers	2018/6/19 PM3:16:00

The f

页 21: [172] 删除的内容	LucidPapers	2018/6/19 PM3:17:00

is aimed

页 21: [172] 删除的内容	LucidPapers	2018/6/19 PM3:17:00

is aimed

页 24: [173] 删除的内容	Microsoft Office 用户	2018/7/15 AM9:14:00

Figure 10. Time series of the initial simulated surface variables for the sensible heat flux sensitivity and Noah land surface experiments: (a) sensible heat flux; (b) latent heat flux; (c) surface temperature; (d) soil moisture content; (e) temperature at 2 m; (f) relative humidity at 2 m; (g) wind speed at 10 m; and (h) wind direction at 10 m.

页 24: [174] 删除的内容	soderb5314	2018/7/14 PM4:56:00

Figure 1. Simulation domains used in the ARW model with (a) the terrain height (shaded, units:m), (b) the land use categories for domains D03 and D04 and (c) photograph of the area around Tazhong station.

Figure 1 Simulation domains used in ARW model with terrain height (shaded, units:m); (b) land use categories for domain D03 and D04Figure 1 Simulation domains used in

ARW model with terrain height (shaded, units:m); (b) land use categories for domain D03 and D04.

Figure 2. Horizontal distribution of the geopotential height (solid lines, units: da gpm), wind speed (shaded, units: knots) and wind barbs from the NCEP FNL analysis at 0800 BJT on 1 July 2016 at (a) 850, (b) 700, (c) 500 and (d) 100 hPa.Figure 2 Horizontal distribution of geopotential height (solid, units: dagpm), wind speed (shaded, units: knot), and wind barbs from the NCEP FNL analysis at 0800 BJT 1 Jul 2016 at (a) 850 hPa, (c) 700 hPa, (e) 500 hPa, and (d) 100hPa.Figure 2 Horizontal distribution of geopotential height (solid, units: dagpm), wind speed (shaded, units: knot), and wind barbs from the NCEP FNL analysis at 0800 BJT 1 Jul 2016 at (a) 850 hPa, (c) 700 hPa, (e) 500 hPa, and (d) 100hPa.

Figure 3. NCEP FNL 700 hPa potential temperature (colors) and mean sea level pressure (white lines) at 0800 BJT on 1 July 2016. The black dot shows the location of Tazhong station in Xingjiang province.Figure 3 NCEP FNL 700hPa potential temperature (colors) and mean sea level pressure (white lines) at 0800 BJT 1 Jul 2016. The black dot shows the location of Tazhong station at Xingjiang

province.Figure 3 NCEP fnl 700hPa potential temperature (colors) and mean sea level pressure (white lines) at 0800 BJT 1 Jul 2016. The black dot shows the location of Tazhong station at Xingjiang province.

Figure 4. Time series of the initial simulated surface variables from the innermost domain of the simulations and the surface observations at Tazhong station (83.63° E, 39.03° N) at 0800 BJT on 1 July 2016: (a) sensible heat flux; (b) latent heat flux; (c) surface temperature; (d) soil moisture content; (e) temperature at 2 m; (f) relative humidity at 2 m; (g) wind speed at 10 m; and (h) wind direction at 10 m.Figure 4 Time series of simulated surface variables from innermost domain of simulations and surface observations at Tazhong station (83.63°E, 39.03°N) initial at 0800 BJT 01July 2016 (a) sensible heat flux (W/m^2), (b) latent heat flux(W/m^2), (c) 2-m temperature (◦C), (d) surface temperature (◦C), (e) 2-m Relative Humidity(%) and (f) 10-m wind speed (m/s) with corresponding observations.

Figure 5. Vertical profiles of the potential temperature (solid line, units: K) and vapor mixing ratio (dashed line, units: g kg^{-1}) from the innermost domain of the simulations and the observations from GPS sounding at Tazhong station (83.63° E, 39.03° N) at (a)

1100, (b) 1400, (c) 1700 and (d) 2000 BJT on 1 July 2016. The profiles of the model output are averaged over a radius of 3.5 km.Figure 5 Vertical profiles of potential temperature (solid line, units: K) and vapor mixing ratio(dash line, units: g/Kg)from innermost domain of simulations and observation of GPS sounding at Tazhong station (83.63°E, 39.03°N) at (a)1100 (b) 1400 (c) 1700 (d) 2000 BJT 01 Jul2016Figure 4 Vertical profiles of potential temperature (units: K) at (a)1100 (b) 1400 (c) 1700 (d) 2000 BJT 01 Jul2016.

Figure 6. Cross-sections along 39.03° N of the horizontal winds (barbs, units: m s^{-1}) at intervals of 5 m s^{-1} superposed with theta (shaded, units: K) and the vapor mixing ratio (contours, units: g kg^{-1}) from the (a) BDY_T1, (c) BDY_T2 and (e) BDY_T3 experiments at 1400 BJT on 1 July 2016 and the (b) BDY_T1, (d) BDY_T2 and (f) BDY_T3 experiments at 2000 BJT on 1 July 2016.Figure 6 cross sections along 39.03°N of horizontal winds (barbs, units: m/s), at intervals of 5 m/s, superposed with theta (shaded, units: K) and vapor mixing ratio(contour, units: g/Kg), from (a)

BDY_T1, (c) BDY_T2, (e) BDY_T3 experiments at1400 BJT 01JUL2016, (b), (d), (f) are the same as (a), (c), (e), but for 2000 BJT 01JUL2016.Figure 7 cross sections along 39.03°N of horizontal winds (barbs, units: m/s), at intervals of 5 m/s, superposed with theta (shaded, units: K) and vapor mixing ratio(contour, units: g/Kg), from (a) BDY_T1, (c) BDY_T2, (e) BDY_T3 experiments at1400 BJT 01JUL2016, (b), (d), (f) are the same as (a), (c), (e), but for 2000 BJT 01JUL2016.

Figure 7. Instantaneous vertical velocity fields (shading: m s−1) at 3000 m for the (a) BDY_T1 (CTRL), (b) BDY_T2, (c) BDY_T3 and (d) Noah experiments at 1400 BJT on 1 July 2016.Figure 7 Instantaneous vertical velocity fields (shading: m/s) at 3000 m for (a) BDY_T1 (CTRL), (b) BDY_T2, (c) BDY_T3, and (d) Noah at 1400 BJT, 1 July 2016.

Figure 8. Vertical cross-sections of the instantaneous vertical velocity fields (shading: m s^{-1}) along A1–A2 in for the (a) BDY_T1 (CTRL), (b) BDY_T2, (c) BDY_T3 and (d) Noah experiments at 1400 BJT on 1 July 2016.Figure 8 Vertical cross-section of instantaneous vertical velocity fields (shading: m/s) along A1-A2 in for for (a)

BDY_T1 (CTRL), (b) BDY_T2, (c) BDY_T3, and (d) Noah at 1400 BJT, 1 July 2016.

Figure 9 Vertical profiles of the potential temperature (solid line, units: K) and vapor mixing ratio (dashed line, units: g kg^{-1}) for the sensible heat flux sensitivity and Noah land surface experiments at (a) 1100, (b) 1400, (c) 1700 and (d) 2000 BJT on 1 July 2016. The profiles of the model output are averaged over a radius of 3.5 km.Figure 9 The same as Figure 5, but for SH flux sensitive and Noah land-surface experimentFigure 8 The same as Figure 4, but for SH flux sensitive experiment.

Figure 10. Time series of the initial simulated surface variables for the sensible heat flux sensitivity and Noah land surface experiments: (a) sensible heat flux; (b) latent heat flux; (c) surface temperature; (d) soil moisture content; (e) temperature at 2 m; (f) relative humidity at 2 m; (g) wind speed at 10 m; and (h) wind direction at 10 m.Figure 10 The same as Figure 4, but for SH flux sensitive and Noah land-surface experiment.

页 24: [175] 带格式的 Microsoft Office 用户 2018/6/22 AM9:37:00

字体:11 pt

页 24: [175] 带格式的 Microsoft Office 用户 2018/6/22 AM9:37:00

字体:11 pt

页 24: [175] 带格式的 Microsoft Office 用户 2018/6/22 AM9:37:00

字体:11 pt

页 24: [175] 带格式的	Microsoft Office 用户	2018/6/22 AM9:37:00

字体:11 pt

页 24: [175] 带格式的	Microsoft Office 用户	2018/6/22 AM9:37:00

字体:11 pt

页 24: [175] 带格式的	Microsoft Office 用户	2018/6/22 AM9:37:00

字体:11 pt

页 24: [175] 带格式的	Microsoft Office 用户	2018/6/22 AM9:37:00

字体:11 pt

页 24: [175] 带格式的	Microsoft Office 用户	2018/6/22 AM9:37:00

字体:11 pt

页 24: [175] 带格式的	Microsoft Office 用户	2018/6/22 AM9:37:00

字体:11 pt

页 24: [175] 带格式的	Microsoft Office 用户	2018/6/22 AM9:37:00

字体:11 pt

页 24: [175] 带格式的	Microsoft Office 用户	2018/6/22 AM9:37:00

字体:11 pt

页 24: [175] 带格式的	Microsoft Office 用户	2018/6/22 AM9:37:00

字体:11 pt

页 24: [175] 带格式的	Microsoft Office 用户	2018/6/22 AM9:37:00

字体:11 pt

页 24: [175] 带格式的	Microsoft Office 用户	2018/6/22 AM9:37:00

字体:11 pt

页 24: [175] 带格式的	Microsoft Office 用户	2018/6/22 AM9:37:00

字体:11 pt

页 24: [175] 带格式的	Microsoft Office 用户	2018/6/22 AM9:37:00

字体:11 pt

页 24: [175] 带格式的	Microsoft Office 用户	2018/6/22 AM9:37:00

字体:11 pt

页 24: [175] 带格式的	Microsoft Office 用户	2018/6/22 AM9:37:00

字体:11 pt

页 24: [175] 带格式的	Microsoft Office 用户	2018/6/22 AM9:37:00

字体:11 pt

页 24: [175] 带格式的	Microsoft Office 用户	2018/6/22 AM9:37:00

字体:11 pt

页 24: [175] 带格式的	Microsoft Office 用户	2018/6/22 AM9:37:00

字体:11 pt

页 24: [175] 带格式的	Microsoft Office 用户	2018/6/22 AM9:37:00

字体:11 pt

页 24: [175] 带格式的	Microsoft Office 用户	2018/6/22 AM9:37:00

字体:11 pt

页 24: [175] 带格式的	Microsoft Office 用户	2018/6/22 AM9:37:00

字体:11 pt

页 24: [175] 带格式的	Microsoft Office 用户	2018/6/22 AM9:37:00

字体:11 pt

页 24: [175] 带格式的	Microsoft Office 用户	2018/6/22 AM9:37:00

字体:11 pt

页 24: [175] 带格式的	Microsoft Office 用户	2018/6/22 AM9:37:00

字体:11 pt

页 24: [175] 带格式的	Microsoft Office 用户	2018/6/22 AM9:37:00

字体:11 pt

页 24: [175] 带格式的	Microsoft Office 用户	2018/6/22 AM9:37:00

字体:11 pt

页 24: [175] 带格式的	Microsoft Office 用户	2018/6/22 AM9:37:00

字体:11 pt

页 24: [175] 带格式的	Microsoft Office 用户	2018/6/22 AM9:37:00

字体:11 pt

页 24: [175] 带格式的	Microsoft Office 用户	2018/6/22 AM9:37:00

字体:11 pt

页 24: [175] 带格式的	Microsoft Office 用户	2018/6/22 AM9:37:00

字体:11 pt

页 24: [175] 带格式的	Microsoft Office 用户	2018/6/22 AM9:37:00

字体:11 pt

页 24: [175] 带格式的	Microsoft Office 用户	2018/6/22 AM9:37:00

字体:11 pt

页 24: [175] 带格式的	Microsoft Office 用户	2018/6/22 AM9:37:00

字体:11 pt

页 24: [175] 带格式的	Microsoft Office 用户	2018/6/22 AM9:37:00

字体:11 pt

页 24: [175] 带格式的	Microsoft Office 用户	2018/6/22 AM9:37:00

字体:11 pt

页 24: [175] 带格式的	Microsoft Office 用户	2018/6/22 AM9:37:00

字体:11 pt

页 24: [175] 带格式的	Microsoft Office 用户	2018/6/22 AM9:37:00

字体:11 pt

页 25: [176] 删除的内容	Microsoft Office 用户	2018/6/22 AM9:29:00

（a） （b）

（c）

页 27: [177] 带格式的	Microsoft Office 用户	2018/6/22 AM9:36:00

字体:11 pt

页 27: [177] 带格式的	Microsoft Office 用户	2018/6/22 AM9:36:00

字体:11 pt

页 27: [177] 带格式的	Microsoft Office 用户	2018/6/22 AM9:36:00

字体:11 pt

页 27: [178] 带格式的	Microsoft Office 用户	2018/6/22 AM9:36:00

字体:11 pt

页 27: [178] 带格式的	Microsoft Office 用户	2018/6/22 AM9:36:00

字体:11 pt

页 30: [179] 删除的内容	Microsoft Office User	2018/4/9 AM11:25:00

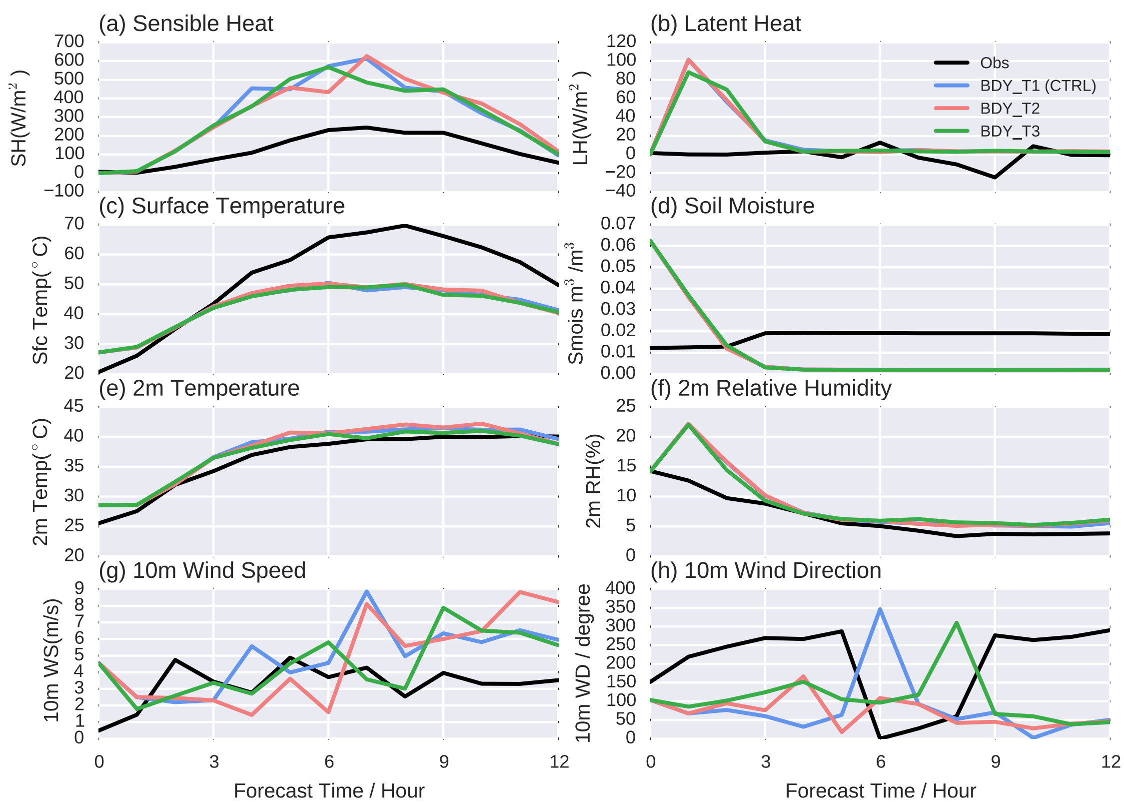

Figure 6 Time series of simulated surface initial at 0800 BJT 01July 2016 (a) sensible heat

flux (W/m²), (b) latent heat flux(W/m²), (c) 2-m temperature (◦C), (d) surface temperature (◦C), (e) 2-m Relative Humidity(%) and (f) 10-m wind speed (m/s) with corresponding observations.

分页

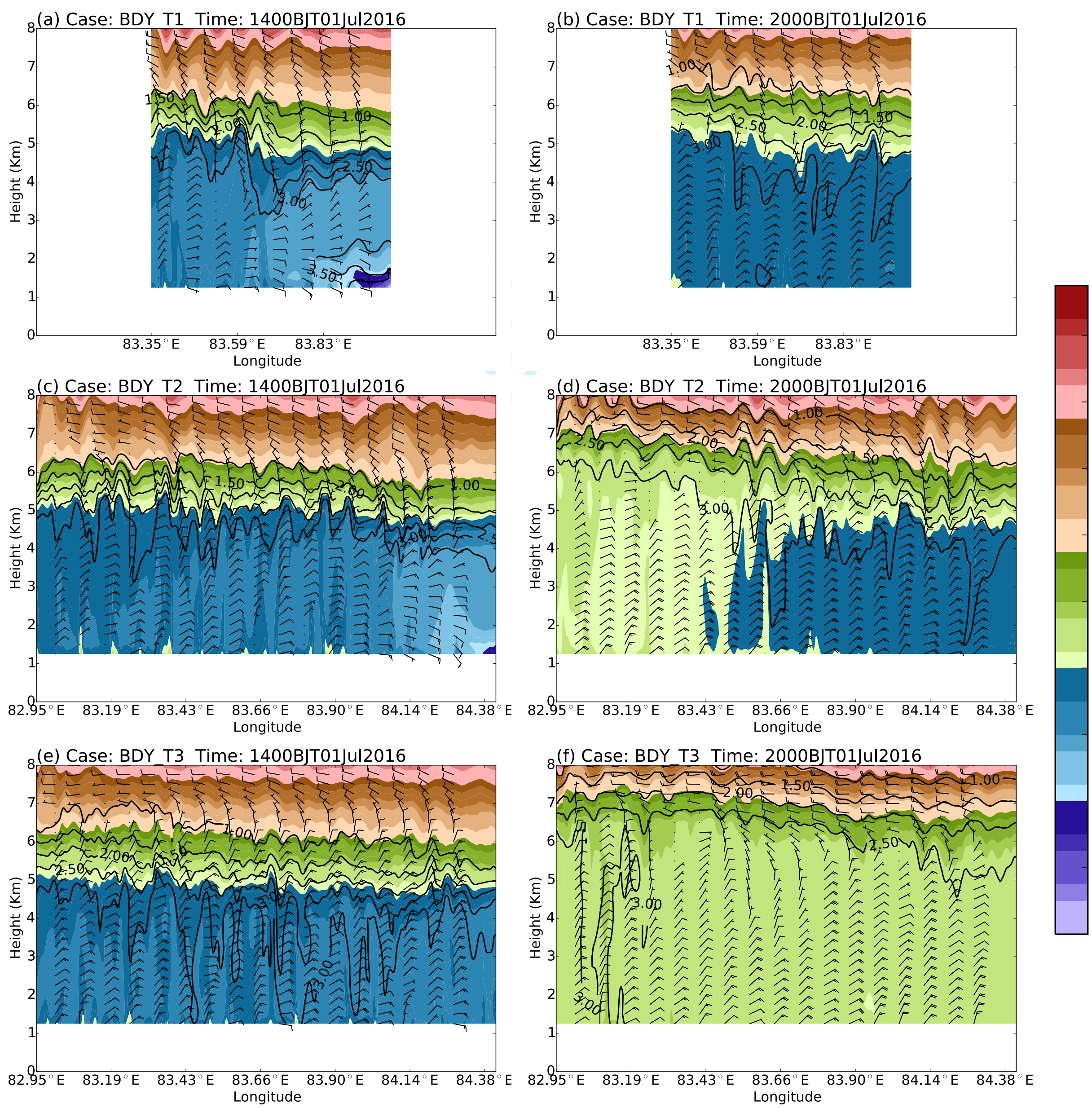

页 30: [180] 带格式的 Unknown

字体:(默认) Times New Roman, 字体颜色: 文字 1

页 30: [180] 带格式的 Unknown

字体:(默认) Times New Roman, 字体颜色: 文字 1

页 30: [181] 带格式的 Microsoft Office 用户 2018/6/22 AM9:35:00

字体:11 pt

页 30: [181] 带格式的 Microsoft Office 用户 2018/6/22 AM9:35:00

字体:11 pt

页 30: [181] 带格式的 Microsoft Office 用户 2018/6/22 AM9:35:00

字体:11 pt

页 30: [182] 删除的内容 LucidPapers 2018/6/19 PM3:33:00

c

页 30: [182] 删除的内容 LucidPapers 2018/6/19 PM3:33:00

c

页 30: [182] 删除的内容 LucidPapers 2018/6/19 PM3:33:00

c

页 30: [182] 删除的内容 LucidPapers 2018/6/19 PM3:33:00

c

页 30: [182] 删除的内容	LucidPapers	2018/6/19 PM3:33:00

c

页 30: [182] 删除的内容	LucidPapers	2018/6/19 PM3:33:00

c

页 30: [182] 删除的内容	LucidPapers	2018/6/19 PM3:33:00

c

页 30: [182] 删除的内容	LucidPapers	2018/6/19 PM3:33:00

c

页 30: [182] 删除的内容	LucidPapers	2018/6/19 PM3:33:00

c

页 30: [182] 删除的内容	LucidPapers	2018/6/19 PM3:33:00

c

页 30: [182] 删除的内容	LucidPapers	2018/6/19 PM3:33:00

c

页 30: [182] 删除的内容	LucidPapers	2018/6/19 PM3:33:00

c

页 30: [182] 删除的内容	LucidPapers	2018/6/19 PM3:33:00

c

页 30: [182] 删除的内容	LucidPapers	2018/6/19 PM3:33:00

c

页 30: [182] 删除的内容	LucidPapers	2018/6/19 PM3:33:00

c

页 30: [182] 删除的内容	LucidPapers	2018/6/19 PM3:33:00

c

页 35: [183] 删除的内容	Microsoft Office User	2018/4/8 PM6:22:00

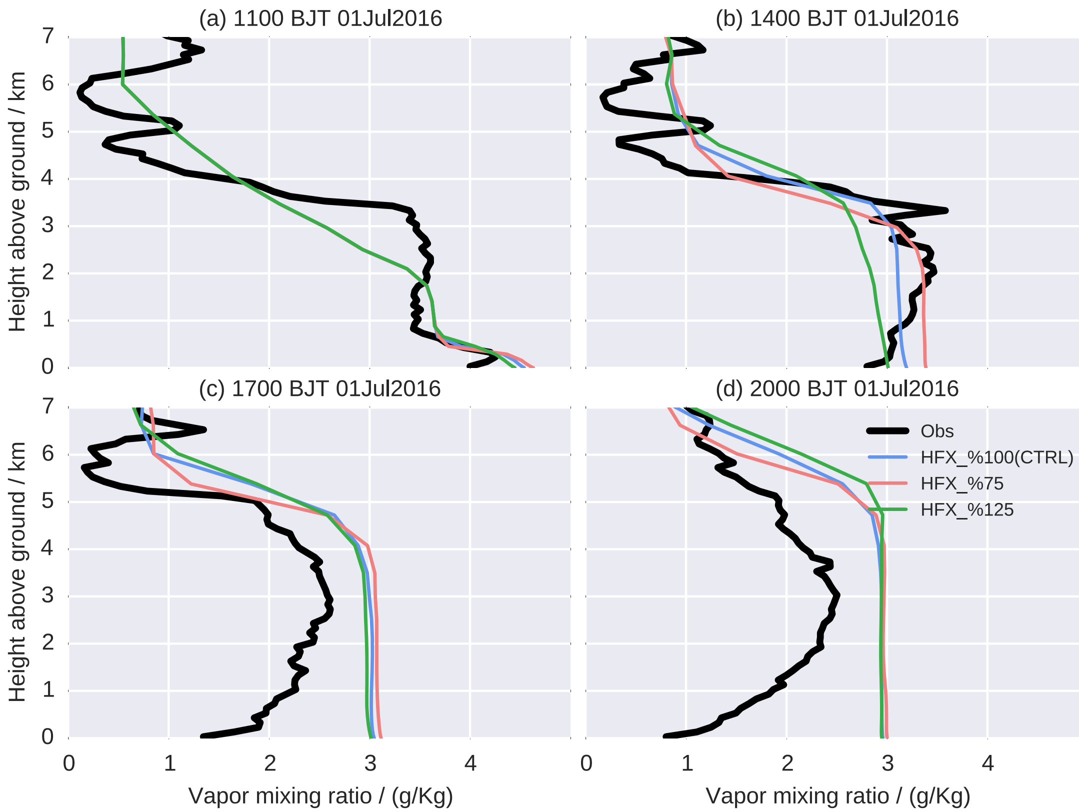

Figure 9 The same as Figure 8, but for vapor mixing ratio (units: g/Kg)

页 35: [184] 删除的内容	LucidPapers	2018/6/19 PM3:43:00

1

页 35: [184] 删除的内容	LucidPapers	2018/6/19 PM3:43:00

1

页 35: [185] 删除的内容	LucidPapers	2018/6/19 PM3:44:00

model grids

页 35: [185] 删除的内容	LucidPapers	2018/6/19 PM3:44:00

model grids

页 35: [185] 删除的内容	LucidPapers	2018/6/19 PM3:44:00

model grids

页 35: [186] 删除的内容	LucidPapers	2018/6/19 PM3:44:00

SH

页 35: [186] 删除的内容	LucidPapers	2018/6/19 PM3:44:00

SH

页 35: [187] 删除的内容	LucidPapers	2018/6/19 PM3:44:00

SH

页 35: [187] 删除的内容	LucidPapers	2018/6/19 PM3:44:00

SH

页 35: [188] 删除的内容	LucidPapers	2018/6/19 PM3:44:00

surface-

页 35: [188] 删除的内容	LucidPapers	2018/6/19 PM3:44:00

surface-

页 36: [189] 删除的内容	LucidPapers	2018/6/19 PM3:45:00

H

页 36: [189] 删除的内容	LucidPapers	2018/6/19 PM3:45:00

H

页 36: [190] 删除的内容	LucidPapers	2018/6/19 PM3:46:00

2m

页 36: [190] 删除的内容	LucidPapers	2018/6/19 PM3:46:00

2m

页 36: [191] 删除的内容	LucidPapers	2018/6/19 PM3:46:00

10m

页 36: [191] 删除的内容	LucidPapers	2018/6/19 PM3:46:00

10m

页 36: [192] 删除的内容	LucidPapers	2018/6/19 PM3:46:00

页 36: [192] 删除的内容	LucidPapers	2018/6/19 PM3:46:00

页 36: [193] 删除的内容	LucidPapers	2018/6/19 PM3:46:00

页 36: [193] 删除的内容	LucidPapers	2018/6/19 PM3:46:00

页 36: [194] 删除的内容	LucidPapers	2018/6/19 PM3:48:00

-

页 36: [194] 删除的内容	LucidPapers	2018/6/19 PM3:48:00

-

页 36: [195] 删除的内容	LucidPapers	2018/6/19 PM3:46:00

页 36: [195] 删除的内容	LucidPapers	2018/6/19 PM3:46:00

页 36: [196] 删除的内容	LucidPapers	2018/6/19 PM3:48:00

-

页 36: [196] 删除的内容	LucidPapers	2018/6/19 PM3:48:00

-

页 36: [197] 删除的内容	LucidPapers	2018/6/19 PM3:46:00

页 36: [197] 删除的内容	LucidPapers	2018/6/19 PM3:46:00

页 36: [198] 删除的内容	LucidPapers	2018/6/19 PM3:46:00

页 36: [198] 删除的内容	LucidPapers	2018/6/19 PM3:46:00

页 36: [199] 删除的内容	LucidPapers	2018/6/19 PM3:47:00

页 36: [199] 删除的内容	LucidPapers	2018/6/19 PM3:47:00

页 36: [200] 删除的内容	LucidPapers	2018/6/19 PM3:47:00

页 36: [200] 删除的内容	LucidPapers	2018/6/19 PM3:47:00

页 36: [201] 删除的内容	LucidPapers	2018/6/19 PM3:47:00

页 36: [201] 删除的内容	LucidPapers	2018/6/19 PM3:47:00

页 36: [202] 删除的内容	LucidPapers	2018/6/19 PM3:47:00

页 36: [202] 删除的内容	LucidPapers	2018/6/19 PM3:47:00

页 36: [203] 删除的内容	LucidPapers	2018/6/19 PM3:47:00

页 36: [203] 删除的内容	LucidPapers	2018/6/19 PM3:47:00

页 36: [204] 删除的内容	LucidPapers	2018/6/19 PM3:47:00

页 36: [204] 删除的内容	LucidPapers	2018/6/19 PM3:47:00

页 36: [205] 删除的内容	LucidPapers	2018/6/19 PM3:48:00

-

页 36: [205] 删除的内容	LucidPapers	2018/6/19 PM3:48:00

-

页 36: [206] 删除的内容	LucidPapers	2018/6/19 PM3:47:00

页 36: [206] 删除的内容	LucidPapers	2018/6/19 PM3:47:00

页 36: [207] 删除的内容	LucidPapers	2018/6/19 PM3:48:00

-

页 36: [207] 删除的内容	LucidPapers	2018/6/19 PM3:48:00

-

页 36: [208] 删除的内容	LucidPapers	2018/6/19 PM3:47:00

页 36: [208] 删除的内容	LucidPapers	2018/6/19 PM3:47:00

页 36: [209] 删除的内容	LucidPapers	2018/6/19 PM3:47:00

页 36: [209] 删除的内容	LucidPapers	2018/6/19 PM3:47:00

页 36: [210] 删除的内容	LucidPapers	2018/6/19 PM3:47:00

页 36: [210] 删除的内容	LucidPapers	2018/6/19 PM3:47:00

页 36: [211] 删除的内容	LucidPapers	2018/6/19 PM3:47:00

页 36: [211] 删除的内容	LucidPapers	2018/6/19 PM3:47:00

页 36: [212] 删除的内容	LucidPapers	2018/6/19 PM3:47:00

页 36: [212] 删除的内容	LucidPapers	2018/6/19 PM3:47:00

页 36: [213] 删除的内容	LucidPapers	2018/6/19 PM3:47:00

页 36: [213] 删除的内容	LucidPapers	2018/6/19 PM3:47:00

页 36: [214] 删除的内容	LucidPapers	2018/6/19 PM3:47:00

页 36: [214] 删除的内容	LucidPapers	2018/6/19 PM3:47:00

页 36: [215] 删除的内容	LucidPapers	2018/6/19 PM3:47:00

页 36: [215] 删除的内容	LucidPapers	2018/6/19 PM3:47:00

页 36: [216] 删除的内容	LucidPapers	2018/6/19 PM3:48:00

-

页 36: [216] 删除的内容	LucidPapers	2018/6/19 PM3:48:00

-

页 36: [217] 删除的内容	LucidPapers	2018/6/19 PM3:47:00

页 36: [217] 删除的内容	LucidPapers	2018/6/19 PM3:47:00

页 36: [218] 删除的内容	LucidPapers	2018/6/19 PM3:48:00

-

页 36: [218] 删除的内容	LucidPapers	2018/6/19 PM3:48:00

-

页 36: [219] 删除的内容	LucidPapers	2018/6/19 PM3:47:00

页 36: [219] 删除的内容	LucidPapers	2018/6/19 PM3:47:00

页 36: [220] 删除的内容	LucidPapers	2018/6/19 PM3:47:00

页 36: [220] 删除的内容	LucidPapers	2018/6/19 PM3:47:00

页 36: [221] 删除的内容	LucidPapers	2018/6/19 PM3:47:00

页 36: [221] 删除的内容	LucidPapers	2018/6/19 PM3:47:00

页 36: [222] 删除的内容	LucidPapers	2018/6/19 PM3:47:00

页 36: [222] 删除的内容	LucidPapers	2018/6/19 PM3:47:00

页 36: [223] 删除的内容	LucidPapers	2018/6/19 PM3:47:00

页 36: [223] 删除的内容	LucidPapers	2018/6/19 PM3:47:00

页 36: [224] 删除的内容	LucidPapers	2018/6/19 PM3:47:00

页 36: [224] 删除的内容	LucidPapers	2018/6/19 PM3:47:00

页 36: [225] 删除的内容	LucidPapers	2018/6/19 PM3:47:00

页 36: [225] 删除的内容	LucidPapers	2018/6/19 PM3:47:00

页 36: [226] 删除的内容	LucidPapers	2018/6/19 PM3:47:00

页 36: [226] 删除的内容	LucidPapers	2018/6/19 PM3:47:00

页 36: [227] 删除的内容	LucidPapers	2018/6/19 PM3:48:00

-

页 36: [227] 删除的内容	LucidPapers	2018/6/19 PM3:48:00

-

页 36: [228] 删除的内容	LucidPapers	2018/6/19 PM3:47:00

页 36: [228] 删除的内容	LucidPapers	2018/6/19 PM3:47:00

页 36: [229] 删除的内容	LucidPapers	2018/6/19 PM3:48:00

-

页 36: [229] 删除的内容	LucidPapers	2018/6/19 PM3:48:00

-

页 36: [230] 删除的内容	LucidPapers	2018/6/19 PM3:47:00

页 36: [230] 删除的内容	LucidPapers	2018/6/19 PM3:47:00

页 36: [231] 删除的内容	LucidPapers	2018/6/19 PM3:47:00

页 36: [231] 删除的内容	LucidPapers	2018/6/19 PM3:47:00

页 36: [232] 删除的内容	LucidPapers	2018/6/19 PM3:47:00

页 36: [232] 删除的内容	LucidPapers	2018/6/19 PM3:47:00

页 36: [233] 删除的内容	LucidPapers	2018/6/19 PM3:47:00

页 36: [233] 删除的内容	LucidPapers	2018/6/19 PM3:47:00

页 36: [234] 删除的内容	LucidPapers	2018/6/19 PM3:47:00

页 36: [234] 删除的内容	LucidPapers	2018/6/19 PM3:47:00

页 36: [235] 删除的内容	LucidPapers	2018/6/19 PM3:47:00

页 36: [235] 删除的内容	LucidPapers	2018/6/19 PM3:47:00

页 36: [236] 删除的内容	LucidPapers	2018/6/19 PM3:47:00

页 36: [236] 删除的内容	LucidPapers	2018/6/19 PM3:47:00

页 36: [237] 删除的内容	LucidPapers	2018/6/19 PM3:47:00

页 36: [237] 删除的内容	LucidPapers	2018/6/19 PM3:47:00

页 36: [238] 删除的内容	LucidPapers	2018/6/19 PM3:48:00

-

页 36: [238] 删除的内容	LucidPapers	2018/6/19 PM3:48:00

-

页 36: [239] 删除的内容	LucidPapers	2018/6/19 PM3:47:00

页 36: [239] 删除的内容	LucidPapers	2018/6/19 PM3:47:00

页 36: [240] 删除的内容	LucidPapers	2018/6/19 PM3:48:00

-

页 36: [240] 删除的内容	LucidPapers	2018/6/19 PM3:48:00

-

页 36: [241] 删除的内容	LucidPapers	2018/6/19 PM3:47:00

页 36: [241] 删除的内容	LucidPapers	2018/6/19 PM3:47:00

页 36: [242] 删除的内容	LucidPapers	2018/6/19 PM3:48:00

页 36: [242] 删除的内容	LucidPapers	2018/6/19 PM3:48:00

页 36: [243] 删除的内容	LucidPapers	2018/6/19 PM3:48:00

页 36: [243] 删除的内容	LucidPapers	2018/6/19 PM3:48:00

页 36: [244] 删除的内容	LucidPapers	2018/6/19 PM3:48:00

页 36: [244] 删除的内容	LucidPapers	2018/6/19 PM3:48:00

页 36: [245] 删除的内容	LucidPapers	2018/6/19 PM3:48:00

页 36: [245] 删除的内容	LucidPapers	2018/6/19 PM3:48:00

页 36: [246] 删除的内容	LucidPapers	2018/6/19 PM3:48:00

页 36: [246] 删除的内容	LucidPapers	2018/6/19 PM3:48:00

页 36: [247] 删除的内容	LucidPapers	2018/6/19 PM3:48:00

页 36: [247] 删除的内容	LucidPapers	2018/6/19 PM3:48:00

页 36: [248] 删除的内容	LucidPapers	2018/6/19 PM3:48:00

-

页 36: [248] 删除的内容	LucidPapers	2018/6/19 PM3:48:00

-

页 36: [249] 删除的内容	LucidPapers	2018/6/19 PM3:48:00

页 36: [249] 删除的内容	LucidPapers	2018/6/19 PM3:48:00

页 36: [250] 删除的内容	LucidPapers	2018/6/19 PM3:48:00

页 36: [250] 删除的内容	LucidPapers	2018/6/19 PM3:48:00

页 36: [251] 删除的内容	LucidPapers	2018/6/19 PM3:48:00

页 36: [251] 删除的内容	LucidPapers	2018/6/19 PM3:48:00

页 36: [252] 删除的内容	LucidPapers	2018/6/19 PM3:48:00

页 36: [252] 删除的内容	LucidPapers	2018/6/19 PM3:48:00

页 36: [253] 删除的内容	LucidPapers	2018/6/19 PM3:48:00

页 36: [253] 删除的内容	LucidPapers	2018/6/19 PM3:48:00

页 36: [254] 删除的内容	LucidPapers	2018/6/19 PM3:48:00

页 36: [254] 删除的内容	LucidPapers	2018/6/19 PM3:48:00

页 36: [255] 删除的内容	LucidPapers	2018/6/19 PM3:48:00

页 36: [255] 删除的内容	LucidPapers	2018/6/19 PM3:48:00

页 36: [256] 删除的内容	LucidPapers	2018/6/19 PM3:45:00

页 36: [256] 删除的内容	LucidPapers	2018/6/19 PM3:45:00

页 37: [257] 删除的内容	Microsoft Office User	2018/4/15 AM11:41:00

页 39: [258] 删除的内容	Microsoft Office User	2018/4/12 AM11:58:00

References